Western&Graduate&PostdoctoralStudies

10-2-2017 2:00 PM

CCN Proteins in Metastatic Melanoma

James Hutchenreuther, *The University of Western Ontario*

Supervisor: Andrew Leask, *The University of Western Ontario*
Co-Supervisor: Lynne Postovit, *The University of Western Ontario*
A thesis submitted in partial fulfillment of the requirements for the Doctor of Philosophy degree in Physiology
© James Hutchenreuther 2017

Recommended Citation

Abstract

Melanoma cells recruit host tissue to become a part of the activated tumour stroma. This stromal microenvironment is similar to that seen in fibrotic tissue. CCN1 and CCN2 are tightly spatiotemporally regulated matricellular proteins involved in development and wound healing, and are abberantly expressed in fibrosis. Additionally they have been seen to be abnormally highly expressed in several cancers, including melanoma. Recent evidence has shown that deletion of CCN2 in the fibroblasts renders mice resistant to several models of fibrosis. Given this, I tested the hypothesis that deletion of CCN1 and CCN2 from fibroblasts could similarly impede the formation of the activated stromal microenvironment in melanoma. I used B16F(10) murine melanoma cells and syngeneic C57 BL6 mice with a tamoxifen-dependent conditional deletion of CCN1 or CCN2 in their fibroblasts. First I determined that loss of CCN2 in the fibroblasts prevents the metastasis of melanoma to the lungs of the mice, while loss of CCN2 in the tumour alone does not. Second I determined that loss of CCN2 from the fibroblasts prevented the expression of myofibroblast marker αSMA and reduced the expression of pluripotency marker SOX2. This loss of CCN2 was accompanied by a reduced tumour vascularisation, and a reduction in tumour cell vasculogenic mimicry. Finally I determined that loss of CCN1 in the fibroblasts results in highly disorganized collagen in the skin, which results in reduced metastasis of the melanoma cells. These observations were supported by *in vitro* experiments showing that deletion of CCN1 or CCN2 from melanoma cells reduce their ability to invade through a collagen basement membrane, and that deletion of CCN2 impedes the ability of melanoma cells to form tubule networks in nutrient-deficient environments. The results presented here suggest that CCN1 and CCN2 in the stromal microenvironment mediate the metastasis of melanoma through different mechanisms, with CCN2 being required for the activated stromal microenvironment and tumour vascularisation, and CCN1 being required for formation of a stiff and organized collagen network that facilitates tumour cell invasion, and thus they might both present novel targets for therapies to improve patient outcome.

Keywords

tumour microenvironment, matricellular protein, CCN1, CCN2, tumour vasculature, angiogenesis, micro-computed tomography, metastasis, melanoma

Co-Authorship Statement

Chapter 2 constitutes a manuscript that has been accepted to a peer-reviewed journal, chapter 3 represents a manuscript being prepared for submission, and chapter 4 will contribute to publication of a manuscript. Contributions to each chapter by authors are as follows:

Chapter 2: *CCN2 Expression by Tumour Stroma is Required for Melanoma Metastasis*

Manuscript published by Journal of Investigative Dermatology as an Original Article. Authors are (in order) Hutchenreuther J, Vincent KM, Carter DE, Postovit LM, Leask A. Vincent KM performed bioinformatic analyses, Carter DE performed Microarray analyses under my oversight, and all other experiments were performed by me. Bioinformatics was performed in the Postovit lab at the University of Alberta, human cell line experiments were performed in both the Postovit lab at the Univerisity of Alberta and in the Leask lab at the University of Western Ontario, Microarray experiments were performed at London Regional Genomics Centre at the University of Western Ontario, and all other experiments were performed in the Leask Lab at the University of Western Ontario. The manuscript was written by Leask A, Postovit LM, and myself.

Chapter 3: *CCN2 Expression by Tumour Stroma is Required for Tumour Vascularization and Formation of a Contractile Stroma*

Bioinformatics experiments were performed by Krista Vincent in the Postovit lab at the University of Alberta. MicroCT scanning was performed by Chris Norley at Robarts Research Institute at the University of Western Ontario. Mass spectrometry was performed by Dylan Dieters-Castator in the LaJoie Lab at the University of Western Ontario. I performed all other experiments in the Leask Lab at the University of Western Ontario and I wrote the manuscript, with revisions suggested by Andrew Leask.

Chapter 4: *CCN1 Expression in Tumour Stroma is Required for Collagen Organization and Melanoma Metastasis*

Microarray analysis was performed by David Carter at the London Regional Genomics Centre at the University of Western Ontario. HPLC-Mass Spectrometry was performed by Yizhi Xiao in the Siqueira Lab at the University of Western Ontario. Transmission Electron

Microscopy was performed by me with the assistance of Richard Gardiner and Karen Nygard with tissue sections cut by Reza Khazaee in the Integrated Microscopy Unit of the Biotron at the University of Western Ontario. I performed all other experiments in the Leask Lab at the University of Western Ontario and I wrote the manuscript, with revisions suggested by Andrew Leask.

Acknowledgments

Table of Contents

vii

ix

List of Tables

List of Figures

Chapter 1

1.1   Introduction

Melanoma, a cancer that develops from melanocytes, is the second most common invasive cancer in young adults, and the incidence of diagnosis among this group is only increasing (Reed, Brewer et al. 2012). Of all skin cancers, melanoma is the most likely to metastasize making it the most likely to be fatal (Society 2013). In 2017 in the US and Canada there will be an estimated 97,000 new cases of melanoma diagnosed, and 11,000 fatalities (Society 2013, Society 2017). Of the three types of skin cancer (basal cell carcinoma, squamous cell carcinoma, and melanoma) it is the least common; it accounts for only 4% of skin cancers, but its highly metastatic nature makes it so deadly that it accounts for over 80% of skin cancer deaths (Miller and Mihm 2006).

1.1.1   Staging and Risk

Melanoma progresses through several stages as it develops, and the survival rate of patients is highly variable based on the stage at which it is diagnosed. The current staging system used to evaluate melanomas is the TNM staging system most recently updated by the American Joint Committee on Cancer in 2009 (Balch, Gershenwald et al. 2009). The TNM system is named for the three factors measured: primary Tumour characteristics (such as thickness, ulceration, and mitotic rate), presence or absence of metastases in regional lymph Nodes, and presence or absence of distant Metastases (Balch, Gershenwald et al. 2009). This system will remain in use until December 31st 2017 when the newly updated TNM system, which removes mitotic rate and puts more emphasis on circulating lactate dehydrogenase (LDH) levels, is implemented (AJCC 2017). Proper staging is important in developing a prognosis for patients diagnosed. For example, a patient diagnosed while the tumour is thin and has not metastasized has a 10-year survival rate of 95%, while a patient with multiple regional lymph node metastases has a 10-year survival rate of only 33% (Balch, Gershenwald et al. 2009).

1.1.2   Progression and Metastasis

Under healthy conditions, melanocytes are found throughout the basal layer of the epidermis at a 1:10 ratio with keratinocytes where they extend their dendrites between keratinocytes to facilitate delivery of melanin (Cichorek, Wachulska et al. 2013). In addition to their presence in the epidermis, melanocytes are also found in hair follicles, the uveal tract of the eye, and in lesser numbers in several other tissues (Shain and Bastian 2016). In the epidermis, each melanocyte and its associated keratinocytes are known as an Epidermal-Melanin Unit (Haass and Herlyn 2005). In this state their association with keratinocytes and their E-cadherin mediated cell-to-cell contacts regulate their proliferation and prevent transformation; in fact, when melanocytes are grown in monoculture they begin expressing surface markers consistent with those acquired during tumourigenesis of melanoma, and these markers disappear when the cells are then co-cultured with undifferentiated keratinocytes (Haass and Herlyn 2005). Typically melanocytes will escape the control of their associated keratinocytes in two circumstances: To divide, which occurs approximately twice a year, or as a result of a mutation (Shain and Bastian 2016). These mutations can be familial (such as mutations in CDKN2A) or somatic (such as mutations in NRAS or BRAF), but these mutations are frequently insufficient to drive melanocytes transformation on their own, and require additional mutations which are frequently acquired through UV exposure (Sample and He 2017).

Once sufficient mutations are accumulated the affected melanocytes will undergo the first stage of melanoma development in which they decouple from their associated keratinocytes, allowing them to proliferate and form a benign nevus – also known as a mole (Miller and Mihm 2006). The majority of nevi enter a senescence-like state in which very few of the melanocytes within them are able to proliferate further until they acquire further mutations, such as inactivating mutations of the p53 tumour-suppressor gene (Miller and Mihm 2006, Shain and Bastian 2016). In this state the nevus is typically symmetrical, smooth, evenly coloured, and does not penetrate the basement membrane (Miller and Mihm 2006).

Once a melanocyte within a benign nevus acquires sufficient mutations to escape its senescence-like state, it progresses to the second stage of development and becomes a dysplastic nevus. Typically at this stage the lesion becomes asymmetrical, with abnormal colouration patterns and the melanocytes within it become irregularly and abnormally shaped (Miller and Mihm 2006). While a benign nevus has very little proliferation once its senescence-like state has set it, it is believed that dysplastic nevi engage in constant, slow proliferation that is offset by attritional factors which are sometimes strong enough to reverse the development of the lesion entirely (Shain and Bastian 2016).

The third stage, known as the radial growth phase is characterized by a cancerous histological phenotype, rapid growth across the epidermis with only minor incursions across the basement membrane, and constitutive activation of ERK signaling to drive rapid clonal cell proliferation (Haass and Herlyn 2005, Miller and Mihm 2006, Shain and Bastian 2016). Explanted cells from lesions in the radial growth phase, or any earlier phase, are typically unable to produce colonies in soft agar, as they are typically reliant on exogenous growth factors (Miller and Mihm 2006, Steck 2014). Since the cells are largely unable to penetrate deeper than the basement membrane, surgical excision up to this stage remains highly effective (Steck 2014).

Once the lesion breaches the basement membrane and begins to expand through intradermal growth it has reached the vertical growth phase (Nesbit and Herlyn 1994, Miller and Mihm 2006). This phase is characterized by a loss of E-cadherin expression, increased N-cadherin expression, and increased $\alpha_V\beta_3$ integrin expression that results in induction of MMP2 to break down the collagen of the basement membrane and BCL-2 to prevent apoptosis in the absence of cell-cell contacts, allowing explanted cells to colonize soft agar (Kuphal, Bauer et al. 2005, Miller and Mihm 2006, Shain and Bastian 2016). Additionally, the shift from E-cadherin to N-cadherin expression allows melanoma cells to interact with fibroblasts and vascular endothelial cells to better facilitate migration and intravasation (Haass and Herlyn 2005). It has been theorized that this newfound ability to communicate and attach to fibroblasts might be instrumental in facilitating the transition from the radial growth phase to the vertical growth phase (Haass and Herlyn 2005). At this point the tumour is fully competent to invade and metastasize to distant

organs, though continuing accumulation of mutations may speed this process (Steck 2014). Once metastasis to distant organs has occurred, the tumour has entered its final stage and becomes metastatic melanoma.

1.1.3 Current Therapies

Despite major advances in therapies for other cancers, melanoma remains difficult to manage. While other cancers are vulnerable to chemo- and radio-therapies, melanoma is largely unaffected by these traditional standbys (Soengas and Lowe 2003). Treatment with dacarbazine, temozolomide, or fotemustine have very low response rates (with complete response in less than 5% of patients and most responses lasting only ~1.5 months) and toxic combinatorial treatments not showing any significant increase in survival (Thompson, Scolyer et al. 2005, Palathinkal, Sharma et al. 2014). Surgical excision is highly effective, but only when melanomas are caught early; while resection of non-metastatic lesions provides an approximately 5-year survival rate of 90%, even the presence of microsatellite metastases (discrete lesions greater than 0.05mm in diameter separated from the primary lesion) decreases this survival rate from 90% to 36% (Homsi, Kashani-Sabet et al. 2005, Cummins, Cummins et al. 2006). Although conventional chemotherapies and surgical excision are of little use in late stage melanoma, there are several promising therapies, primarily in two major categories: molecularly targeted inhibitors (primarily targeting the BRAF mutation) and anti-angiogenic therapies.

1.1.3.1 BRAF inhibitors

BRAF is a protein kinase of the RAF family that functions downstream of RAS to help stimulate cell growth and survival by phosphorylation of MEK to activate ERK (Chan, Singh et al. 2017). In 2002, large-scale sequencing of genes in the RAS-RAF-MEK-ERK-MAPK pathway revealed a mutation in the BRAF gene that resulted in constitutive activation of this pathway (Davies, Bignell et al. 2002). The vast majority (92%) of these mutations were in the same codon: BRAFV600E, which prevents folding of BRAF in its inactive state and instead results in a new conformation that has 10-12 fold increased kinase activity (Davies, Bignell et al. 2002, DeLuca, Srinivas et al. 2008). Present in

approximately 60% of melanomas, BRAF mutations drive melanoma progression from the earliest stages, and even contribute to the formation of a benign nevus (Miller and Mihm 2006). While it is insufficient on its own to generate a cancerous lesion, when a melanocytes acquires secondary mutations BRAF becomes a major driver of disease progression (Miller and Mihm 2006, DeLuca, Srinivas et al. 2008). Since the discovery of the BRAFV600E mutation, several inhibitors of its activity have been developed. The two most promising inhibitors are vemurafenib and dabrafenib, both of which have gone through phase III clinical trials. Although they both show significant increases in both overall and progression-free survival, they also have approximately 50% response rates, and both only increased overall survival by ~4 months (DeLuca, Srinivas et al. 2008, Lim, Menzies et al. 2017). Whereas intrinsic resistance to BRAF inhibition is only present in approximately 10% of BRAFV600E mutant melanomas, acquired resistance is rapidly acquired by almost all patients (Lim, Menzies et al. 2017). The exact mechanism behind this resistance is still being studied, but potential mechanisms include expression of splice variants with reduced inhibitor affinity, BRAF allele amplification, overexpression of alternative RAF isoforms, and activation of alternative ERK signaling pathways (Lim, Menzies et al. 2017). One of the side-effects of the inhibition of BRAFV600E is a paradoxical activation of wild-type BRAF in non-mutant cells. This has been shown to occur not only in wild-type BRAF melanomas, but also in the cancer associated fibroblasts of the stroma which results in increased contractility and matrix deposition (Hirata, Girotti et al. 2015). When BRAFV600E cells are grown in the presence of cancer associated fibroblasts, or when plated on an ECM layered rigid substrate they displayed BRAF inhibitor resistance that was disrupted by inhibition of integrin β1 or FAK indicating that the stiff matrix created by activation of the fibroblasts in the stroma was conferring BRAF resistance through an alternate ERK signaling pathway that relied upon integrin-mediated attachment to ECM (Figure 1) (Hirata, Girotti et al. 2015). Collectively, these data suggest that disruption of this activated, stiff matrix might represent a strategy to overcome resistance to BRAF inhibitors.
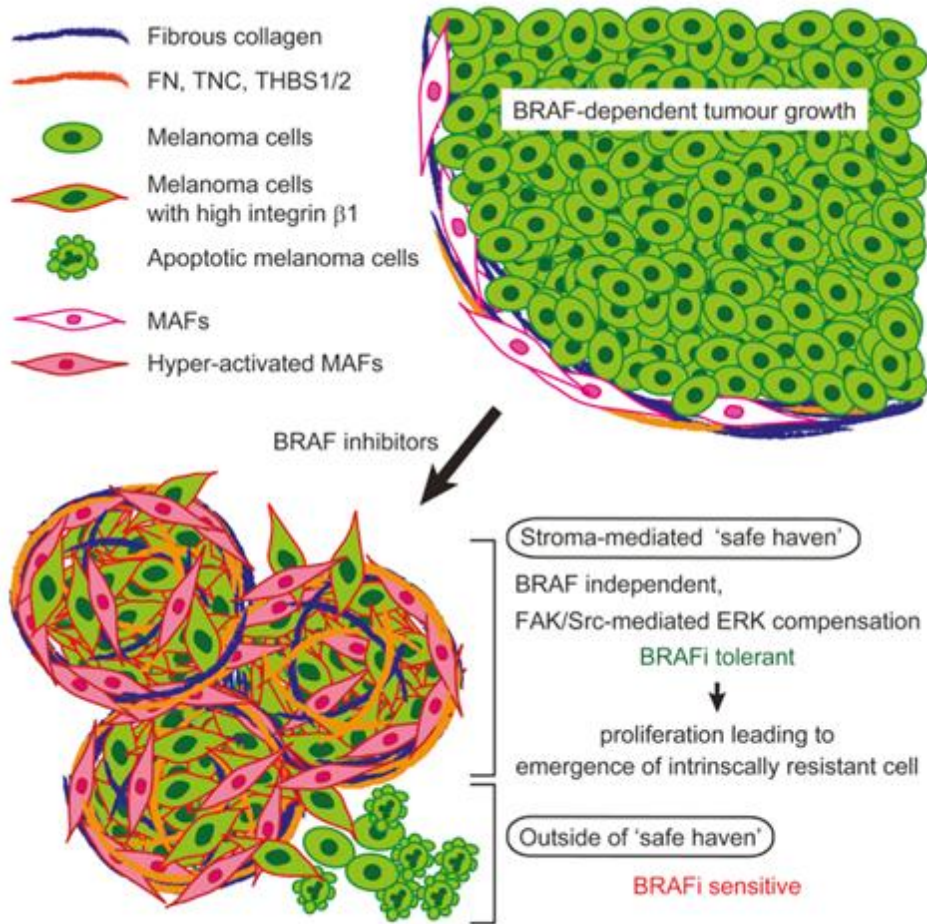
Figure 1-1 BRAF inhibition is overcome by alternate ERK signaling by hyperactivated stroma

Cells driven by a BRAFV600E mutation are sensitive to BRAF inhibition until they migrate to the hyperactivated stromal microenvironment. In this microenvironment an alternate ERK signaling pathway stimulated by integrin-mediated attachment to the ECM compensates for the inhibition of BRAF.

Reprinted from (Hirata, Girotti et al. 2015)

1.1.3.2   Immune therapy

As melanoma is an immunogenic tumour, it must develop methods of evading immune responses in the host as the cancer progresses (Anderson, Stromnes et al. 2017, Pulluri, Kumar et al. 2017). As such, therapies to increase the effectiveness of the body's immune response have been developed to combat melanoma. Therapies such as high dose interleukin-2 inducing proliferation in T cell populations have been developed, but show limited efficacy and high rates of severe toxicity (Pulluri, Kumar et al. 2017). More recently, however, targeted therapies such as immune checkpoint inhibition and adoptive T cell therapy have been developed and show more promise. Adoptive T cell therapy is a therapy in which T cells are isolated from a patient and expanded *in vitro* before being re-introduced back into the patient (Perica, Varela et al. 2015). While the cells are being expanded *in vitro* they can be genetically engineered to recognize tumour-specific antigens, but this process is extremely expensive as a new line of T cells must be developed for each individual patient (Perica, Varela et al. 2015, Anderson, Stromnes et al. 2017). Additionally, these T cells are still susceptible to the immunosuppressive mechanisms developed by the tumour microenvironment (Figure 2). Activation of cancer associated fibroblasts into an αSMA expressing phenotype results in increased deposition of collagen-rich extracellular matrix which can act as a physical barrier preventing T cells from reaching the tumour, secretion of C-X-C motif chemokine 12 which coats tumour cells and prevents T cell infiltration, increased secretion of pro-inflammatory cytokines that create an immunosuppressive microenvironment by recruiting regulatory T cells and myeloid derived suppressor cells, as well as increasing the expression of programmed cell death ligand 1 (PD-L1) in tumour cells and the cells of the stromal microenvironment (Anderson, Stromnes et al. 2017, Frydenlund and Mahalingam 2017, Pulluri, Kumar et al. 2017). PD-L1 is a membrane-bound protein which serves as a checkpoint of self-identification for the immune system by interacting with programmed cell death protein 1 (PD-1) on T cells to inhibit their activity (Frydenlund and Mahalingam 2017). Melanoma cells expressing high levels of PD-L1 have been shown to provoke fewer anti-tumour immune responses, and the expression of PD-L1 by stromal cells has been hypothesized to contribute to immune resistance as well (Frydenlund and Mahalingam 2017).
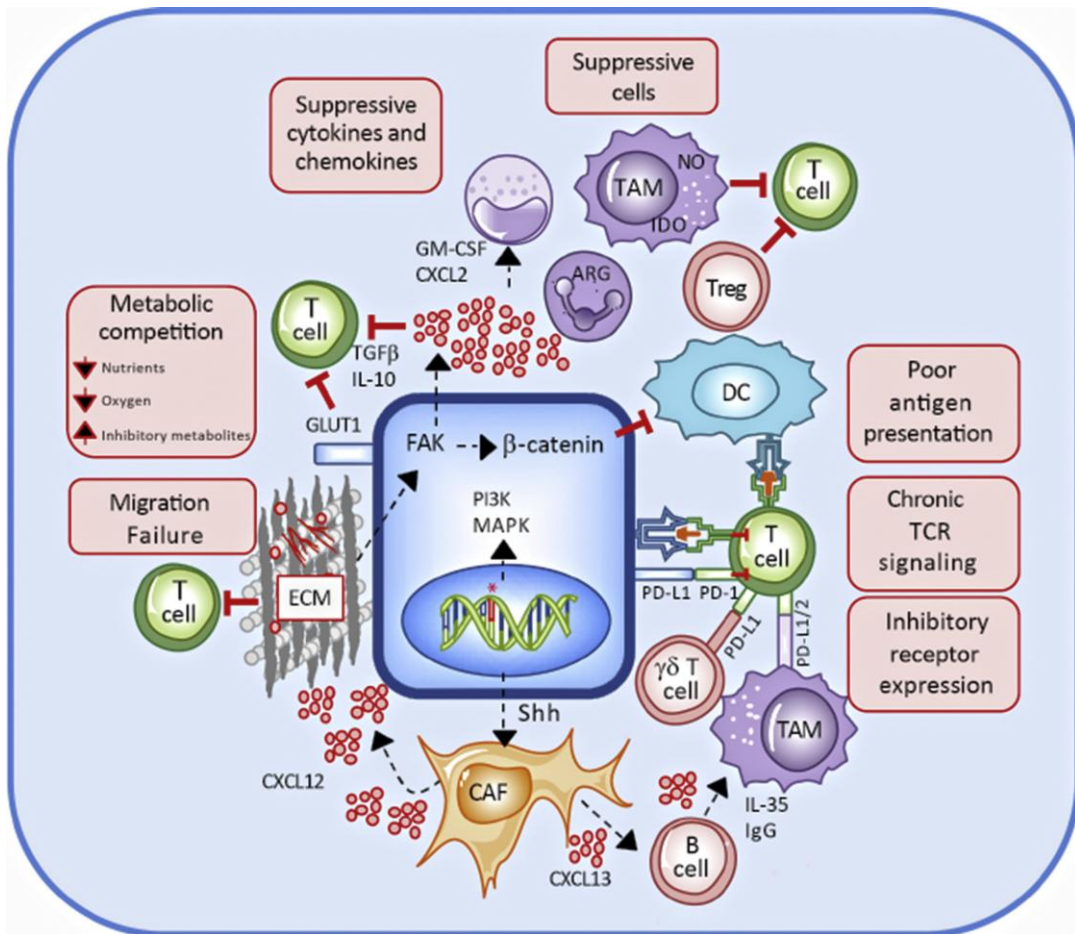
Figure 1-2 Immunosuppressive mechanisms of the activated tumour stroma

Tumour cells activate cancer associated fibroblasts (CAF), which produce a thick extracellular matrix (ECM) and secrete CXCL12 that impede access of the T cells to the tumour. Tumour cells secrete suppressive cytokines and chemokines that reduce the proliferation and activity of T cells, as well as attract suppressive cells like regulatory T cells and Tumour Associated Macrophages. Expression of inhibitory ligands by both tumour and stromal cells reduce T cell activity.

Reprinted from (Anderson, Stromnes et al. 2017)

One method of impairing the immunosuppressive defenses of melanoma has been the inhibition of immune checkpoints like PD-1 or cytotoxic T-lymphocyte associated protein 4 (CTLA-4), a protein that is expressed in response to increased T cell proliferation and reduces immune response (Pulluri, Kumar et al. 2017). While these therapies have shown the capacity to increase overall survival rates of patients with advanced melanoma, they do not show universal efficacy with CTLA-4 antagonist therapies showing a response rate of 15% and PD-1 antagonist therapies showing an approximately 40% response rate (Emens, Ascierto et al. 2017, Pulluri, Kumar et al. 2017). These low response rates are likely due to the fact that T cells targeted by these inhibitors are still subject to the immunosuppresive mechanisms detailed above (Anderson, Stromnes et al. 2017). Additionally, immune checkpoint inhibitors are expensive, with treatments potentially costing hundreds of thousands of dollars per patient per year (Frydenlund and Mahalingam 2017).

1.1.3.3   Anti-angiogenic therapies

As avascular tumours are theoretically limited in size to ~2mm^3, the development of therapies that disrupt the vascular networks of tumours held great promise to not only limit the growth of smaller tumours, but also cause regression of larger lesions (Zaki, Basu et al. 2012, Maj, Papiernik et al. 2016). In light of this, a large variety of anti-angiogenic therapies have been developed, most of which fall into three major categories: monoclonal antibodies attacking the VEGF pathway (either anti-VEGF or anti-VEGFR), decoy receptor VEGF-trap peptides, or small molecule tyrosine kinase inhibitors (Maj, Papiernik et al. 2016). Despite effective inhibition of VEGF signaling resulting from these therapies, no study has shown a significant increase in overall survival from anti-angiogenic monotherapy (Felcht and Thomas 2015, Maj, Papiernik et al. 2016). Additionally, while anti-VEGF therapy combined with chemotherapy in colorectal cancer shows an increase in progression-free survival, different trials showed mixed results for overall survival (Maj, Papiernik et al. 2016). Tumours exhibit two different patterns of anti-angiogenic therapies: Intrinsic resistance, where the tumour fails to respond to therapy immediately, or acquired resistance, where there is an initial response to therapy

followed by a resurgence of tumour growth and progression (Bergers and Hanahan 2008, Lupo, Caporarello et al. 2016, Maj, Papiernik et al. 2016).

The reasons the therapies fail are multi-factorial, with most intrinsic resistance stemming from preexisting oncogenic activation of non-VEGF reliant pro-angiogenic pathways, the presence of inflammatory cell-mediated protection of vasculature, and vascular co-option while acquired resistance is typically driven by new activation of alternative (VEGF-independent) pro-angiogenic pathways, compensatory vasculogenic mimicry and vascular co-option, increased progenitor cell recruitment from bone marrow, and vascular normalization (Bergers and Hanahan 2008, Pastushenko, Vermeulen et al. 2014, Felcht and Thomas 2015). In addition, even when the treatment is successful, long-term hypoxia in the tumour increases genetic instability, vascular permeability, and triggers paradoxically increased VEGF production (Lupo, Caporarello et al. 2016).

In preclinical data using a pancreatic neuroendocrine cancer model, mice that were subjected to anti-VEGFR inhibition experienced a brief period of responsiveness to therapy before tumours began to regrow (Bergers and Hanahan 2008). During tumour regression, these tumours had regions of hypoxia which began to express high levels of pro-angiogenic factors Fibroblast Growth Factor 1 (FGF1), FGF2, ephrin A1, ephrin A2, and angiopoeitin 1, and the treatment of these tumours with an FGF-trap protein was able to slow revascularization and tumour regrowth indicating that FGF is one part of the mechanism by which these tumours acquire resistance to anti-angiogenic therapies (Bergers and Hanahan 2008). Other studies have found similar pro-angiogenic factors upregulated, with anti-VEGF therapies in human patients resulting in increased expression of placental growth factor, FGF2, and interleukin 8 as well as persistent upregulation of mTOR signaling (Maj, Papiernik et al. 2016). Additionally, untreated late stage breast cancers show an increased tolerance for anti-VEGF therapy as well as elevated expression of pro-angiogenic factors like FGF2, suggesting that in addition to playing a role in acquired resistance these pathways are able to be activated and grant intrinsic resistance as well (Bergers and Hanahan 2008). Similarly, in experiments performed using anti-VEGF therapies in mouse models a heterogeneous response to treatment was seen, where tumours with high levels of infiltrating inflammatory cells

prior to treatment showed a reduced response, likely due to pro-angiogenic factors being secreted by the inflammatory cells (Bergers and Hanahan 2008).

Another barrier to effective inhibition of angiogenesis in tumours stems from the fact that sprouting and maturation are driven by competing signals: When VEGF is overexpressed, a tumour will develop a large number of blood vessels, but this VEGF expression will prevent the association of perivascular cells like pericytes which drive vessel stability and maturation (Maj, Papiernik et al. 2016). When anti-VEGF therapies block this overexpression, the vessels which have already been formed begin to recruit perivascular cells and undergo a process known as vessel normalization, which leads to increased vascular organization, decreased vessel permeability, increased vessel diameter, and more reliable delivery of nutrients throughout the tumour (Helfrich and Schadendorf 2011, Maj, Papiernik et al. 2016). Since the association of perivascular cells protects these newly normalized vessels from anti-VEGF therapy-associated regression, it also explains why tumours in highly vascularized tissues such as brain metastases and cutaneous melanomas are more able to withstand anti-angiogenic therapies: A significant portion of their vascular networks are formed by vascular co-option, in which they hijack already mature vasculature which do not undergo regression when deprived of VEGF (Felcht and Thomas 2015).

Anti-angiogenic therapies have also been associated with high levels of side-effects. Complications from anti-VEGF antibody therapies include endocrine dysfunction, cardiac toxicity, gastrointestinal perforation, thrombosis, and impaired wound healing with tyrosine kinase inhibitors also showing malaise, fatigue, hypothyroidism, and cardiac failure due to off-target kinase inhibition (Lupo, Caporarello et al. 2016, Maj, Papiernik et al. 2016). Additionally, even in cases where the therapy is successful in causing vascular regression it is possible that both antibody therapy and tyrosine kinase inhibitors may promote metastasis by damaging vascular walls that normally serve as a barrier to extravasation while simultaneously inducing a more invasive tumour cell phenotype (Bergers and Hanahan 2008, Lupo, Caporarello et al. 2016).

1.2   Tumour-host interactions

As a tumour develops it not only alters the cells carrying oncogenetic mutations, but also begins to recruit host tissue cells to form an active stroma that participates in the development and progression of the disease (Le Bitoux and Stamenkovic 2008). As the tumour grows it begins to secrete cytokines that recruit and activate several different cells types which develop into macrophages, mast cells, adipocytes, and carcinoma-associated fibroblasts which begin to secrete cytokines, disrupt existing extracellular matrix, and deposit new extracellular matrix in a fashion that can play a significant role in the progression of the disease (Le Bitoux and Stamenkovic 2008).

1.2.1   Skin

While melanoma can arise from any pigmented tissue in the body, including mucous membranes and the eye, the most common site for it to develop is the skin. Skin is composed of four major layers: The epidermis, the dermis, a basement membrane that separates them, and finally the hypodermis (Kanitakis 2002). Each of these is further subdivided, and most melanomas arise from the epidermis.

1.2.1.1   The Epidermis

The epidermis serves as a barrier to protect the body from dehydration, toxins, mechanical perturbation, and microorganism intrusion. In order to serve this purpose it is avascular, stratified, and composed of four layers of epithelium which undergo considerable transformation as they move from deep to superficial tissue (Simpson, Patel et al. 2011).

1.2.1.1.1   Keratinocytes

The most common cells in the epidermis, keratinocytes (and the corneocytes to which they will eventually differentiate), are produced in the stratum basale which is a single layer of cells attached to the basement membrane between the epidermis and the dermis (Kanitakis 2002). This layer of cells is composed of proliferating stem cells which proliferate asymmetrically, with the daughter cell deeper in the tissue remaining a stem cell and the superficial one being a keratinocyte which becomes part of the stratum

spinosum (Kanitakis 2002, Proksch, Brandner et al. 2008). The cell polarity that allows this asymmetry of proliferation is possible because of the strong attachment to the basement membrane by hemidesmosomes (Kanitakis 2002, Simpson, Patel et al. 2011).

As keratinocytes differentiate off of the proliferating stem cells of the stratum basale, they begin a process of differentiation which begins with large, polygonal cells with a distinct nucleus and organelles and ends with completely squamous cells lacking both nuclei and organelles (Simpson, Patel et al. 2011). This process progresses as the keratinocytes move through each of the layers of the epidermis. Keratinocytes of the stratum spinosum stop proliferating, are connected to each other by a strong network of intracellular connections, and form a 5-15 cell thick layer. Cells are pushed superficially by continually proliferating stem cells in the stratum basale, and as they move superficially they are subjected to gradually increasing calcium concentrations which eventually trigger differentiation (Bikle, Jiang et al. 2016). These differentiating cells begin to produce lamellar bodies, which will eventually help form a barrier to hydrophilic substances that helps prevent water loss through the skin (Kanitakis 2002, Proksch, Brandner et al. 2008). As calcium continues to increase and the cells enter the stratum granulosum, the lamellar bodies move from the Golgi where they are produced, and fuse with the plasma membrane to release their contents into the extracellular matrix (Proksch, Brandner et al. 2008). While this process occurs the keratinocytes begin to flatten out, and form a layer 1-3 cells thick (Kanitakis 2002). Finally, in the stratum corneum the cells differentiate from keratinocytes into corneocytes by degrading their major organelles with lysosomal enzymes (Simpson, Patel et al. 2011). This layer is composed of highly squamous cells which are crosslinked together in order to form the primary barrier against chemicals and microbes, as well as allowing the cells to withstand mechanical forces (Proksch, Brandner et al. 2008, Simpson, Patel et al. 2011).

1.2.1.1.2   Melanocytes

While 90-95% of cells within the epidermis are keratinocytes, there are several other important cell types present throughout. Langerhans cells are present throughout the epidermis, and within the stratum basale there are Merkel cells, lymphocytes, and melanocytes (Kanitakis 2002). In most areas of the skin the stratum basale is made up of

a 1:10 ratio of melanocytes to proliferating stem cells. Melanocytes are anchored to the basement membrane, with dendrites extending up through the epidermis to form an associated epidermal-melanin unit each consisting of a single melanocytes making contact with 30-40 keratinocytes (Kanitakis 2002, Cichorek, Wachulska et al. 2013). The epidermal-melanin unit has several important functions, with keratinocytes receiving protection from UV irradiation from the melanin secreted by melanocytes and with keratinocytes using both paracrine signaling and cell-cell adhesions with melanocytes to regulate melanocytes proliferation (Haass, Smalley et al. 2005, Cichorek, Wachulska et al. 2013). While in the epidermis melanocytes typically do not proliferate. This is believed to be in large part due to cell-cell adhesions with keratinocyte progenitor cells suppressing proliferation, as melanocytes grown *in vitro* display proliferative capacity that is suppressed when co-cultured with undifferentiated keratinocyte progenitors (Cichorek, Wachulska et al. 2013, Wang, Fukunaga-Kalabis et al. 2016). Due to this lack of proliferation, combined with an accumulation of reactive oxygen species most humans show a 10-20% decrease in number of epidermal melanocytes per decade over the age of 30, with older melanocytes becoming larger and more dendritic to reach more keratinocytes (Cichorek, Wachulska et al. 2013).

In addition to control by cell-cell contact, keratinocytes can exert control over melanocytes through paracrine signaling. This method of control is typically associated with exposure of keratinocytes to UV radiation, which causes secretion of stem cell factor, endothelin 1, and pro-inflamatory cytokines like interleukin 1 (Cichorek, Wachulska et al. 2013, Wang, Fukunaga-Kalabis et al. 2016). These factors serve to activate several signal transduction pathways, with stem cell factor activating mitogen-activated protein kinases and endothelin 1 activating protein kinase C to increase transcription of genes associated with melanocyte dendricity and melanogenesis, and interleukin 1β upregulating melanocytes expression of CCN3 which acts in an autocrine fashion to enhance adhesion to the basement membrane of the epidermis (Cichorek, Wachulska et al. 2013, Wang, Fukunaga-Kalabis et al. 2016). Melanocytes also receive paracrine signals from dermal fibroblasts, who secrete stem cell factor and neuroregulin 1 to help alter melanocytes function (Cichorek, Wachulska et al. 2013).

In addition to being found throughout the stratum basale, melanocytes can also be found in hair follicles, mostly at the apex of the dermal papilla and in the sebaceous glands associated with hair (Cichorek, Wachulska et al. 2013). Here melanocytes are found in higher numbers, with a ratio that is usually closer to 1:5 than the 1:10 ratio found in most of the epidermis (Haass and Herlyn 2005, Cichorek, Wachulska et al. 2013). While they undergo a lot of the same processes, there are several key differences between melanocytes found in the follicle. Unlike epidermal melanocytes there is considerable turnover in follicular melanocytes, with all fully differentiated melanocytes undergoing apoptosis every 3-8 years and being replaced by resident melanoblasts located superficially in the follicle. Additionally, their melanogenesis is regulated independently of UV exposure, with melanogenesis only taking place during the anagen phase when hair is growing, and not during catagen or telogen phases where there is little to no growth (Cichorek, Wachulska et al. 2013).

Between the epidermis and the dermis is the basement membrane, which is composed of 4 layers: First is a layer of keratin and plectin attached to the basal plasma membrane of keratinocyte progenitor cells and melanocytes by hemidesmosomes, second is anchoring filaments composed of laminins, third is a the lamina densa which is composed of collagen IV and laminin V, and finally is the sub-basal lamina filamentous zone composed of collagen VII fibres anchoring the basement membrane to the dermis (Kanitakis 2002, Proksch, Brandner et al. 2008).

1.2.1.2   The Dermis

The dermis is a vascularized region composed primarily of large amounts of extracellular matrix, fibroblasts, and macrophages (Kanitakis 2002). It is divided into two layers: the papillary dermis, which lies just below the basement membrane and is named for fingerlike dermal papillae it forms in order to increase surface area of attachment with the basement membrane, and the reticular dermis (Kanitakis 2002). The papillary dermis consists of loose connective tissue that supports capillary networks which deliver oxygen and nutrients to both the dermis and the epidermis, as well as tactile sensors, while the reticular dermis is characterized by thicker connective tissue which provides strength to the dermis, and the presence of larger blood vessels which feed the capillaries of the

papillary dermis (Kanitakis 2002, Oosterhoff, Sluijter et al. 2012). The reticular dermis also houses the roots of hair follicles, along with sebaceous and sweat glands (Kanitakis 2002). The vast majority of the mass of the dermis is made up of collagen fibres (mainly types I and III) with 90% of the fibres being collagen, providing the dermis with a high tensile strength (Kanitakis 2002, Arora, Falto-Aizpurua et al. 2017). In addition to collagen, elastin and elastic fibres are present (mostly in the reticular dermis), making up another 2-4% of the dermis by mass, with the rest being composed of cells and a mixture of glycoproteins and proteoglycans known as ground substance (Kanitakis 2002, Arora, Falto-Aizpurua et al. 2017). The extracellular matrix of the dermis is undergoing constant maintenance and has a high rate of turnover, with the synthesis of new connective tissue being conducted by spindle shaped cells called fibroblasts (Kanitakis 2002, McAnulty 2007). Fibroblasts regulate the extracellular matrix of the dermis by producing matrix metalloproteinases, which degrade extracellular matrix components, and by producing the majority of extracellular matrix components themselves (McAnulty 2007). In addition to their role in maintaining healthy extracellular matrix, fibroblasts are also key players in responding to tissue injury. When tissue is damaged, cytokines are released that recruit fibroblasts to the wound to assist in deposition of new extracellular matrix and they are activated into a myofibroblast phenotype that is characterized by expression of α-smooth muscle actin stress fibers which allow them to assist with contraction and closure of the wound (McAnulty 2007).

The deepest section of the skin is known as the hypodermis. It is mostly composed of adipocytes surrounded by loose connective tissue, fibroblasts, nerves, and blood vessels, and it helps with storage of energy, thermoregulation, and protection from mechanical forces (Kanitakis 2002).

1.2.2   Collagen Fibril Assembly

Dermal collagen consists of a little less than 90% type I collagen, 10% type III collagen, and approximately 2% type V collagen (Krieg and Aumailley 2011). Collagens are transcribed and synthesized as α chains of procollagen monomers before undergoing extensive post-translational modifications in the rough endoplasmic reticulum and Golgi

apparatus involving the hydroxylation of specific prolyl and lysyl residues and glycosylation of others (Kadler, Baldock et al. 2007, Krieg and Aumailley 2011). Prolyl hydroxylation is required for each monomer to fold into a left-handed helix, at which point three α chain monomers supercoil into a right-handed triple helix, which is then stabilized with hydrogen bonds inside the rough endoplasmic reticulum (Mienaltowski and Birk 2014, Bella 2016). Once this triple helix is properly formed the collagen molecules are released from the endoplasmic reticulum and can enter the extracellular space (Kadler, Baldock et al. 2007). Once outside the cell the collagen molecules can be formed into fibrils through numerous mechanisms: They can self-assemble around nucleators, they can be directed to assemble by cell-directed organizers, and their growth can be controlled by regulator molecules and enzymes (Mienaltowski and Birk 2014, Du, Pang et al. 2017).

While type I and type III collagen can self-assemble *in vitro*, it is only after considerable lag and is not seen to occur *in vivo*, where despite production and secretion of type I and III collagen molecules, they do not form into fibrils without type V collagen to act as a nucleator (Mienaltowski and Birk 2014). In concert with nucleators, cells can direct the assembly of fibrils by assembling fibronectin into fibrils using integrins, forming fibronectin networks that contain binding sites that assist with collagen fibril assembly (Mienaltowski and Birk 2014). Blocking the fibronectin binding sites, or alteration of integrins that assemble the fibronectin organizer complex, can result in alterations to collagen fibril assembly. Regulator molecules like small leucine-rich proteoglycans and some non-fibril forming collagens are not necessary for the initiation of fibril assembly, but can alter the rate at which collagen fibrils grow, and also the characteristics that result from growth. Disruption of these regulators can result in abnormally large fibril diameters which have functional defects (Mienaltowski and Birk 2014).

Once fibrils have begun to form, their maturation into a stable network is governed by a balance of enzymatic activity. Fibrils are stabilized by the formation of intramolecular and intermolecular cross-links after oxidative deamination by a class of enzymes called lysyl oxidases, and hydroxylation by lysyl hydroxylases (Krieg and Aumailley 2011). The key enzyme in mediating the hydroxylation of lysyl residues in type I collagen is

lysyl hydroxylase 2, which is encoded by the gene *PLOD2,* with decreased levels of *PLOD2* expression in tumour stroma correlating with decreased lysine aldehyde-derived crosslinks (Du, Pang et al. 2017). Additionally the extent of lysyl residue hydroxylation can have effects on the circumference of the triple helical domain of collagens, resulting in changes in fibril assembly (Mienaltowski and Birk 2014). Once collagen networks are formed, matured, and stabilized they can be remodeled by the activity of matrix metalloproteinases MMP1 and MMP13 (Krieg and Aumailley 2011, Moro, Mauch et al. 2014).

1.2.3   Fibrosis: Cancer as a wound that won't heal

When tissue experiences an injury or insult it goes through several stages in attempting to resolve the damage: Hemostasis (when the injury has caused bleeding), Inflammation, Proliferation of new tissues, and finally Remodelling of the newly formed tissue (Buganza Tepole and Kuhl 2013). In the case of cancer, however, the insult is not easily resolved by these processes, and so the cancer cells persist, stimulating a wound healing response that is unable to resolve (Horimoto, Polanska et al. 2012, Kalluri 2016). This results in sustained inflammation, and the recruitment of a wide variety of cells to form an activated stroma, similar to what occurs in fibrotic diseases like scleroderma. In fact, activated tumour stroma and fibrosis are both characterized by high numbers of activated fibroblasts and an increased deposition of extracellular matrix (Kalluri 2016). The link between cancer and fibrosis is reinforced by the fact that co-morbidity of cancer and scleroderma has been show to occur quite frequently with the incidence of melanoma being 3.3 times as high among patients diagnosed with scleroderma as among the general population (Videtic, Lopez et al. 1997, O'Byrne and Dalgleish 2001, Coussens and Werb 2002, Hill, Nguyen et al. 2003, Shah, Rosen et al. 2010, Franks and Slansky 2012). In addition to this increased incidence, there is a notable temporal proximity between diagnoses of cancer and fibroproliferative diseases, with almost 50% of breast cancer diagnoses amongst scleroderma patients occurring very close to the diagnoses of scleroderma itself (Shah, Rosen et al. 2010). There is considerable debate as to what is causing this increased association of not only the incidence, but also time of onset between cancer and fibroproliferative diseases. One theory is that the overactive

fibroproliferative processes in diseases such as scleroderma not only lay down excessive extracellular matrix which can lead to organ failure, but they also produce a tumour stroma which is conducive to the progression of malignancy (O'Byrne and Dalgleish 2001, Rakoff-Nahoum 2006). Additionally, the inflammatory cascade produced by an initial injury or insult produces high amounts of oxidative stress, resulting in the production of reactive oxygen species that not only perpetuate the inflammatory cascade but also cause DNA damage leading to DNA breaks, single base mutations, and genomic instability which are known to lead to tumourigenesis (Le Bitoux and Stamenkovic 2008, Elinav, Nowarski et al. 2013). Cytokines like tumour necrosis factor α, interleukin 1β, and transforming growth factor (TGF)β1, that are elevated in the fibrotic microenvironment, trigger signaling cascades that introduce mutations in the genes encoding p53 and Myc which contribute to oncogenesis (Elinav, Nowarski et al. 2013). These cytokines also induce nuclear factor-κB signaling, which increases pro-inflammatory, proliferative, and survival gene expression from both tumour and stromal cells (Le Bitoux and Stamenkovic 2008, Kalluri 2016).

Once oncogenesis has occurred, a diverse tumour stroma is recruited, most importantly including the recruitment of immune cells and the recruitment and activation of activated cancer associated fibroblasts (CAFs) (Le Bitoux and Stamenkovic 2008, Horimoto, Polanska et al. 2012, Kalluri 2016). Recruited immune cells play several roles, with activated macrophages producing cytokines to increase inflammatory signaling throughout the stroma, recruit additional immune cells like leukocytes, inhibit immune response, increase pro-angiogenic signaling, and promote gene expression associated with survival (Le Bitoux and Stamenkovic 2008). Additional immune cells recruited by macrophages serve to amplify the signals secreted by macrophages, activate resident fibroblasts, and secrete proteolytic enzymes which can reduce physical barriers to tumour spread and cause the release of sequestered growth factors from the extracellular matrix (Le Bitoux and Stamenkovic 2008, Horimoto, Polanska et al. 2012).

The activated fibroblasts of the tumour stroma have proven to be key drivers in the progression of many different cancers. CAFs induce invasion of non-invasive cells in

many cancer models by secreting matrix metalloproteinases, which help remodel stromal matrix to increase stiffness and align extracellular matrix components to facilitate invasion, and TGFβ, allowing improved adhesion of cancer cells to the extracellular matrix: CAFs have also been shown to be highly migratory (Horimoto, Polanska et al. 2012, Kalluri 2016). Additionally, CAFs secrete tenascin C and periostin, which have both been shown to be mediators of the development of a "cancer stem cell" phenotype that is able to take root in distant organs after metastasis and form metastatic sites (Horimoto, Polanska et al. 2012). CAFs are a highly heterogeneous population: although there are several markers which are absent in inactivated normal fibroblasts, such as fibroblast specific protein 1, vimentin, α-smooth muscle actin, PDGF receptor α and β, these markers are neither exclusive to activated fibroblasts, nor expressed by all cancer associated fibroblasts (Kalluri 2016). For example, fibroblast specific protein 1 also identifies immune cells, vimentin is expressed widely in mesenchymally-derived cells, and PDGF receptors are also present in the perivasculature (Kalluri 2016). This heterogeneous pattern of marker expression pattern may simply reflect that CAFs are likely to originate from a variety of different sources. Indeed, CAFs have been suggested to arise from bone marrow-derived precursors, mesenchymal stem cells, endothelial cells, resident fibroblasts, epithelial cells, pericytes, smooth muscle cells, and adipocytes (Bhattacharyya, Wei et al. 2012, Horimoto, Polanska et al. 2012, Kalluri 2016). In fibrotic diseases, recruitment and proliferation of these cell types has been induced inflammatory cytokines, and differentiation has been seen to be caused by several different mechanisms. Resident fibroblasts can be differentiated in to myofibroblasts by TGFβ1 signaling or by mechanical strain being transduced through integrins (Koivisto, Heino et al. 2014). Blocking integrins $\alpha_v\beta_5$ or $\alpha_v\beta_3$ *in vitro* is able to prevent this differentiation, as is deletion if integrin β1 *in vivo* (Liu, Xu et al. 2010, Koivisto, Heino et al. 2014). The protein Phosphatase and tensin homolog (PTEN), which inactivates pro-adhesive signaling and is frequently mutated in cancers, can suppress myofibroblast differentiation of resident fibroblasts and loss of PTEN not only accelerates cancer progression, but when it is deleted from fibroblasts *in vivo* it results in spontaneous

generation of fibrosis (Horimoto, Polanska et al. 2012, Parapuram, Thompson et al. 2015). Damage to microvasculature has also been seen to cause pericyte differentiation into myofibroblasts in patients with scleroderma, and in mouse models of fibrosis myofibroblasts were observed to express pericyte/progenitor marker genes NG2 and SOX2 (Rajkumar, Sundberg et al. 1999, Tsang and Leask 2015). Additionally, lineage tracing revealed some fibrotic myofibroblasts are derived from dermal progenitor cells, and the process requires expression of matricellular protein CCN2 which is highly upregulated in fibrotic diseases (Liu, Herault et al. 2014, Tsang and Leask 2015).

1.2.4   Tumour vascularization

Tumour vascularization is essential for the progression, growth, and metastasis of any tumour. Since oxygen can only diffuse approximately 100-150µm through tissue avascular tumours are limited in the maximum size they can achieve (Felcht and Thomas 2015). While it has been estimated that an avascular tumour can reach up to 2-3mm^3 in volume, vascularization typically begins when a tumour reaches approximately 1mm^3, or the distance between two blood vessels is larger than 100-250µm (Helfrich and Schadendorf 2011, Zaki, Basu et al. 2012). As tumours grow, they develop regions of hypoxia which are either too far removed from vasculature, or which have had their blood supply cut off when the vessels feeding them are occluded by the growing tumour (Muz, de la Puente et al. 2015). Intratumoural hypoxia alters the balance between pro- and anti-angiogenic signals, primarily by signaling through the Hypoxia Inducible Factor (HIF) pathway, triggering what is known as the "Angiogenic Switch" when pro-angiogenic signals are stronger than anti-angiogenic signals (Helfrich and Schadendorf 2011, Muz, de la Puente et al. 2015). This balance can also be altered by other factors like mechanical stress, inflammation, or genetic mutation (Helfrich and Schadendorf 2011). Once this switch is flipped, there are 4 major forms of neovascularization that take place within a tumour: sprouting angiogenesis, vascular co-option (where the tumour will simply grow around an existing vessel and thus hijack it), vasculogenic mimicry and mosaic vessels, and bone marrow-derived vasculogenesis (Pastushenko, Vermeulen et al. 2014, Felcht and Thomas 2015).

1.2.4.1   Mechanisms of neovascularization

Sprouting angiogenesis is a recapitulation of the angiogenesis that occurs during development and wound healing in which the growth of new capillaries occurs starting from existing vessels (Pastushenko, Vermeulen et al. 2014). Although there are many factors that can trigger this process, the most predominant one is VEGF secretion from the tumour. Not only does HIF signaling induce VEGF expression, but several oncogenes can cause constitutive overexpression of VEGF by the tumour through MEK activation, PI3K activation, NFκB activation, and ROS production (Pastushenko, Vermeulen et al. 2014, Muz, de la Puente et al. 2015). When VEGF reaches the endothelial cells of a blood vessel, it causes them to reduce their cell-cell contacts (which help to keep endothelial cells quiescent and non-proliferative) with each other, increase their mitogenesis, proliferation, survival, and migration signals (Zaki, Basu et al. 2012, Mongiat, Andreuzzi et al. 2016). Once these cell junctions loosen, there is extravasation of plasma proteins, which help serve as a scaffold for endothelial cell migration and organization, and the initiation of a proteolytic cascade involving matrix-metalloproteases, which degrade both the basement membrane of the existing vessel and the extracellular matrix between the endothelial cells and the source of VEGF secretion resulting in both a path for endothelial cells to migrate through and release of bound pro-angiogenic factors (Zaki, Basu et al. 2012, Pastushenko, Vermeulen et al. 2014, Mongiat, Andreuzzi et al. 2016). As the process progresses endothelial cells will migrate in a specific pattern, with a polarized tip cell breaking off to migrate across the extracellular matrix, followed by some rapidly proliferating stalk cells which will begin to form the lumen of the new vessel, and lastly phalanx cells which have recruited perivascular cells, like pericytes, through secretion of Transforming Growth Factor β, and PDGF to help mature and stabilize them (Helfrich and Schadendorf 2011, Pastushenko, Vermeulen et al. 2014, Felcht and Thomas 2015, Muz, de la Puente et al. 2015). The expression of Angiopoietin-1 by perivascular cells binds to Tie-2 receptors on endothelial cells, inducing quiescence (Helfrich and Schadendorf 2011).

In addition to sprouting angiogenesis melanoma makes great use of vascular co-option, (Pastushenko, Vermeulen et al. 2014, Felcht and Thomas 2015). Vascular co-option is

more prevalent in melanoma than some other cancers (for example breast cancer tends to grow primarily through sprouting angiogenesis) and while this process occurs in the primary tumour, it is especially prevalent in distant metastatic sites where the freshly extravasated melanoma cells will grow around the existing vasculature (Felcht and Thomas 2015). These newly co-opted vessels are typically more mature and stable than newly formed vasculature within the tumour (Helfrich and Schadendorf 2011).

Both sprouting angiogenesis and vascular co-option are ways in which the tumour can incorporate endothelial cells into its vascular network, but when that process proves insufficient to meet nutrient and waste disposal needs of rapidly proliferating cells the tumour can begin to reprogram its own cells to serve the same purpose in a process known as vasculogenic mimicry (Pastushenko, Vermeulen et al. 2014, Felcht and Thomas 2015). Vessels created by vasculogenic mimicry can either be tube structures composed of either reprogrammed tumour cells or a mixture of endothelial cells and tumour cells which closely resemble normal endothelial lined blood vessels, or they can be patterned matrices consisting of collagens, heparin sulfate proteoglycans and laminins that closely resemble the basement membrane of a blood vessel but which lack any cellular lining (Pastushenko, Vermeulen et al. 2014, Pinto, Sotomayor et al. 2016). In either case the melanoma cells lining them begin to express markers that are characteristic of endothelial cells, such as CD31 or vascular endothelial (VE)-cadherin (Pinto, Sotomayor et al. 2016). Additionally, both tubular and non-tubular examples of vasculogenic mimicry have been shown to stain positive for periodic-acid Schiff (PAS) stain, and contain red blood cells in histological sections, indicating that they are both successful at conducting blood throughout the tumour (Pastushenko, Vermeulen et al. 2014, Pinto, Sotomayor et al. 2016).

Finally, new vasculature can be generated by recruitment of bone marrow-derived progenitor cells which will be integrated into new vessels and differentiated into endothelial cells by VEGF signaling (Pastushenko, Vermeulen et al. 2014, Felcht and Thomas 2015, Muz, de la Puente et al. 2015). Several factors secreted by both tumour and stromal components have been identified in the recruitment process, including

VEGF, stromal derived factor-1, placental growth factor, stem cell factor, and interleukin-6 (Bergers and Hanahan 2008, Maj, Papiernik et al. 2016).

1.2.4.2 Tumour vascular environment

Despite the formation of new vasculature, the oxygenation of intratumoural tissue is far from consistent. Due to high levels of VEGF secretion by tumour cells, highly heterogeneous makeup of vasculature, and periodic blood vessel occlusion tumours contain areas of acute, chronic, and cycling hypoxia (Helfrich and Schadendorf 2011, Muz, de la Puente et al. 2015)

Tumour hypoxia can come in three major forms, with different consequences for each: acute hypoxia is a short term interruption in blood flow that is generally resolved in less than 72 hours and triggers autophagy to allow cells to survive, induces spontaneous metastasis and a more invasive phenotype; chronic hypoxia is a sustained state of low oxygen availability which impairs DNA repair systems and increases accumulation of DNA damage, leading to increased genomic instability and mutagenesis; cycling hypoxia is frequently caused by short-term occlusion of blood vessels, and results in recurring fluctuations in tissue oxygen levels which has been shown to increase reactive oxygen species production, and increase tumour cell survival and aggressiveness (Muz, de la Puente et al. 2015, Lupo, Caporarello et al. 2016).

In addition to occlusion of vasculature, hypoxia can result from the disorganized and largely immature vasculature found within a tumour. While high levels of VEGF secretion by tumour cells is helpful in generating new vasculature, it does not subside when the new vasculature has been established, and so the normal blood vessel phenotype that includes pericytes instructing endothelial cells to form tight junctions to prevent fluid leak does not occur: Continuous VEGF expression acts on endothelial cells preventing them from entering their quiescent state, and prevents pericyte coverage of vessels by disrupting PDGF signaling (Greenberg, Shields et al. 2008, Helfrich and Schadendorf 2011). Additionally, this non-quiescent endothelial cell phenotype results in increased vascular permeability, which increases intra-tumoural interstitial pressure and augments hypoxia (Zaki, Basu et al. 2012).

1.2.5   CCN Proteins

The CCN proteins are a family of matricellular proteins named for the first three members (**C**YR61, **C**TGF, and **N**OV) characterized by a highly conserved modular structure consisting of an insulin-like growth factor binding domain, a Von Willebrand factor type C domain, a thrombospondin type 1 domain, and a C-terminal domain (Leask and Abraham 2006). Matricellular proteins are non-structural, secreted proteins that modulate cellular reactions to external stimuli, and as such the CCN proteins are highly spatiotemporily regulated (Leask and Abraham 2006, Jun and Lau 2011). Their activity is primarily mediated through direct binding to adhesion receptors like integrins and heparin sulphate proteoglycans (HSPGs), but they can also bind to other receptors like lipoprotein receptor-related proteins (LRPs) and modulate the expression and bioavailability of a wide variety of growth factors, cytokines and matrix metalloproteinases (Chen and Lau 2009, Jun and Lau 2011). CCN protein expression is sensitive to signals from growth factors, UV radiation, hypoxia, mechanical forces, and inflammatory cytokines, allowing them to be regulated in response to a wide variety of stimuli (Chen and Lau 2009). Each protein's function is highly context dependent: CCN1, CCN2, and CCN3 promote apoptosis in fibroblasts when bound as cell adhesion substrates, but when they bind to endothelial cells they serve as protection against apoptosis due to different integrin expression patterns between the cell types (Chen and Lau 2009, Jun and Lau 2011). CCN1-3 are pro-angiogenic *in vivo*, and promote cell adhesion, migration, proliferation, and tubule formation of endothelial cells *in vitro* (Leask and Abraham 2006). Given these pro-angiogenic roles it is unsurprising that CCN1 is required for the formation of a cardiovascular system during embryonic development, and mice lacking CCN2 display severe vascular defects (Jun and Lau 2011, Mongiat, Andreuzzi et al. 2016).

CCN1 and CCN2 are upregulated in wound healing, with CCN2 being released from platelets and both CCN1 and CCN2 being transcriptionally upregulated in response to TGFβ signaling. During wound healing they act as adhesion substrates for platelets and inflammatory cells, as well as modulating TGFβ activity on fibroblasts and unmasking

the cytotoxic effects of TNFα to facilitate the apoptosis of fibroblasts (Jun and Lau 2011).

Both CCN1 and CCN2 are also highly upregulated during fibrosis, but while CCN1 and CCN2 have been shown to have similar functions *in vitro*, it has been proposed that they have different functions *in vivo*, with CCN1 inducing a senescence-like phenotype in while CCN2 potentiates TGFβ signaling (Leask and Abraham 2006, Jun and Lau 2011). CCN2 expression in fibroblasts is essential for the development of fibrosis, and mice with *Ccn2* deleted from their fibroblasts are resistant to both bleomycin-induced skin fibrosis and PTEN deficiency-induced fibrosis (Liu, Shi-wen et al. 2011, Liu, Parapuram et al. 2013).

Given the similarities between activated tumour stroma and fibrosis, the overexpression of CCN1 and CCN2 during fibrosis, and the pro-angiogenic activities of CCN1 and CCN2, the following study investigates the role of CCN1 and CCN2 in the progression of metastatic melanoma. My hypothesis is that CCN1 and CCN2 play different, but complementary roles in the progression of melanoma, with CCN2 promoting the vascularization of the tumour and facilitating the development of a collagen producing activated stroma, and CCN1 promoting the processing and stabilization of produced collagen.

1.3   References

AJCC. (2017). "8th edition implementation project." 2017, from https://cancerstaging.org/8thEdImplementation/Pages/default.aspx.

Anderson, K. G., I. M. Stromnes and P. D. Greenberg (2017). "Obstacles Posed by the Tumor Microenvironment to T cell Activity: A Case for Synergistic Therapies." Cancer Cell **31**(3): 311-325.

Arora, H., L. Falto-Aizpurua, A. Cortes-Fernandez, S. Choudhary and P. Romanelli (2017). "Connective Tissue Nevi: A Review of the Literature." Am J Dermatopathol **39**(5): 325-341.

Balch, C. M., J. E. Gershenwald, S. J. Soong, J. F. Thompson, M. B. Atkins, D. R. Byrd, A. C. Buzaid, A. J. Cochran, D. G. Coit, S. Ding, A. M. Eggermont, K. T. Flaherty, P. A. Gimotty, J. M. Kirkwood, K. M. McMasters, M. C. Mihm, Jr., D. L. Morton, M. I. Ross,

A. J. Sober and V. K. Sondak (2009). "Final version of 2009 AJCC melanoma staging and classification." J Clin Oncol **27**(36): 6199-6206.

Bella, J. (2016). "Collagen structure: new tricks from a very old dog." Biochem J **473**(8): 1001-1025.

Bergers, G. and D. Hanahan (2008). "Modes of resistance to anti-angiogenic therapy." Nat Rev Cancer **8**(8): 592-603.

Bhattacharyya, S., J. Wei, W. G. Tourtellotte, M. Hinchcliff, C. G. Gottardi and J. Varga (2012). "Fibrosis in systemic sclerosis: common and unique pathobiology." Fibrogenesis Tissue Repair **5**(Suppl 1): S18.

Bikle, D. D., Y. Jiang, T. Nguyen, Y. Oda and C. L. Tu (2016). "Disruption of Vitamin D and Calcium Signaling in Keratinocytes Predisposes to Skin Cancer." Front Physiol **7**: 296.

Buganza Tepole, A. and E. Kuhl (2013). "Systems-based approaches toward wound healing." Pediatr Res **73**(4 Pt 2): 553-563.

Chan, X. Y., A. Singh, N. Osman and T. J. Piva (2017). "Role Played by Signalling Pathways in Overcoming BRAF Inhibitor Resistance in Melanoma." Int J Mol Sci **18**(7).

Chen, C. C. and L. F. Lau (2009). "Functions and mechanisms of action of CCN matricellular proteins." Int J Biochem Cell Biol **41**(4): 771-783.

Cichorek, M., M. Wachulska, A. Stasiewicz and A. Tyminska (2013). "Skin melanocytes: biology and development." Postepy Dermatol Alergol **30**(1): 30-41.

Coussens, L. M. and Z. Werb (2002). "Inflammation and cancer." Nature **420**(6917): 860-867.

Cummins, D. L., J. M. Cummins, H. Pantle, M. A. Silverman, A. L. Leonard and A. Chanmugam (2006). "Cutaneous malignant melanoma." Mayo Clin Proc **81**(4): 500-507.

Davies, H., G. R. Bignell, C. Cox, P. Stephens, S. Edkins, S. Clegg, J. Teague, H. Woffendin, M. J. Garnett, W. Bottomley, N. Davis, E. Dicks, R. Ewing, Y. Floyd, K. Gray, S. Hall, R. Hawes, J. Hughes, V. Kosmidou, A. Menzies, C. Mould, A. Parker, C. Stevens, S. Watt, S. Hooper, R. Wilson, H. Jayatilake, B. A. Gusterson, C. Cooper, J. Shipley, D. Hargrave, K. Pritchard-Jones, N. Maitland, G. Chenevix-Trench, G. J. Riggins, D. D. Bigner, G. Palmieri, A. Cossu, A. Flanagan, A. Nicholson, J. W. Ho, S. Y. Leung, S. T. Yuen, B. L. Weber, H. F. Seigler, T. L. Darrow, H. Paterson, R. Marais, C. J. Marshall, R. Wooster, M. R. Stratton and P. A. Futreal (2002). "Mutations of the BRAF gene in human cancer." Nature **417**(6892): 949-954.

DeLuca, A. M., A. Srinivas and R. M. Alani (2008). "BRAF kinase in melanoma development and progression." Expert Rev Mol Med **10**: e6.

Du, H., M. Pang, X. Hou, S. Yuan and L. Sun (2017). "PLOD2 in cancer research." Biomed Pharmacother **90**: 670-676.

Elinav, E., R. Nowarski, C. A. Thaiss, B. Hu, C. Jin and R. A. Flavell (2013). "Inflammation-induced cancer: crosstalk between tumours, immune cells and microorganisms." Nat Rev Cancer **13**(11): 759-771.

Emens, L. A., P. A. Ascierto, P. K. Darcy, S. Demaria, A. M. M. Eggermont, W. L. Redmond, B. Seliger and F. M. Marincola (2017). "Cancer immunotherapy: Opportunities and challenges in the rapidly evolving clinical landscape." Eur J Cancer **81**: 116-129.

Felcht, M. and M. Thomas (2015). "Angiogenesis in malignant melanoma." J Dtsch Dermatol Ges **13**(2): 125-136.

Franks, A. L. and J. E. Slansky (2012). "Multiple associations between a broad spectrum of autoimmune diseases, chronic inflammatory diseases and cancer." Anticancer Res **32**(4): 1119-1136.

Frydenlund, N. and M. Mahalingam (2017). "PD-L1 and immune escape: insights from melanoma and other lineage-unrelated malignancies." Hum Pathol **66**: 13-33.

Greenberg, J. I., D. J. Shields, S. G. Barillas, L. M. Acevedo, E. Murphy, J. Huang, L. Scheppke, C. Stockmann, R. S. Johnson, N. Angle and D. A. Cheresh (2008). "A role for VEGF as a negative regulator of pericyte function and vessel maturation." Nature **456**(7223): 809-813.

Haass, N. K. and M. Herlyn (2005). "Normal human melanocyte homeostasis as a paradigm for understanding melanoma." J Investig Dermatol Symp Proc **10**(2): 153-163.

Haass, N. K., K. S. Smalley, L. Li and M. Herlyn (2005). "Adhesion, migration and communication in melanocytes and melanoma." Pigment Cell Res **18**(3): 150-159.

Helfrich, I. and D. Schadendorf (2011). "Blood vessel maturation, vascular phenotype and angiogenic potential in malignant melanoma: one step forward for overcoming anti-angiogenic drug resistance?" Mol Oncol **5**(2): 137-149.

Hill, C. L., A. M. Nguyen, D. Roder and P. Roberts-Thomson (2003). "Risk of cancer in patients with scleroderma: a population based cohort study." Ann Rheum Dis **62**(8): 728-731.

Hirata, E., M. R. Girotti, A. Viros, S. Hooper, B. Spencer-Dene, M. Matsuda, J. Larkin, R. Marais and E. Sahai (2015). "Intravital imaging reveals how BRAF inhibition generates drug-tolerant microenvironments with high integrin beta1/FAK signaling." Cancer Cell **27**(4): 574-588.

Homsi, J., M. Kashani-Sabet, J. L. Messina and A. Daud (2005). "Cutaneous melanoma: prognostic factors." Cancer Control **12**(4): 223-229.

Horimoto, Y., U. M. Polanska, Y. Takahashi and A. Orimo (2012). "Emerging roles of the tumor-associated stroma in promoting tumor metastasis." Cell Adh Migr **6**(3): 193-202.

Jun, J. I. and L. F. Lau (2011). "Taking aim at the extracellular matrix: CCN proteins as emerging therapeutic targets." Nat Rev Drug Discov **10**(12): 945-963.

Kadler, K. E., C. Baldock, J. Bella and R. P. Boot-Handford (2007). "Collagens at a glance." J Cell Sci **120**(Pt 12): 1955-1958.

Kalluri, R. (2016). "The biology and function of fibroblasts in cancer." Nat Rev Cancer **16**(9): 582-598.

Kanitakis, J. (2002). "Anatomy, histology and immunohistochemistry of normal human skin." Eur J Dermatol **12**(4): 390-399; quiz 400-391.

Koivisto, L., J. Heino, L. Hakkinen and H. Larjava (2014). "Integrins in Wound Healing." Adv Wound Care (New Rochelle) **3**(12): 762-783.

Krieg, T. and M. Aumailley (2011). "The extracellular matrix of the dermis: flexible structures with dynamic functions." Exp Dermatol **20**(8): 689-695.

Kuphal, S., R. Bauer and A. K. Bosserhoff (2005). "Integrin signaling in malignant melanoma." Cancer Metastasis Rev **24**(2): 195-222.

Le Bitoux, M. A. and I. Stamenkovic (2008). "Tumor-host interactions: the role of inflammation." Histochem Cell Biol **130**(6): 1079-1090.

Leask, A. and D. J. Abraham (2006). "All in the CCN family: essential matricellular signaling modulators emerge from the bunker." J Cell Sci **119**(Pt 23): 4803-4810.

Lim, S. Y., A. M. Menzies and H. Rizos (2017). "Mechanisms and strategies to overcome resistance to molecularly targeted therapy for melanoma." Cancer **123**(S11): 2118-2129.

Liu, S., Y. Herault, G. Pavlovic and A. Leask (2014). "Skin progenitor cells contribute to bleomycin-induced skin fibrosis." Arthritis Rheumatol **66**(3): 707-713.

Liu, S., S. K. Parapuram and A. Leask (2013). "Fibrosis caused by loss of PTEN expression in mouse fibroblasts is crucially dependent on CCN2." Arthritis Rheum **65**(11): 2940-2944.

Liu, S., X. Shi-wen, D. J. Abraham and A. Leask (2011). "CCN2 is required for bleomycin-induced skin fibrosis in mice." Arthritis Rheum **63**(1): 239-246.

Liu, S., S. W. Xu, K. Blumbach, M. Eastwood, C. P. Denton, B. Eckes, T. Krieg, D. J. Abraham and A. Leask (2010). "Expression of integrin beta1 by fibroblasts is required for tissue repair in vivo." J Cell Sci **123**(Pt 21): 3674-3682.

Lupo, G., N. Caporarello, M. Olivieri, M. Cristaldi, C. Motta, V. Bramanti, R. Avola, M. Salmeri, F. Nicoletti and C. D. Anfuso (2016). "Anti-angiogenic Therapy in Cancer: Downsides and New Pivots for Precision Medicine." Front Pharmacol **7**: 519.

Maj, E., D. Papiernik and J. Wietrzyk (2016). "Antiangiogenic cancer treatment: The great discovery and greater complexity (Review)." Int J Oncol **49**(5): 1773-1784.

McAnulty, R. J. (2007). "Fibroblasts and myofibroblasts: their source, function and role in disease." Int J Biochem Cell Biol **39**(4): 666-671.

Mienaltowski, M. J. and D. E. Birk (2014). "Structure, physiology, and biochemistry of collagens." Adv Exp Med Biol **802**: 5-29.

Miller, A. J. and M. C. Mihm, Jr. (2006). "Melanoma." N Engl J Med **355**(1): 51-65.

Mongiat, M., E. Andreuzzi, G. Tarticchio and A. Paulitti (2016). "Extracellular Matrix, a Hard Player in Angiogenesis." Int J Mol Sci **17**(11).

Moro, N., C. Mauch and P. Zigrino (2014). "Metalloproteinases in melanoma." Eur J Cell Biol **93**(1-2): 23-29.

Muz, B., P. de la Puente, F. Azab and A. K. Azab (2015). "The role of hypoxia in cancer progression, angiogenesis, metastasis, and resistance to therapy." Hypoxia (Auckl) **3**: 83-92.

Nesbit, M. and M. Herlyn (1994). "Adhesion receptors in human melanoma progression." Invasion Metastasis **14**(1-6): 131-146.

O'Byrne, K. J. and A. G. Dalgleish (2001). "Chronic immune activation and inflammation as the cause of malignancy." Br J Cancer **85**(4): 473-483.

Oosterhoff, D., B. J. Sluijter, B. N. Hangalapura and T. D. de Gruijl (2012). "The dermis as a portal for dendritic cell-targeted immunotherapy of cutaneous melanoma." Curr Top Microbiol Immunol **351**: 181-220.

Palathinkal, D. M., T. R. Sharma, H. B. Koon and J. S. Bordeaux (2014). "Current systemic therapies for melanoma." Dermatol Surg **40**(9): 948-963.

Parapuram, S. K., K. Thompson, M. Tsang, J. Hutchenreuther, C. Bekking, S. Liu and A. Leask (2015). "Loss of PTEN expression by mouse fibroblasts results in lung fibrosis through a CCN2-dependent mechanism." Matrix Biol **43**: 35-41.

Pastushenko, I., P. B. Vermeulen, G. G. Van den Eynden, A. Rutten, F. J. Carapeto, L. Y. Dirix and S. Van Laere (2014). "Mechanisms of tumour vascularization in cutaneous malignant melanoma: clinical implications." Br J Dermatol **171**(2): 220-233.

Perica, K., J. C. Varela, M. Oelke and J. Schneck (2015). "Adoptive T cell immunotherapy for cancer." Rambam Maimonides Med J **6**(1): e0004.

Pinto, M. P., P. Sotomayor, G. Carrasco-Avino, A. H. Corvalan and G. I. Owen (2016). "Escaping Antiangiogenic Therapy: Strategies Employed by Cancer Cells." Int J Mol Sci **17**(9).

Proksch, E., J. M. Brandner and J. M. Jensen (2008). "The skin: an indispensable barrier." Exp Dermatol **17**(12): 1063-1072.

Pulluri, B., A. Kumar, M. Shaheen, J. Jeter and S. Sundararajan (2017). "Tumor microenvironment changes leading to resistance of immune checkpoint inhibitors in metastatic melanoma and strategies to overcome resistance." Pharmacol Res **123**: 95-102.

Rajkumar, V. S., C. Sundberg, D. J. Abraham, K. Rubin and C. M. Black (1999). "Activation of microvascular pericytes in autoimmune Raynaud's phenomenon and systemic sclerosis." Arthritis Rheum **42**(5): 930-941.

Rakoff-Nahoum, S. (2006). "Why cancer and inflammation?" Yale J Biol Med **79**(3-4): 123-130.

Reed, K. B., J. D. Brewer, C. M. Lohse, K. E. Bringe, C. N. Pruitt and L. E. Gibson (2012). "Increasing incidence of melanoma among young adults: an epidemiological study in Olmsted County, Minnesota." Mayo Clin Proc **87**(4): 328-334.

Sample, A. and Y. Y. He (2017). "Mechanisms and prevention of UV-induced melanoma." Photodermatol Photoimmunol Photomed.

Shah, A. A., A. Rosen, L. Hummers, F. Wigley and L. Casciola-Rosen (2010). "Close temporal relationship between onset of cancer and scleroderma in patients with RNA polymerase I/III antibodies." Arthritis Rheum **62**(9): 2787-2795.

Shain, A. H. and B. C. Bastian (2016). "From melanocytes to melanomas." Nat Rev Cancer **16**(6): 345-358.

Simpson, C. L., D. M. Patel and K. J. Green (2011). "Deconstructing the skin: cytoarchitectural determinants of epidermal morphogenesis." Nat Rev Mol Cell Biol **12**(9): 565-580.

Society, A. C. (2013). "Melanoma Skin Cancer." Retrieved January 6, 2013, from http://www.cancer.org/cancer/skincancer-melanoma/detailedguide/index.

Society, C. C. (2017). "Melanoma Skin Cancer Statistics." 2017, from http://www.cancer.ca/en/cancer-information/cancer-type/skin-melanoma/statistics/?region=on.

Soengas, M. S. and S. W. Lowe (2003). "Apoptosis and melanoma chemoresistance." Oncogene **22**(20): 3138-3151.

Steck, M. B. (2014). "The role of melanocortin 1 receptor in cutaneous malignant melanoma: along the mitogen-activated protein kinase pathway." <u>Biol Res Nurs</u> **16**(4): 421-428.

Thompson, J. F., R. A. Scolyer and R. F. Kefford (2005). "Cutaneous melanoma." <u>Lancet</u> **365**(9460): 687-701.

Tsang, M. and A. Leask (2015). "CCN2 is required for recruitment of Sox2-expressing cells during cutaneous tissue repair." <u>J Cell Commun Signal</u> **9**(4): 341-346.

Videtic, G. M., P. G. Lopez and J. V. Jones (1997). "A case of melanoma concurrent with progressive systemic sclerosis." <u>Cancer Invest</u> **15**(3): 224-226.

Wang, J. X., M. Fukunaga-Kalabis and M. Herlyn (2016). "Crosstalk in skin: melanocytes, keratinocytes, stem cells, and melanoma." <u>J Cell Commun Signal</u> **10**(3): 191-196.

Zaki, K. A., B. Basu and P. Corrie (2012). "The role of angiogenesis inhibitors in the management of melanoma." <u>Curr Top Med Chem</u> **12**(1): 32-49.

Chapter 2

2 CCN2 Expression by Tumour Stroma is Required for Melanoma Metastasis

2.1 Introduction

Melanoma is the second most common invasive cancer in young adults, and the incidence of diagnosis among this group is increasing (Reed, Brewer et al. 2012). Of skin cancers, melanoma is the most likely to metastasize making it the most likely to be fatal: Approximately 5% of patients diagnosed with metastatic melanoma survive for 5 years after diagnosis, whereas patients with no metastases have a 5 year survival rate approaching 90% (Cummins, Cummins et al. 2006).

Melanocytes, protective cells found in the skin, are subjected to assault by UV radiation on a routine basis, and thus require a strong resistance to apoptosis. Unfortunately this resistance is retained when melanocytes progress into melanoma, leaving the cancer largely unaffected by chemotherapy and radiotherapy (Soengas and Lowe 2003, Cummins, Cummins et al. 2006, Gray-Schopfer, Wellbrock et al. 2007). Given this high resistance to conventional therapies and the effectiveness of surgical excision in the absence of metastasis (Cummins, Cummins et al. 2006), discovering methods of preventing metastasis is vital to increasing patient survival.

For melanoma to metastasize, tumour cells must migrate through the extracellular matrix, which is built by cells in the stromal microenvironment. Following the degradation of the extracellular matrix, tumour cells must migrate by forming new adhesive sites closer to their destination and degrading old adhesive sites further away. The formation and degradation of these sites are governed by integrins, and the communication between cells and their surrounding matrix is mediated by a class of non-structural secreted proteins known as matricellular proteins (Steeg 2006).

It has long been recognized that expression of the CCN family of matricellular proteins, is highly associated with certain cancers (Bleau, Planque et al. 2005, Perbal 2013). CCN2 (formerly known as connective tissue growth factor, CTGF) is a member of the CCN family of matricellular proteins, which act primarily in two ways; by directly binding to adhesion receptors like integrins, and by acting as co-factors for other regulatory molecules (Chen and Lau 2009, Perbal 2013). Abnormal expression patterns of CCN proteins have been associated with progression of breast, prostate and pancreatic cancers (Xie, Nakachi et al. 2001, Yang, Tuxhorn et al. 2005, Dornhofer, Spong et al. 2006, Sha and Leask 2011, Wong and Rustgi 2013) and overexpression of CCN2 has been associated with malignant melanoma (Sha and Leask 2011). CCN2 expression can also be stimulated in surrounding tissues by the inflammatory response caused by tumour formation (Coussens and Werb 2002, Leask and Abraham 2006, Wong and Rustgi 2013). While these observations suggest that CCN2 plays a role in the metastasis of melanoma, the majority of studies involving the role of CCN proteins in cancer have only correlated expression levels of the proteins with tumour progression without incorporating loss of function studies. Recently CCN2 was shown to be regulated by the Hippo pathway in melanoma cell lines (Nallet-Staub, Marsaud et al. 2014). Moreover, an antibody to CCN2 was shown to revert established metastatic melanoma in a murine model (Finger, Cheng et al. 2014); however, the mechanism underlying CCN2 action is unclear. In particular, neither the relative roles of tumour- or stroma- derived CCN2 in melanoma metastasis, nor the downstream effectors of CCN2, are clear.

In this report, we use a syngeneic B16F(10) murine melanoma model (cells derived from C57 BL6 mice) (Wack, Kirst et al. 2002) and C57 BL6 mice lacking CCN2 in fibroblasts to investigate the differential roles of cancer cell versus niche-derived CCN2 in melanoma invasion and metastasis.

2.2 Methods

2.2.1 Cell Culture and Western Blotting

B16(F10) murine melanoma cells were purchased (ATCC) and cultured in high glucose Dulbecco's Modified Eagle's Medium (DMEM), 10% fetal bovine serum (FBS) and 1%

antibiotic/antimycotic solution (Invitrogen). C8161 and c81-61 cells were provided by Mary Hendrix, and experiments using them were performed at the University of Alberta. Cells were cultured until confluence prior to harvesting for mRNA or protein extraction. Where indicated, cells were treated with 10µM Bisindolylmaleimide I (BIM), a pan-PKC inhibitor (EMD Millipore), for 6 hours prior to RNA extraction. Cells were cultured until confluence prior to harvesting for mRNA or protein extraction. CCN2 levels were detected by co-incubating cultures with 50µg/mL sodium heparin (Sigma). Sodium heparin was included to prevent rapid internalization and degradation of CCN2 via LRP1 as endogenous CCN2 is known to be rapidly degraded by mouse cells through this mechanism (Segarini, Nesbitt et al. 2001). 1mL conditioned culture media was collected for every treatment, and total protein were concentrated using methanol/chloroform precipitation as previously described (Friedman, Hoving et al. 2009). Periostin protein levels were assessed by extraction of total protein [using ice-cold TG lysis buffer (20 mM Tris- HCl [pH 8], 1% Triton X-100, 10% glycerol, 137 mM NaCl, 1.5 mM $MgCl_2$, 1 mM EGTA, 50 mM NaF, 1 mM Na_3VO_4, 1 mM phenylmethylsulfonyl fluoride, 20 µM leupeptin, 10 µg of aprotinin ml^{-1})]. The concentration of protein was detected (Pierce) and equal amounts of protein (100 μg) were subjected to SDS/PAGE on a 4-12% gradient gel (Invitrogen). Gels were then blotted onto nitrocellulose (BioRad) and CCN2 was detected using a goat anti-CCN2 antibody (1:200 dilution, Santa Cruz) followed by a HRP-conjugated anti-goat antibody (1:2000; Jackson), a chemiluminescent detection kit (Pierce) and X-Ray film (Kodak). Alternatively, Periostin was detected using a rabbit anti-POSTN (1:1000 dilution; Santa Cruz) followed by a HRP-conjugated anti-rabbit antibody (1:2000; Jackson), a chemiluminescent detection kit (Pierce) and X-Ray film (Kodak). When indicated, cells were transfected with CTGF (CCN2) shRNA Lentiviral or control shRNA Lentiviral Particles (Santa Cruz) using polybrene and selected for using puromycin as described by the manufacturer (Santa Cruz), or with CTGF (CCN2) siRNA or control siRNA using Lipofectamine 2000 transfection kit (Thermo Fisher Scientific) as per manufacturer instructions.

2.2.2 Real Time RT-PCR

B16(F10) murine melanoma cells were grown in high glucose DMEM containing 10% FBS until 75% confluence after which the media was replaced with low glucose DMEM containing 0.5% FBS and grown for 24 hours. RNA was harvested using Trizol (Invitrogen) and used for Real-Time RT-PCR. 25 ng of RNA was reverse transcribed and amplified using TaqMan Assays on Demand (Applied Biosystems) in a 15μl reaction containing primers for mouse CCN2 and POSTN (Assays on Demand; Applied Biosystems) and 6-carboxyfluroscein labelled TaqMan MGB probe. Reverse Transcriptase One-Step Mastermix was added to samples and the ABI Prism 7900 HT sequence detector (Applied Biosystems) was used according to manufacturer's instructions to detect amplified sequences. Samples were run in triplicate, expression values were standardized to control values from EUK18S primers using the ΔΔCt method. Statistical analysis was done using one way ANOVA and Tukey's post-hoc test on GraphPad.

2.2.3 Expression Profiling

Expression profiling was performed as described in prior publications (Guo, Carter et al. 2011, Guo, Carter et al. 2011) All sample labeling and processing was handled at the London Regional Genomics Centre (Robarts Research Institute, London, Ontario, Canada; http://www.lrgc.ca). Briefly, RNA quality was assessed on an Agilent 2100 Bioanalyzer (Agilent Technologies Inc.) and the RNA 6000 Nano kit (Caliper Life Sciences) before 5.5 μg of single-stranded cDNA was synthesized from 200 ng of total RNA, end-labeled, and hybridized, for 16 hours at 45 °C, to Human Gene 1.0 ST arrays. GeneChips were scanned with the GeneChip Scanner 3000 7G and probe level (.CEL file) data were generated using Affymetrix Command Console v3.2.4. Probes were summarized to gene level data in Partek Genomics Suite v6.6 (Partek) using the RMA algorithm. Experiments were performed twice, and fold changes and *P*-values were generated using analysis of variance in Partek. Genes that significantly changed (at least 1.5 fold change, *P*-value <0.05) in response to CCN2 knockdown were compiled and exported into DAVID (http://david.abcc.ncifcrf.gov/) for further analysis.

2.2.4 Immunohistochemistry

Tissue was stained for CCN2 and Periostin using the Vectastain ABC Kit (Vector Laboratories). Briefly, sections (0.5 μm) were cut using a microtome (Leica), collected on Superfrost Plus slides (Fisher Scientific), de-waxed in xylene, and rehydrated by successive immersion in descending concentrations of alcohol. Antigen retrieval was performed by immersing slides in Na-citrate solution (pH 6.0) for 30 minutes at 98°C. After cooling, slides were rinsed, and non-specific binding was blocked by incubation with diluted normal serum. Sections were incubated with primary antibodies in diluted normal serum (1:100 goat anti-CCN2, or 1:100 rabbit anti-POSTN), followed by incubation with biotinylated secondary antibody solution and Vectastain ABC Reagent. After incubations, the sections were incubated in ImmPACT DAB peroxidise substrate (Vector Laboratories) and counterstained with hematoxylin.

2.2.5 *In vitro* Invasion Assay

10,000 Parental untreated, CCN2 shRNA, and Control shRNA B16(F10) cells were seeded in growth medium containing 0.5% FBS (and 5μg/mL puromycin hydrochloride for shRNA cells) onto a transwell filter insert with a pore size of 8 μm coated with 100μL of 10μg/mL purified bovine collagen (Advanced Biosystems) as previously described (Chen 2005). The transwell filter insert was suspended in a plate filled with growth medium containing 10% FBS (to create a chemotactic incentive to invade) and allowed to incubate at 37°C for 24 hours. After incubation all excess collagen and non-invasive cells were removed from the inside of the transwell filter insert. The remaining cells were fixed in methanol, and stained with 1μg/mL DAPI to allow for counting with microscopy.

2.2.6 Animals

Mice possessing a tamoxifen-dependent Cre recombinase under the control of a fibroblast-specific regulatory sequence from the proα2(I) collagen gene (Zheng, Zhang et al. 2002) were crossed with mice homozygous for a conditional CCN2 allele to generate Cre/CCN2 heterozygote mice, which were mated to generate mice hemizygous for Cre and homozygous for CCN2. Animals used for experiments were genotyped by

polymerase chain reaction (PCR) as described previously (Zheng, Zhang et al. 2002, Liu, Shi-wen et al. 2011). To delete CCN2 (CCN2$^{-/-}$) in fibroblasts, 3-week-old mice were given intraperitoneal injections of tamoxifen suspension (0.1 ml of 10 mg/mL 4-hydroxitamoxifen, Sigma) over 5 days. Littermate mice of identical genotype were injected with corn oil and were used as controls (CCN2$^{fl/fl}$). All animal protocols were approved by the animal care committee at the University of Western Ontario.

2.2.7 *In vivo* Tumour Growth and Metastasis

Subconfluent melanoma cells in the exponential growth phase were harvested by exposure to 0.25% trypsin/0.02% EDTA solution, resuspended in serum-free DMEM at a concentration of 3300 cells/µL, and 330,000 cells were injected subcutaneously into the right flank of each mouse. Upon appearance of a palpable tumour the volume of the tumour was measured daily using calipers and the following equation: Tumour Volume $(mm^3) = 1/2$(Length of Longest Tumour Dimension) x (Length of Narrowest Tumour Dimension)^2. Tumour growth was evaluated over the course of 14 days, and mice were euthanized on the 14th day. After euthanasia the lungs and tumour were collected from the mice and fixed in a 4% paraformaldehyde solution. After fixation, tissues were processed, embedded in paraffin, and prepared for histological sectioning. Lung sections were stained with hematoxylin and eosin (H&E; Fisher Scientific) to locate dense metastatic foci. Three non-serial sections per lung were examined. To examine macroscopic metastasis in the lungs, tumours were allowed to grow for 21 days, and collected lungs were stained with Bouin's solution and rinsed with 70% ethanol to visualize the metastases.

2.2.8 Datasets and Analysis of Patient Samples

Level 3 TCGA RNAseqV2 gene expression data was obtained from the TCGA Data Portal in March 2015. SKCM TCGA mutational data was obtained from the USCS Xena browser for calls generated at the Broad Institute Genome Sequencing Center using the MutDect method in April 2015 (genome cancer.ucsc.edu/download/public/xena/TCGA/TCGA.SKCM.sampleMap/mutation_broad).

Stromal and immune scores were defined for tumours by the ESTIMATE algorithm (Estimation of STromal and Immune cells in MAlignant Tumour tissues using Expression data) using tumour RNASeqV2 data and the ESTIMATE package in R (Yoshihara, Shahmoradgoli et al. 2013). Pearson's correlation coefficient was used to calculate the association of specific genes to stromal signatures.

We conducted all analyses and visualizations in the RStudio programming environment (v0.98.501). R/Bioconductor packages ggplot2, plyr, and ESTIMATE were used where appropriate.

2.3 Results

2.3.1 Loss of CCN2 expression by B16(F10) murine melanoma cells results in impaired invasion but not proliferation

Initial experiments were conducted using B16(F10) melanoma cells which were stably transfected with either CCN2 shRNA or scrambled control shRNA. Extent of CCN2 knockdown relative to GAPDH control was determined by real time PCR and Western blot analyses (Figure 1A). To assess the invasive ability of the resultant melanoma cells, B16(F10) cells were subjected a transwell filter invasion assay. After incubation at 37°C for 24 hours, collagen and non-invasive cells were removed from the inside of the transwell insert, and the number of remaining cells was calculated. B16(F10) melanoma cells deficient in CCN2 showed markedly reduced invasion of collagen type I compared with either wild type B16(F10) melanoma cells or control B16(F10) melanoma cells stably transfected with scrambled control shRNA (Figure 1B, C). In order to ensure the loss of invasive ability with CCN2 deficiency was also present in human melanomas, the transwell filter invasion assay was also used to test C8161 and C81-61 cells. Both C8161 and its poorly aggressive counterpart were derived from metastases from the abdominal wall, and mRNA and protein analysis revealed that C81-61 expressed significantly less CCN2 (Seftor, Brown et al. 2005) (Figure 2A). Using siRNA transfection the CCN2 expression in C8161 cells was reduced (Figure 2A). Both the C8161 CCN2 siRNA cells, and the C81-61 cells showed markedly reduced invasion as compared to control C8161

a

CCN2 mRNA Expression is Reduced in CCN2 shRNA cells
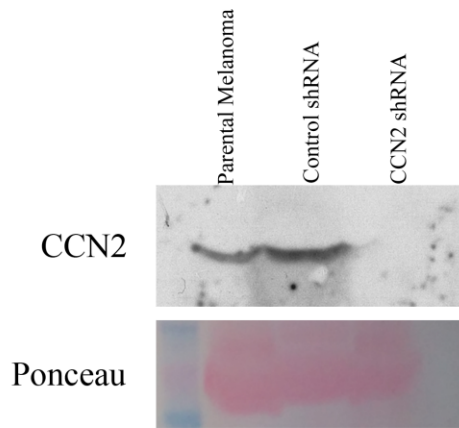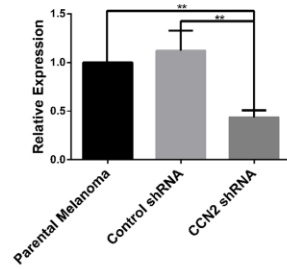
b

Parental Melanoma

Control shRNA

CCN2 shRNA

100μm

CCN2

Ponceau

c
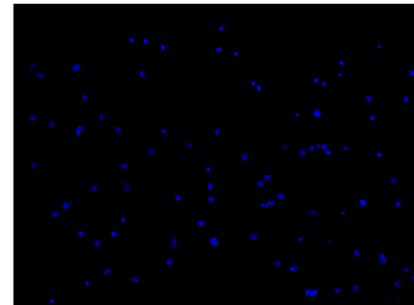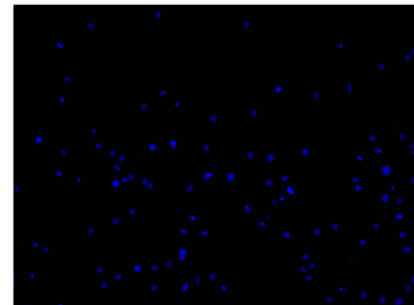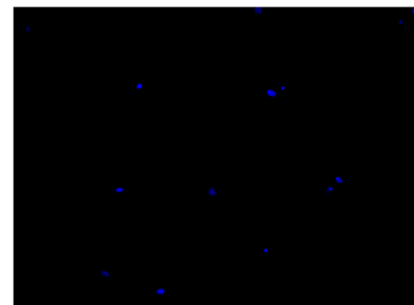
Invasion of Cells Through Collagen
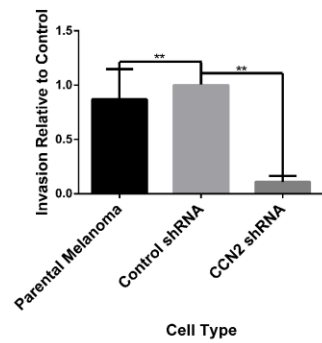
Figure 2-1 Loss of CCN2 impairs the invasive ability of melanoma cells *in vitro*.

B16(F10) murine melanoma cells were transfected with either *Ccn2* shRNA, to produce a knockdown in *Ccn2* mRNA expression, or a scrambled shRNA, to act as a control. **(a)** Cells treated with the *Ccn2* shRNA lentiviral particles showed a significant decrease in *Ccn2* mRNA expression compared to both untreated B16(F10) cells, and cells treated with the scrambled control shRNA. (n=3, ** = $p < 0.005$) and a decrease in CCN2 protein present in growth media **(b)** Each cell line was subjected to a Boyden chamber assay to assess their ability to invade through a collagen matrix. After being given 24 hours to invade through the collagen towards a chemotactic incentive the non-invasive cells and collagen were removed and the invasive cells were stained with DAPI. **(c)** Cells deficient in CCN2 were significantly less invasive than both untreated B16(F10) cells, and cells treated with the scrambled control shRNA. (n = 3, *= $p<0.05$, **= $p<0.01$)

a **CCN2 mRNA Expression**

b

c **Relative Invasion**
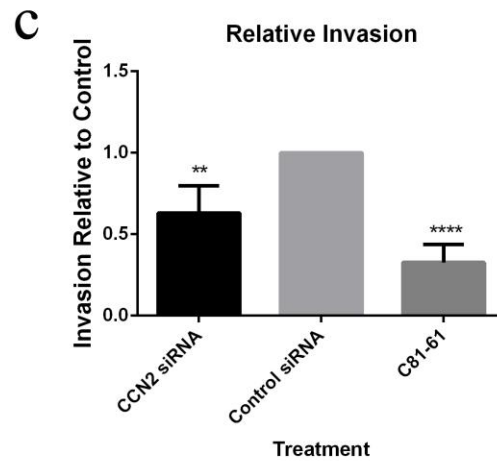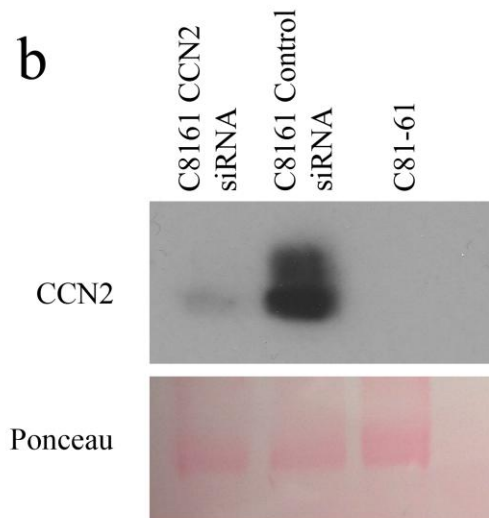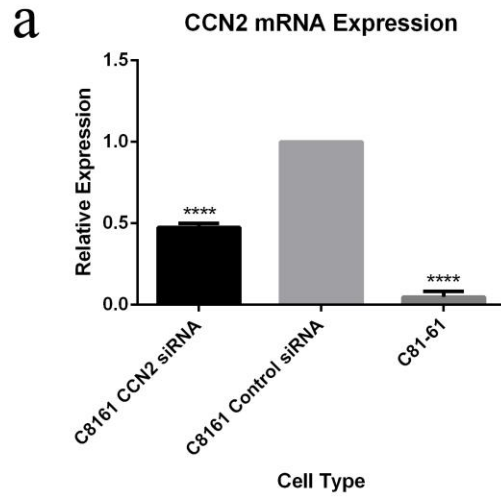
Figure 2-2 CCN2 deficiency impairs invasive ability in human C8161 cells

C8161 cells were transfected with CCN2 siRNA, to produce a knockdown in CCN2 expression, or scrambled siRNA, to act as a control. **(a, b)** CCN2 siRNA transfected C8161 cells, and poorly aggressive C81-61 show a significant decrease in CCN2 mRNA and protein expression when compared to cells treated with scrambled control siRNA. **(c)** Control siRNA transfected C8161 cells, CCN2 siRNA transfected C8161 cells, and C81-61 cells were subjected to a Boyden chamber assay to assess their invasive ability. After being given 24 hours to invade towards a chemotactic incentive, non-invasive cells were removed and invasive cells were stained with DAPI. CCN2 siRNA transfected C8161 cells and C81-61 cells showed significantly decreased invasion compared to C8161 cells transfected with scrambled control siRNA (n = 4, ** = $p<0.01$, **** = $p<0.0001$)

cells (Figure 2 B, C). Of note, the reduced invasion observed with the loss of CCN2 was not due to alterations in proliferation (Supplemental Figure 1A).

2.3.2 Loss of CCN2 expression by tumour stroma results in impaired metastasis, but not tumour growth, *in vivo*

To extend our *in vitro* data supporting a role for CCN2 in melanoma invasion, we next ascertained the *in vivo* effects of CCN2 loss on melanoma growth and invasion. To perform these analyses, we employed a syngeneic model using B16(F10) melanoma cells (which are derived from C57/BL6 mice) deleted or not for CCN2 and C57/BL6 mice deleted or not for CCN2 in fibroblasts. Three weeks post-deletion of CCN2, we subcutaneously injected mice with B16(F10) melanoma cells or B16(F10) melanoma cells deleted for CCN2. Fourteen days later, tumour growth and metastasis were examined. Growth of subcutaneous tumours over 14 days was unaffected by loss of CCN2 expression (Supplemental Figure 1B), consistent with our *in vitro* data suggesting that proliferation of melanoma cells was unaffected by loss of CCN2 (Supplemental Figure 1A). When melanoma cells were injected into wild-type mice, loss of CCN2 in melanoma cells did not significantly affect metastasis to the lung, measured using H&E stained sections. Indeed, loss of CCN2 expression from stromal cells resulted in increased metastasis in wild-type mice, likely due to a compensatory effect of stromal CCN2 (Figure 3B). However, loss of CCN2 expression by tumour stroma resulted in significant reduction in metastasis, regardless of whether CCN2 was knockdown in the melanoma cells (Figure 3A, B). Loss of CCN2 from the tumour stroma of C57 BL6 mice deleted for CCN2 after 14 days of tumour growth was confirmed by immunohistochemical analysis using anti-CCN2 antibody (Figure 4A). Results indicating that loss of CCN2 by tumour stroma resulted in impaired metastasis were confirmed by gross examination of Bouin`s-fixed lungs of mice deleted or not for CCN2 after 21 days of tumour growth (Figure 3C, D). Collectively, these results indicate that CCN2 expression by the tumour stroma could compensate for loss of CCN2 by tumour cells and that CCN2 expression by the tumour stroma is required for metastasis *in vivo*.

a

Mouse:

	CCN2$^{fl/fl}$	CCN2$^{-/-}$

Tumour:

Parental Melanoma

CCN2 shRNA

300μm

b **Area of Lung Occupied by Melanoma**

- CCN2$^{fl/fl}$ mouse
- CCN2$^{-/-}$ mouse

% of Lung Area

Parental Melanoma
CCN2 shRNA
Parental Melanoma
CCN2 shRNA

Melanoma Cells Implanted

c Parental Melanoma cells implanted in CCN2$^{fl/fl}$ mouse

3 mm
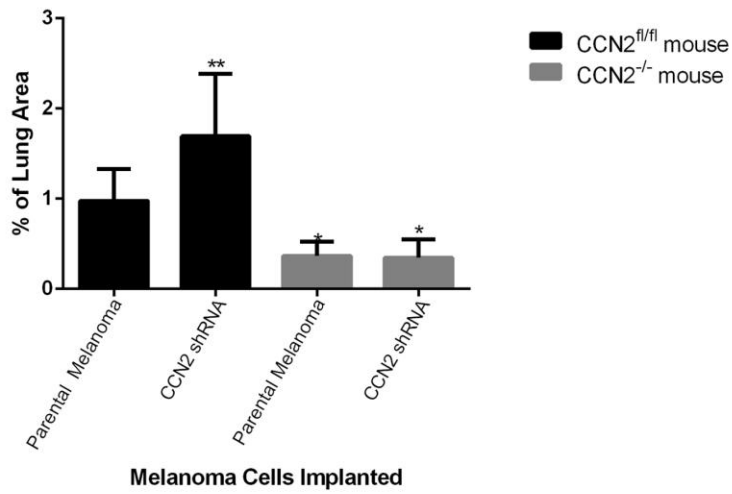
d Parental Melanoma cells implanted in CCN2$^{-/-}$ mouse

3 mm

Figure 2-3 Loss of CCN2 in tumour stroma fibroblasts impairs metastasis *in vivo*.

(a) Representative images of lung sections from wild type or *Ccn2* Knockout mice (mice deleted for CCN2 in fibroblasts) following subcutaneous implantation with Parental or CCN2 shRNA melanoma cells after 14 days of tumour growth. H&E staining detects sites of pulmonary metastasis by staining the dense metastatic foci purple (indicated by arrow). **(b)** The graph quantifies the total area of the lung section covered by metastases. Deletion of CCN2 in fibroblasts of the recipient mice results in a significant decrease in metastasis compared to cells implanted into wild type mice (N = 8, * = P < 0.05). **(c)** Images of lungs fixed with Bouin's 21 days after tumour growth of parental melanoma cells into wild type or *Ccn2* Knockout mice. Note dark areas (indicated by an arrow), indicating metastasized tumours, in wild type but not in **(d)** *Ccn2* Knockout mice (mice deleted for CCN2 in fibroblasts). N=3, representative images are shown.

a

| Mouse: | CCN2$^{fl/fl}$ | CCN2$^{-/-}$ |

Tumour:

Parental
Melanoma

CCN2
shRNA

50μm

b

| Mouse: | CCN2$^{fl/fl}$ | CCN2$^{-/-}$ |

Tumour:

Parental
Melanoma

CCN2
shRNA

50μm
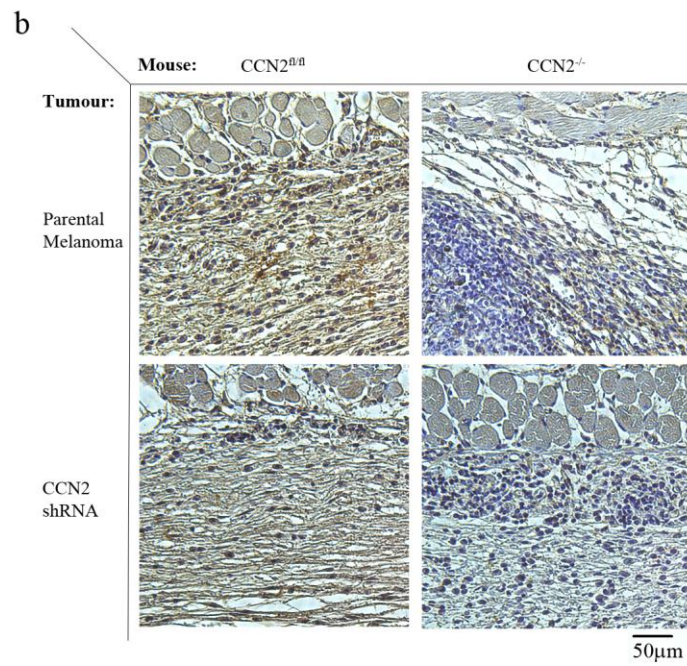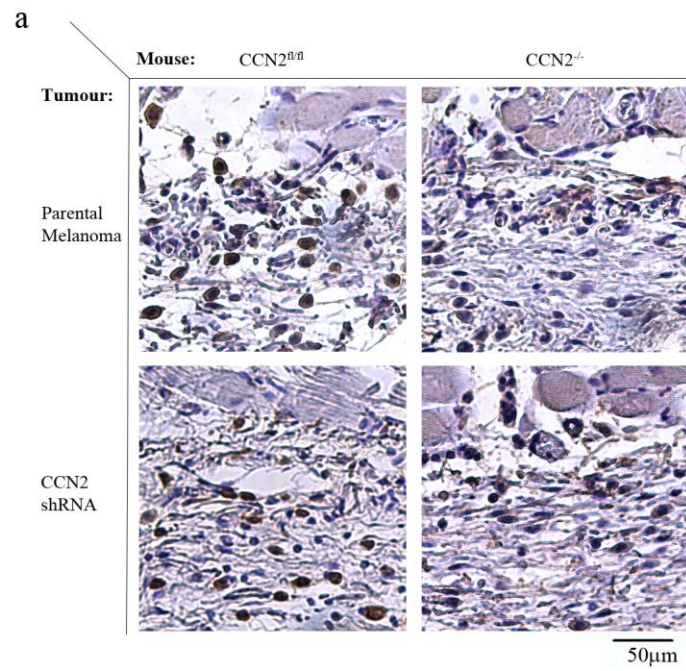
Figure 2-4 Loss of CCN2 and periostin expression in tumour stroma in mice deleted for CCN2 in fibroblasts.

Sections of tumour stroma from wild type or *Ccn2* Knockout mice (mice deleted for CCN2 in fibroblasts) stained with **(a)** anti-CCN2 or **(b)** anti-periostin antibody (N=3, representative images are shown). Mice were examined after 14 days of tumour growth of parental melanoma cells or melanoma cells deleted for CCN2. Note that CCN2 appeared be localized to the cells (red arrow) whereas periostin appeared to be localized to the matrix.

2.3.3 Impaired invasive ability of CCN2-deficient B16(F10) melanoma cells is rescued by recombinant periostin

To begin to address the underlying mechanism of CCN2-dependent action, we performed genome-wide expression profiling of B16(F10) melanoma cells stably transfected with CCN2 shRNA and scrambled control shRNA. We found that expression of 115 mRNA were reduced greater than 1.5-fold in CCN2 shRNA-transfected B16(F10) melanoma cells (Supplemental file). Of these, we noted that expression of perostin, a matricellular protein previously implicated in cell migration, depended on CCN2 (Hamilton 2008). Thus, we selected periostin for further analysis. Genome-wide expression profiling analysis showing that periostin expression depended on CCN2 was confirmed by real time PCR and Western blot analysis (Figure 5A). Addition of recombinant periostin rescued the invasive defect of CCN2-deficient cells (Figure 5B,C). Loss of periostin from the tumour stroma of C57/BL6 mice deleted for CCN2 after 14 days of tumour growth was confirmed by immunohistochemical analysis using anti-periostin antibody (Figure 4B). These results suggest that the lack of invasive ability of CCN2-deficient melanoma cells is due to lack of periostin expression.

2.3.4 In human melanoma patient samples, CCN2 and POSTN expression are correlated with stromal content, and each other

To investigate the role of *CCN2* and *POSTN* in human melanoma samples, we looked at the expression levels of both genes in 104 primary and 368 metastatic melanoma patient samples from The Cancer Genome Atlas (TCGA). Stromal scores were calculated for each sample by use of the ESTIMATE algorithm and correlated with *CCN2* and *POSTN* expression as determined by RNA sequencing. We found that both CCN2 and POSTN correlated strongly with stromal scores (r=0.57 and 0.49, respectively), comparable to the strength of the correlation between stromal scores and expression of fibroblast activation protein (r=0.57), the quintessential tumour-associated stromal protein (Figure 6, Supplemental Figure 2). We also found that *CCN2* and *POSTN* expression positively correlated with each other (r=0.33), providing support for a relationship between *CCN2*

a **POSTN mRNA Expression**
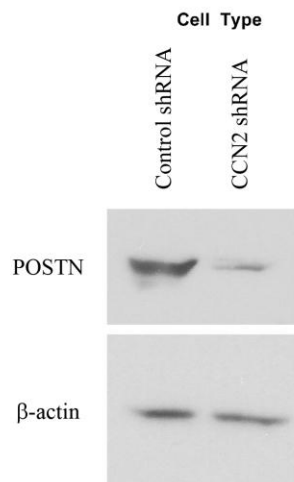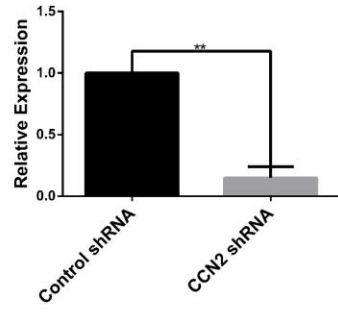
b Control shRNA
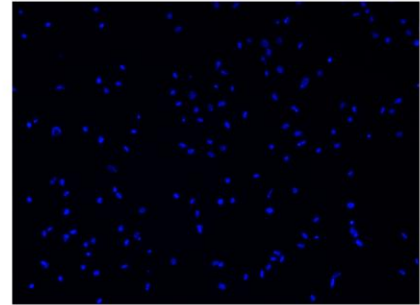
CCN2 shRNA
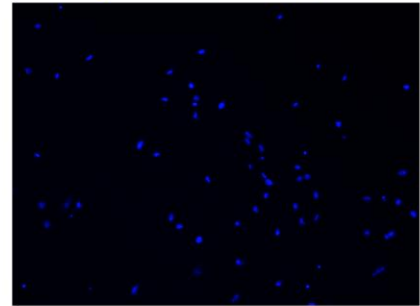
CCN2 shRNA+
150ng/mL rPOSTN

POSTN

β-actin
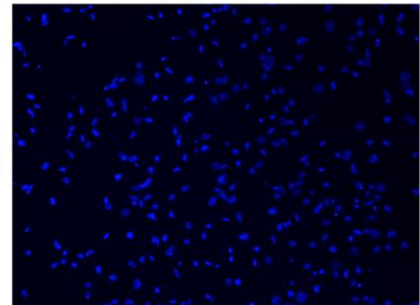
c **Invasion of Cells Through Collagen**
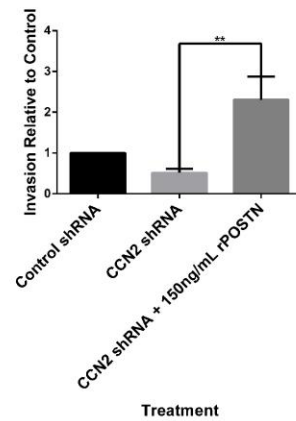
Figure 2-5 Rescuing Periostin deficiency rescues impaired invasion phenotype.

B16(F10) melanoma cells were transfected with either *Ccn2* shRNA, to produce a knockdown in *Ccn2* mRNA expression, or a scrambled shRNA, to act as a control. **(a)** Cells treated with the *Ccn2* shRNA showed a significant decrease in *Postn* mRNA and protein expression compared to cells treated with scrambled control shRNA. **(b)** Cells treated with *Ccn2* shRNA were treated with 150ng/mL rPOSTN and subjected to a Boyden chamber assay to assess their ability to invade through a collagen matrix. After being given 24 hours to invade through the collagen towards a chemotactic incentive the non-invasive cells and collagen were removed and the invasive cells were stained with DAPI. **(c)** Cells treated with 150ng/mL rPOSTN showed a rescue of the impaired invasion phenotype displayed by *Ccn2* shRNA treated cells (n = 3, **= $p < 0.01$)

a *CCN2* expression value vs Stromal score — Pearson's ρ = 0.57, *P* < 2.2e−16

b *POSTN* expression value vs Stromal score — Pearson's ρ = 0.49, *P* < 2.2e−16

c *POSTN* expression value vs *CCN2* expression value — Pearson's ρ = 0.33, *P* < 7.9e−14
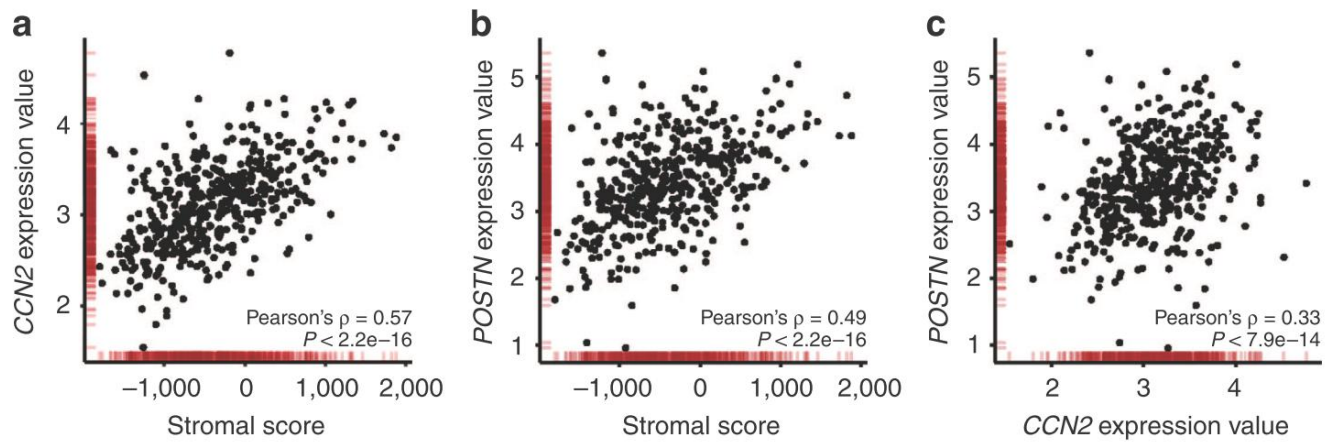
Figure 2-6 *CCN2* and *POSTN* expression correlate with stromal content

Stromal scores for primary (n=104) and metastatic (n=368) melanoma patient samples from The Cancer Genome Atlas (TCGA) were calculated by use of the ESTIMATE method. Stromal scores were analyzed for correlation with **(a)** *CCN2* and **(b)** *POSTN* gene expression values (log10(RSEM normalized count)) as determined by RNA sequencing (Illumina HiSeq 2000 RNA Sequencing Version 2 analysis). Both *CCN2* and *POSTN* were found to highly correlate with the stromal scores (*r*=0.57 and 0.49, respectively). **(c)** Scatterplot comparison of *CCN2* and *POSTN* gene expression values (log10(RSEM normalized count)) revealed a correlation between the expression of those two genes in patient samples (*r*=0.33). Rug plots show the density of the data for given values.

and *POSTN* that extends to human melanoma patient samples (Figure 6). Intriguingly, *CCN2* (Supplemental Figure 3 A, B) and *POSTN* (Supplemental Figure 3 C, D) expression did not correlate with the presence of B-RAF mutations in melanoma patients. Conversely, CCN expression correlated with the activation state of protein kinase C in human melanomas, and protein kinase C inhibition reduced CCN2 mRNA expression in human and mouse melanoma cells (Supplemental Figure 4 A, B).

Collectively, these data confirm our in vitro and animal studies, and suggest that CCN2 and POSTN are highly stromally expressed and that these matricellular proteins are co-regulated.

2.4   Discussion

Our results demonstrated that CCN2 expression by tumour stroma is required for melanoma metastasis. An emerging concept is that alterations in the tumour microenvironment promote invasion and metastasis and thus that targeting these alterations may result in effective anti-cancer therapies (Jewer, Findlay et al. 2012, Quail, Taylor et al. 2012). Matricellular proteins such as CCN2 and periostin are secreted into the extracellular matrix (ECM) that are highly spatiotemporally regulated and, although they are not structural ECM components, alter adhesive signaling in response to ECM and growth factors and hence can have profound localized effects on cellular behavior. The CCN family of matricellular proteins, at least in part due to its ability to promote signaling via integrins, has recently been proposed to play significant roles in altering the tumour microenvironment hence contributing to tumour growth and metastasis. Previous studies have found that CCN2 is abundant in cancers such as pancreatic cancer, and that this overexpression is related to cancer progression (Aikawa, Gunn et al. 2006, Dornhofer, Spong et al. 2006, Kondo, Kubota et al. 2006, Bennewith, Huang et al. 2009, Sodek, Ringuette et al. 2009, Mao, Ma et al. 2011). Our results showing that fibroblast-derived CCN2 contributes to melanoma metastasis suggest that CCN2 may be a good target for drug intervention in melanoma. Our data are consistent with and extend previous data showing that CCN2 is upregulated in cancer cells in response to hypoxia, oncogenic ras, and YAP/TAZ/hippo and that an antibody against CCN2 blocks

progression in animal models of pancreatic cancer and melanoma (Aikawa, Gunn et al. 2006, Sha and Leask 2011, Finger, Cheng et al. 2014, Nallet-Staub, Marsaud et al. 2014)

Periostin, like CCN2, is a matricellular protein upregulated in conditions wherein the ECM is being remodeled (Hamilton 2008). Our data suggesting that periostin operates downstream of CCN2 to promote invasion is consistent with prior data using periodontal ligament cells that showed rCCN2 induced periostin expression (Asano, Kubota et al. 2005); however, our data is the first to link CCN2 and periostin in terms of tumour metastasis. In this regard, it is interesting to note that CCN2 appeared to be largely localized to the cell, whereas periostin appeared to be present in the ECM. Previous data has linked periostin expression with metastasis in some tumours including in invasive melanoma (Tilman, Mattiussi et al. 2007, Kotobuki, Yang et al. 2014). Moreover, periostin has been shown to be upregulated in fibroblasts in the tumour microenvironment (Kikuchi, Kunita et al. 2014) and studies indicate that it promotes the invasiveness of pancreatic tumour cells (Baril, Gangeswaran et al. 2007). However, this is the first report to link tumour invasion in melanoma with periostin expression, consistent with the notion that targeting periostin may prove to be a viable anti-cancer therapy.

40–60% of all cutaneous melanoma patients possess position 600 mutations in *BRAF*; in these patients, tumours shrink in response to the BRAF inhibitors vemurafenib and dabrafenib (Fedorenko, Gibney et al. 2015). However, patients develop resistance to these drugs (Fedorenko, Gibney et al. 2015). That neither periostin nor CCN2 expression correlate with BRAF mutations suggest that anti-periostin or anti-CCN2 therapies may represent novel therapeutic strategies with an entirely different mechanism of action. As CCN2 expression appears to be downstream of PKC, possibly CCN2 elicits its effects by mediating combined protein kinase C/MAP kinase or protein kinase C/Akt pathways (Musi, Ambrosini et al. 2014).

In summation, herein we have provided data that suggest that CCN2 present in the tumour stroma is required for melanoma metastasis. These data are consistent with the

hypothesis that blocking CCN2 action may be a novel approach to mitigate progression of melanoma.

a BrdU Incorporation after 6 Hours of Growth   BrdU Incorporation after 24 Hour of Growth

b Tumour Growth After 14 Days
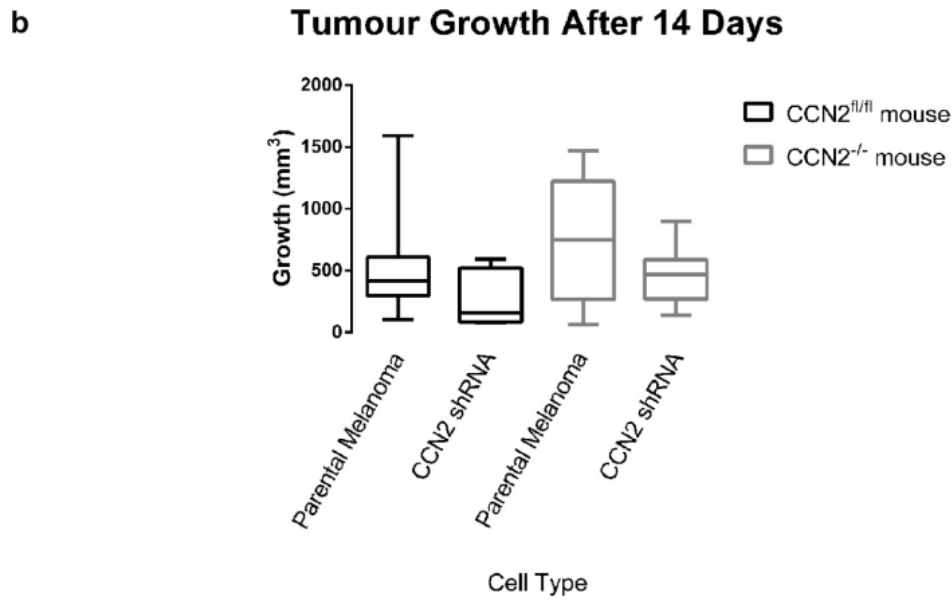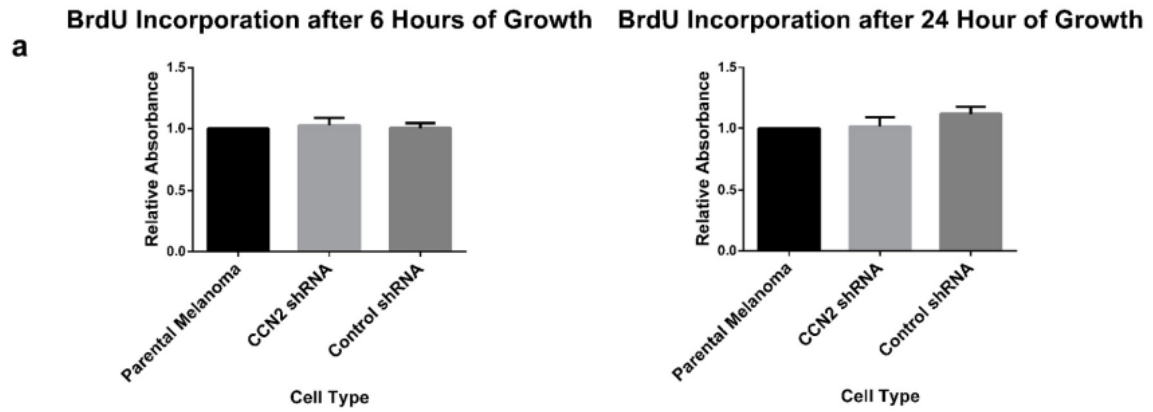
Supplemental Figure 1: Loss of CCN2 does not affect the proliferation of melanoma cells.

(a) B16(F10) murine melanoma cells were transfected with either CCN2 shRNA, to produce a knockdown in *Ccn2* mRNA expression, or a scrambled shRNA, to act as a control. Proliferation of the cells was then determined by measuring the rate of BrdU incorporation into newly synthesized DNA after for 6 or 24 hours. There was no significant difference in the rates of BrdU incorporation between cells, indicating that DNA was synthesized at the same rate, and thus cell proliferation was unaffected (n = 3). **(b)** Parental or CCN2 shRNA B16(F10) melanoma cells were implanted subcutaneously into mice whose fibroblasts were either CCN2 competent or deficient, and allowed to grow for 14 days. Neither reduced CCN2 expression in the tumour cells nor the stroma altered tumour growth. Kruskal-Wallis analysis shows no significant difference in growth at any time point. (N = 8)

a) Pearson's rho = 0.05
p = 0.23

HMGA2 expression value vs Stromal score

b) Pearson's rho = 0.57
p = 2.2e-16

FAP expression value vs Stromal score
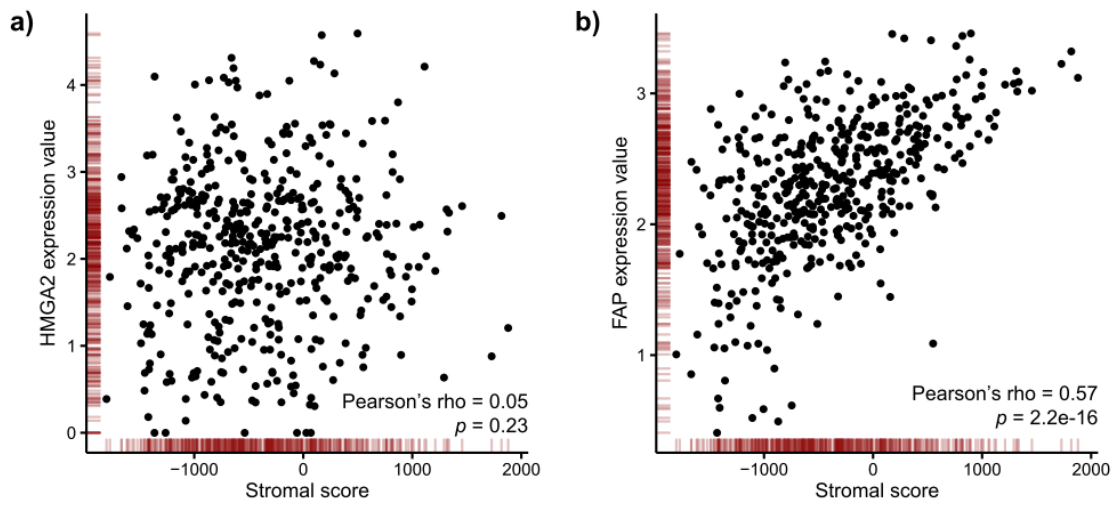
Supplemental Figure 2. Correlation of *HMGA2* and *FAP* to stromal content.

Stromal scores for primary (n=104) and metastatic (n=368) melanoma patient samples from The Cancer Genome Atlas (TCGA) were calculated by use of the ESTIMATE method. Stromal scores were analyzed for correlation with **(a)** *HMGA2* and **(b)** *FAP* gene expression values (log10(RSEM normalized count)) as determined by RNA sequencing (Illumina HiSeq 2000 RNA Sequencing Version 2 analysis). *FAP* was found to highly correlate with the stromal scores (*r*=0.57). Rug plots show the density of the data for given values.
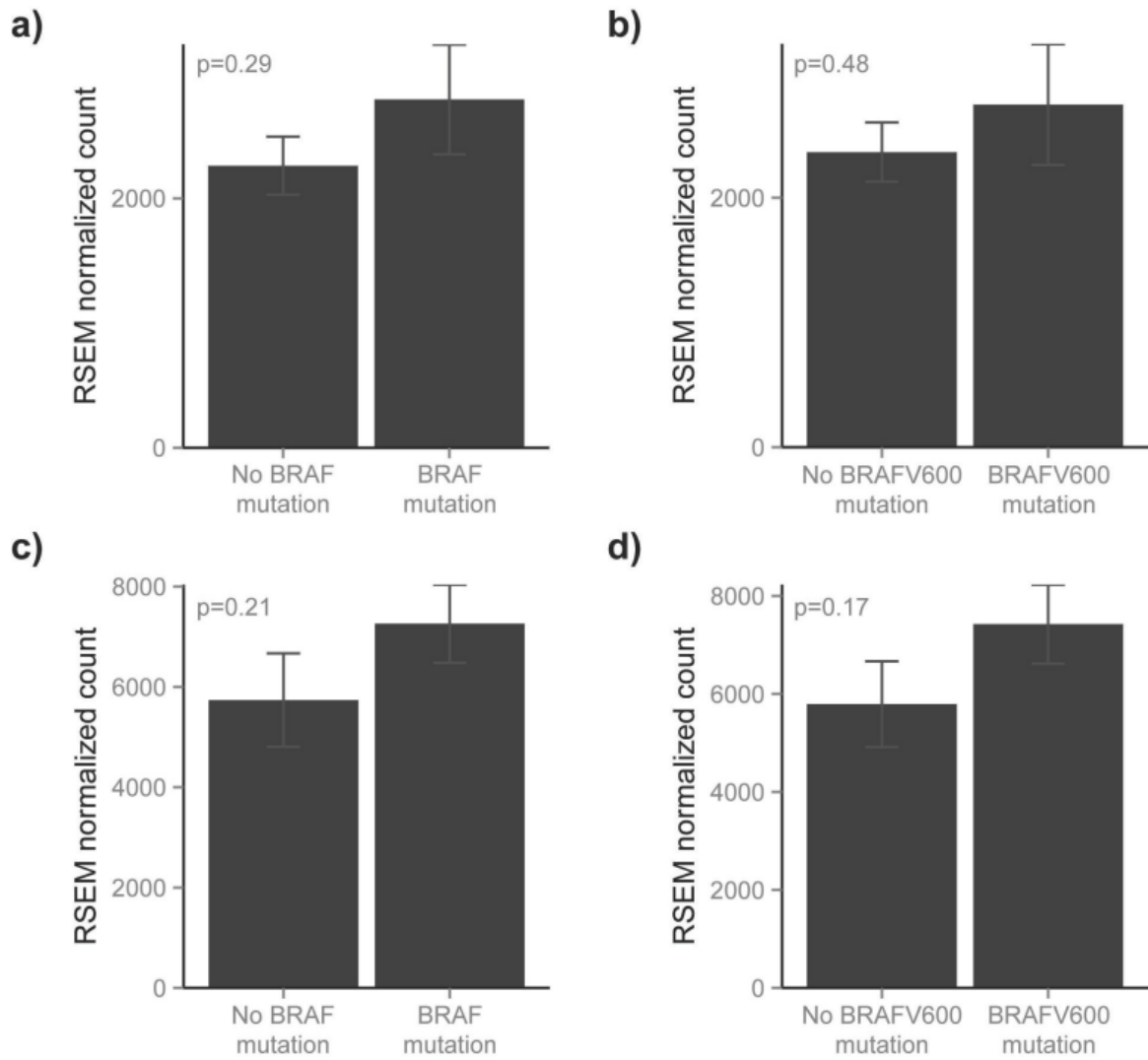
Supplemental Figure 3. *CCN2* and *POSTN* **expression do not correlate with B-RAF mutation**

Barplots show no significant difference in the expression levels of **(a, b)** *CCN2* and **(c,d)** *POSTN* in **(a,c)** BRAF mutated or **(b,d)** BRAF^{V600} mutated human melanoma tumour samples from The Cancer Genome Atlas. (mean+/-SEM, n=296, significance determined by t test)

a

Pearson's *r* = 0.29
p < 0.01

PKC alpha pS657 Protein Expression (RPPA)

CCN2 expression value

b

CCN2 mRNA Expression

Relative Expression

B16F10 DMSO   B16F10 BIM

Treatment

CCN2 mRNA Expression

Relative Expression

C8161 DMSO   C8161 BIM

Treatment
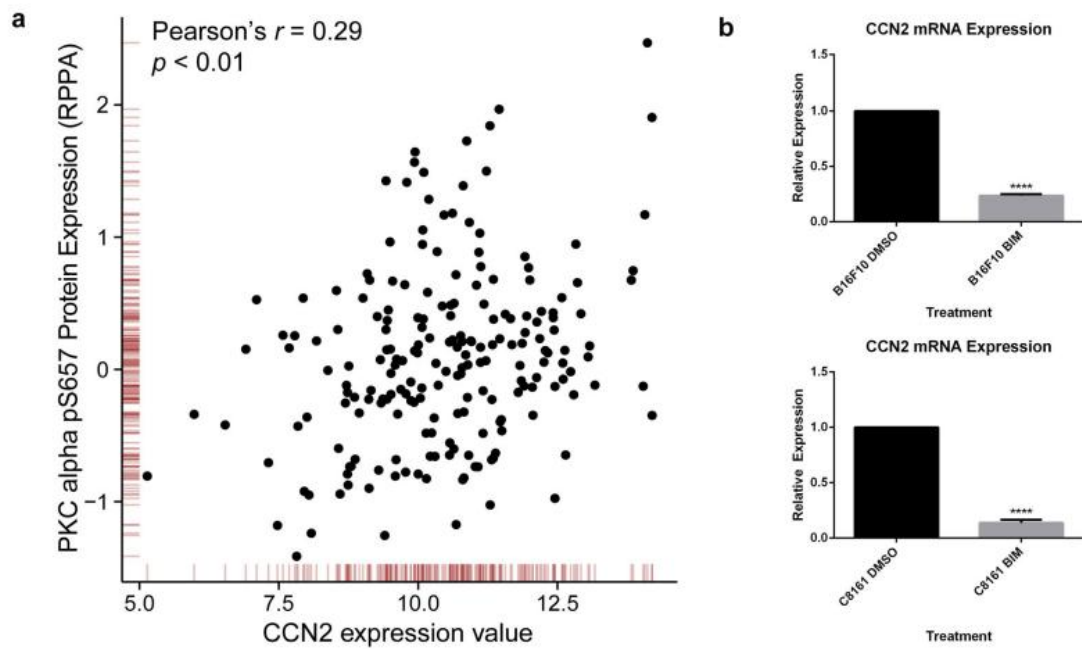
Supplemental Figure 4. CCN2 Expression is elevated in a PKC dependent fashion.

a) Scatterplot displaying the positive correlation between CCN2 expression values (RNA-sequencing, log(RSEM normalized count)) and PKC alpha pS657 protein levels (RPPA) in TCGA melanoma patient samples. Rug plots show the density of the data for given values. Pearson correlation coefficient = 0.29, p<0.01. **(b)** Treatment with 10μM Bisindolylmaleimide I (BIM) showed a significant reduction in CCN2 mRNA expression in both B16F10 and C8161 cells (n = 3, **** = p<0.001)

2.5   References

Aikawa, T., J. Gunn, S. M. Spong, S. J. Klaus and M. Korc (2006). "Connective tissue growth factor-specific antibody attenuates tumor growth, metastasis, and angiogenesis in an orthotopic mouse model of pancreatic cancer." Mol Cancer Ther **5**(5): 1108-1116.

Asano, M., S. Kubota, T. Nakanishi, T. Nishida, T. Yamaai, G. Yosimichi, K. Ohyama, T. Sugimoto, Y. Murayama and M. Takigawa (2005). "Effect of connective tissue growth factor (CCN2/CTGF) on proliferation and differentiation of mouse periodontal ligament-derived cells." Cell Commun Signal **3**: 11.

Baril, P., R. Gangeswaran, P. C. Mahon, K. Caulee, H. M. Kocher, T. Harada, M. Zhu, H. Kalthoff, T. Crnogorac-Jurcevic and N. R. Lemoine (2007). "Periostin promotes invasiveness and resistance of pancreatic cancer cells to hypoxia-induced cell death: role of the beta4 integrin and the PI3k pathway." Oncogene **26**(14): 2082-2094.

Bennewith, K. L., X. Huang, C. M. Ham, E. E. Graves, J. T. Erler, N. Kambham, J. Feazell, G. P. Yang, A. Koong and A. J. Giaccia (2009). "The role of tumor cell-derived connective tissue growth factor (CTGF/CCN2) in pancreatic tumor growth." Cancer Res **69**(3): 775-784.

Bleau, A. M., N. Planque and B. Perbal (2005). "CCN proteins and cancer: two to tango." Front Biosci **10**: 998-1009.

Chen, C. C. and L. F. Lau (2009). "Functions and mechanisms of action of CCN matricellular proteins." Int J Biochem Cell Biol **41**(4): 771-783.

Chen, H. C. (2005). "Boyden chamber assay." Methods Mol Biol **294**: 15-22.

Coussens, L. M. and Z. Werb (2002). "Inflammation and cancer." Nature **420**(6917): 860-867.

Cummins, D. L., J. M. Cummins, H. Pantle, M. A. Silverman, A. L. Leonard and A. Chanmugam (2006). "Cutaneous malignant melanoma." Mayo Clin Proc **81**(4): 500-507.

Dornhofer, N., S. Spong, K. Bennewith, A. Salim, S. Klaus, N. Kambham, C. Wong, F. Kaper, P. Sutphin, R. Nacamuli, M. Hockel, Q. Le, M. Longaker, G. Yang, A. Koong and A. Giaccia (2006). "Connective tissue growth factor-specific monoclonal antibody therapy inhibits pancreatic tumor growth and metastasis." Cancer Res **66**(11): 5816-5827.

Fedorenko, I. V., G. T. Gibney, V. K. Sondak and K. S. Smalley (2015). "Beyond BRAF: where next for melanoma therapy?" Br J Cancer **112**(2): 217-226.

Finger, E. C., C. F. Cheng, T. R. Williams, E. B. Rankin, B. Bedogni, L. Tachiki, S. Spong, A. J. Giaccia and M. B. Powell (2014). "CTGF is a therapeutic target for metastatic melanoma." Oncogene **33**(9): 1093-1100.

Friedman, D. B., S. Hoving and R. Westermeier (2009). "Isoelectric focusing and two-dimensional gel electrophoresis." Methods Enzymol **463**: 515-540.

Gray-Schopfer, V., C. Wellbrock and R. Marais (2007). "Melanoma biology and new targeted therapy." Nature **445**(7130): 851-857.

Guo, F., D. E. Carter and A. Leask (2011). "Mechanical tension increases CCN2/CTGF expression and proliferation in gingival fibroblasts via a TGFbeta-dependent mechanism." PLoS One **6**(5): e19756.

Guo, F., D. E. Carter, A. Mukhopadhyay and A. Leask (2011). "Gingival fibroblasts display reduced adhesion and spreading on extracellular matrix: a possible basis for scarless tissue repair?" PLoS One **6**(11): e27097.

Hamilton, D. W. (2008). "Functional role of periostin in development and wound repair: implications for connective tissue disease." J Cell Commun Signal **2**(1-2): 9-17.

Jewer, M., S. D. Findlay and L. M. Postovit (2012). "Post-transcriptional regulation in cancer progression : Microenvironmental control of alternative splicing and translation." J Cell Commun Signal **6**(4): 233-248.

Kikuchi, Y., A. Kunita, C. Iwata, D. Komura, T. Nishiyama, K. Shimazu, K. Takeshita, J. Shibahara, I. Kii, Y. Morishita, M. Yashiro, K. Hirakawa, K. Miyazono, A. Kudo, M. Fukayama and T. G. Kashima (2014). "The niche component periostin is produced by cancer-associated fibroblasts, supporting growth of gastric cancer through ERK activation." Am J Pathol **184**(3): 859-870.

Kondo, S., S. Kubota, Y. Mukudai, N. Moritani, T. Nishida, H. Matsushita, S. Matsumoto, T. Sugahara and M. Takigawa (2006). "Hypoxic regulation of stability of connective tissue growth factor/CCN2 mRNA by 3'-untranslated region interacting with a cellular protein in human chondrosarcoma cells." Oncogene **25**(7): 1099-1110.

Kotobuki, Y., L. Yang, S. Serada, A. Tanemura, F. Yang, S. Nomura, A. Kudo, K. Izuhara, H. Murota, M. Fujimoto, I. Katayama and T. Naka (2014). "Periostin accelerates human malignant melanoma progression by modifying the melanoma microenvironment." Pigment Cell Melanoma Res **27**(4): 630-639.

Leask, A. and D. J. Abraham (2006). "All in the CCN family: essential matricellular signaling modulators emerge from the bunker." J Cell Sci **119**(Pt 23): 4803-4810.

Liu, S., X. Shi-wen, D. J. Abraham and A. Leask (2011). "CCN2 is required for bleomycin-induced skin fibrosis in mice." Arthritis Rheum **63**(1): 239-246.

Mao, Z., X. Ma, Y. Rong, L. Cui, X. Wang, W. Wu, J. Zhang and D. Jin (2011). "Connective tissue growth factor enhances the migration of gastric cancer through downregulation of E-cadherin via the NF-kappaB pathway." Cancer Sci **102**(1): 104-110.

Musi, E., G. Ambrosini, E. de Stanchina and G. K. Schwartz (2014). "The phosphoinositide 3-kinase alpha selective inhibitor BYL719 enhances the effect of the protein kinase C inhibitor AEB071 in GNAQ/GNA11-mutant uveal melanoma cells." Mol Cancer Ther **13**(5): 1044-1053.

Nallet-Staub, F., V. Marsaud, L. Li, C. Gilbert, S. Dodier, V. Bataille, M. Sudol, M. Herlyn and A. Mauviel (2014). "Pro-invasive activity of the Hippo pathway effectors YAP and TAZ in cutaneous melanoma." J Invest Dermatol **134**(1): 123-132.

Perbal, B. (2013). "CCN proteins: A centralized communication network." J Cell Commun Signal **7**(3): 169-177.

Quail, D. F., M. J. Taylor and L. M. Postovit (2012). "Microenvironmental regulation of cancer stem cell phenotypes." Curr Stem Cell Res Ther **7**(3): 197-216.

Reed, K. B., J. D. Brewer, C. M. Lohse, K. E. Bringe, C. N. Pruitt and L. E. Gibson (2012). "Increasing incidence of melanoma among young adults: an epidemiological study in Olmsted County, Minnesota." Mayo Clin Proc **87**(4): 328-334.

Seftor, E. A., K. M. Brown, L. Chin, D. A. Kirschmann, W. W. Wheaton, A. Protopopov, B. Feng, Y. Balagurunathan, J. M. Trent, B. J. Nickoloff, R. E. Seftor and M. J. Hendrix (2005). "Epigenetic transdifferentiation of normal melanocytes by a metastatic melanoma microenvironment." Cancer Res **65**(22): 10164-10169.

Segarini, P. R., J. E. Nesbitt, D. Li, L. G. Hays, J. R. Yates, 3rd and D. F. Carmichael (2001). "The low density lipoprotein receptor-related protein/alpha2-macroglobulin receptor is a receptor for connective tissue growth factor." J Biol Chem **276**(44): 40659-40667.

Sha, W. and A. Leask (2011). "CCN2 expression and localization in melanoma cells." J Cell Commun Signal **5**(3): 219-226.

Sodek, K. L., M. J. Ringuette and T. J. Brown (2009). "Compact spheroid formation by ovarian cancer cells is associated with contractile behavior and an invasive phenotype." Int J Cancer **124**(9): 2060-2070.

Soengas, M. S. and S. W. Lowe (2003). "Apoptosis and melanoma chemoresistance." Oncogene **22**(20): 3138-3151.

Steeg, P. S. (2006). "Tumor metastasis: mechanistic insights and clinical challenges." Nat Med **12**(8): 895-904.

Tilman, G., M. Mattiussi, F. Brasseur, N. van Baren and A. Decottignies (2007). "Human periostin gene expression in normal tissues, tumors and melanoma: evidences for periostin production by both stromal and melanoma cells." Mol Cancer **6**: 80.

Wack, C., A. Kirst, J. C. Becker, W. K. Lutz, E. B. Brocker and W. H. Fischer (2002). "Chemoimmunotherapy for melanoma with dacarbazine and 2,4-dinitrochlorobenzene

elicits a specific T cell-dependent immune response." <u>Cancer Immunol Immunother</u> **51**(8): 431-439.

Wong, G. S. and A. K. Rustgi (2013). "Matricellular proteins: priming the tumour microenvironment for cancer development and metastasis." <u>Br J Cancer</u> **108**(4): 755-761.

Xie, D., K. Nakachi, H. Wang, R. Elashoff and H. P. Koeffler (2001). "Elevated levels of connective tissue growth factor, WISP-1, and CYR61 in primary breast cancers associated with more advanced features." <u>Cancer Res</u> **61**(24): 8917-8923.

Yang, F., J. A. Tuxhorn, S. J. Ressler, S. J. McAlhany, T. D. Dang and D. R. Rowley (2005). "Stromal expression of connective tissue growth factor promotes angiogenesis and prostate cancer tumorigenesis." <u>Cancer Res</u> **65**(19): 8887-8895.

Yoshihara, K., M. Shahmoradgoli, E. Martinez, R. Vegesna, H. Kim, W. Torres-Garcia, V. Trevino, H. Shen, P. W. Laird, D. A. Levine, S. L. Carter, G. Getz, K. Stemke-Hale, G. B. Mills and R. G. Verhaak (2013). "Inferring tumour purity and stromal and immune cell admixture from expression data." <u>Nat Commun</u> **4**: 2612.

Zheng, B., Z. Zhang, C. M. Black, B. de Crombrugghe and C. P. Denton (2002). "Ligand-dependent genetic recombination in fibroblasts : a potentially powerful technique for investigating gene function in fibrosis." <u>Am J Pathol</u> **160**(5): 1609-1617.

Chapter 3

3 CCN2 expression in tumour stroma is required for tumour vascularization and formation of a contractile stroma

3.1 Introduction

Melanoma is an invasive cancer that is increasing in frequency, and due to its metastatic ability and resistance to therapies is highly fatal with only 5% of metastatic melanoma patients expected to survive for 5 years after diagnosis (Cummins, Cummins et al. 2006, Reed, Brewer et al. 2012). There has been a large amount of effort directed towards finding therapies to improve patient outcomes in melanoma, but these efforts have yielded limited results so far. Although initially regarded as promising breakthroughs, small molecule inhibitors targetting the BRAF mutation show limited windows of efficacy before the tumour rapidly adapts, with almost all patients acquiring resistance to the therapy (Lim, Menzies et al. 2017). One theory as to what causes this resistance and subsequent tumour resurgence is that inhibition of growth and survival signals by BRAF inhibitors can be overcome by activation of alternate signaling pathways driven by β1 integrin-mediated pro-adhesive associations with the extracellular matrix (Hirata, Girotti et al. 2015).

Another promising area of investigation is in disrupting the vascular networks feeding tumours, since avascular tumours are limited in size by the distance that oxygen can diffuse through tissue to reach the core of the tumour (Zaki, Basu et al. 2012, Maj, Papiernik et al. 2016). In addition to allowing for the delivery of oxygen and the removal of metabolic waste products from proliferating cancer cells, the vasculature of a tumour provides easy access to the circulatory system of the body, and thus is a potential pathway for metastasis (van Zijl, Krupitza et al. 2011). While there are many different strategies and specific targets, the majority of anti-angiogenic therapies developed to date have focused on disruption of the VEGF signaling pathway (Maj, Papiernik et al. 2016) Despite some promising preclinical results, these therapies have also been largely ineffective in melanoma due to the upregulation of non-VEGF derived vascularization

mechanisms within the tumour and associated stroma. These can include activation of alternate pathways for inducing endothelial cell based angiogenesis, co-option of endogenous vascular networks, and a process called Vasculogenic Mimicry involving the acquisition of endothelial-like phenotypes by melanoma cells allowing them to form vascular networks independent of endothelial cell angiogenesis (Bergers and Hanahan 2008, Pastushenko, Vermeulen et al. 2014, Felcht and Thomas 2015).

While VEGF is the primary signaling pathway involved in sprouting angiogenesis, as seen in development and wound healing, there are many other molecules within the extracellular matrix that are integrally involved in the process of tumour vascularization as well: Matrix metalloproteinases are involved in degrading extracellular matrix and liberating bound pro-angiogenic factors, Transforming Growth Factor β is involved in the recruitment of perivascular cells which stabilize newly formed vasculature, and several different collagens promote angiogenesis through integrin signaling (Pastushenko, Vermeulen et al. 2014, Felcht and Thomas 2015, Mongiat, Andreuzzi et al. 2016). The CCN family of matricellular proteins serve as regulators and modulators of how cells interact with their environment by mediating signaling of growth factors, extracellular matrix components, and other cytokines to cell surface receptors (Leask and Abraham 2006, Mongiat, Andreuzzi et al. 2016). CCN2 (formerly known as CTGF) is expressed by activated fibroblasts like those found in the tumour stroma, and is involved in angiogenesis by promoting pericyte recruitment and basement membrane organization; in fact, CCN2 null mice exhibit severe vascular defects and die shortly after birth (Mongiat, Andreuzzi et al. 2016).

In this report we use a syngeneic model of C57 BL6 mice with a conditional CCN2 deletion in fibroblasts and B16F(10) murine melanoma cells to investigate the role of stromal CCN2 in the activation of a contractile, α-SMA expressing stroma and tumour vascularization.

3.2　　Methods

3.2.1 Cell Culture

B16(F10) murine melanoma cells were purchased (ATCC) and cultured in high glucose Dulbecco's Modified Eagle's Medium (DMEM), 10% fetal bovine serum (FBS) and 1% antibiotic/antimycotic solution (Invitrogen). When indicated, cells were transfected with CTGF (CCN2) shRNA Lentiviral or control shRNA Lentiviral Particles (Santa Cruz) using polybrene and selected for using puromycin as described by the manufacturer (Santa Cruz).

3.2.2 *In vivo* tubule formation assay

50μL of Geltrex LDEV-free reduced growth factor basement membrane matrix (Thermo Fisher Scientific) was added to each well of a 96-well plate, and incubated at 37°C to allow polymerization. 10,000 cells were seeded in serum-free DMEM and incubated for 8 hours. Formed tubules were imaged on Carl Zeiss Imager M2m microscope (Carl Zeiss, Jena, Germany) using Zen Pro 2012 software. Tubule area and number of tubules and nodes were quantified using ImageJ 1.48v (National Institutes of Health, Bethesda, MD, USA).

3.2.3 Conditioned Media (CM) sample preparation

To prepare CM for LC-MS/MS, ~20 mL of CM was concentrated using a Amicon Ultra-15 3kDa MWCO ultracentrifugal units spun at 3000x g at 4C for 1.5 hours in a swinging bucket rotor. CM was subsequent rinsed with PBS to remove excess dye. Concentrated CM was lyophilized overnight and then dissolved in 8M Urea, 50mM ammonium bicarbonate (ABC), 10mM dithiothreitol (DTT), 2% SDS lysis buffer the following day. CM was quantifed using a Pierce™ 660nm Protein Assay (ThermoFisher Scientific) with ionic detegent compatibility reagent (ThermoFisher Scientific) and ~25ug of CM proteins were reduced in 10mM DTT for 30 minutes and alkylated in 100mM iodoacetamide (IAA) for 30 minutes at room temperature in the dark. CM proteins were subsequently precipitated in chloroform/methanol in 1.5mL microfuge tubes according to Wessel and Flügge (Wessel and Flugge 1984). Briefly, CM samples were topped up to 150μL with

50mM ABC, mixed with 600µL of -20°C methanol followed by 150µL of -20°C chloroform and vortexed thoroughly. An additional volume of 450µL of 4°C water was added before additional vortexing and centrifugation at 14, 000 xg for 5 min. The upper aqueous/methanol phase was carefully removed to avoid disturbing the precipitated protein interphase. A second 450µL volume of cold methanol was added to each sample followed by vigorous vortexing and centrifugation at 14, 000 xg for 5 min. The remaining chloroform/methanol was discarded and the precipitated protein pellet was left to air dry in a fume hood.

3.2.4 CM protein digestion

On-pellet protein digestion was performed similarly to Duan *et al.*(Duan, Young et al. 2009). Briefly, 100µL of 50mM ABC (pH 8) plus LysC/Trypsin (Promega) (1:50 ratio) was added to precipitated CM proteins and vortexed vigorously. CM samples were incubated at 37°C overnight (~18h) in a water bath shaker (Polyscience) at 190 rpm. An additional volume of trypsin (Promega)(1:100 ratio) was added the next day for ~4 hours before acidifying to pH 3-4 with 10% fumaric acid (FA). CM digests were centrifuged at 14,000 xg to pellet insoluble material before SCX peptide fractionation.

3.2.5 SCX peptide fractionation

Tryptic peptides recovered from CM digests were fractionated using SCX StageTips similarly to Kulak *et al.*(Kulak, Pichler et al. 2014). Briefly, peptides were acidified with 1% trifluoroacetic acid (TFA) and loaded onto a pre-rinsed 12-plug SCX StageTips. In total total, 7 SCX fractions were collected by eluting in 50,75, 125, 200, 250, 300 mM ammonium acetate/20% ACN followed by a final elution in 5 mM ammonium hydroxide/80% acetonitrile (ACN). SCX fractions were dried in a SpeedVac (Thermo Fisher), resuspended in ddH$_2$O, and dried again to evaporate residual ammonium acetate. All samples were resuspended in 0.1% FA prior to LC-MS/MS analysis.

3.2.6 LC-MS/MS

SCX fractions were analyzed using an nanoAquity UPLC system (Waters) connected to a Orbitrap Elite mass spectrometer (Thermo Scientific). Buffer A consisted of water/0.1%

FA and Buffer B consisted of ACN/0.1%FA. Peptides (~1μg estimated by BCA) were initially loaded onto an ACQUITY UPLC C18 Trap Column, 5 μm, 180 μm x 20 mm and trapped for 5 minutes at a flow rate of 10 μl/min at 99% A/1% B. Peptides were separated on an ACQUITY UPLC Peptide BEH C18 Column, 130Å, 1.7μm, 75μm x 250mm operating at a flow rate of 300 nL/min at 35°C using a non-linear gradient starting at 5% B then 7.5% B over 1 minute, 7-25% B over 179 minutes and 25-32.5% B over 30 minutes before increasing to 95% B and washing. MS precursor scans were acquired in the Orbitrap at a resolution of 60K (m/z window of 400-1450). MS/MS was performed on the top 20 most intense precursor ions in linear ion trap operating in rapid CID mode (isolation width of 2.0 m/z). A dynamic exclusion width of 30 seconds was used (dynamic exclusion mass width low and high were set to 0.5 and 1.5 respectively). An AGC target of 10000 and maximum injection time of 50 ms was used for MS/MS in the ion trap. A minimum signal threshold of 1000 and normalized collision energy of 35% was used for fragmentation. The lock mass was 445.120025 for ppm correction.

3.2.7 Data Analysis

All raw MS raw files were searched in MaxQuant (1.5.2.8) using the Mouse Uniprot database (reviewed only; updated Dec 2015). Missed cleavages were set to 3 and I=L. Cysteine carbamidomethylation was set as a fixed modification. Oxidation (M), N-terminal Acetylation (protein), and Deamidation (NQ) were set as a variable modifications (max. number of modifications per peptide = 5) and all other setting were left as default. Precursor mass deviation was left at 20 ppm and 4.5 ppm for first and main search, respectively. Fragment mass deviation was left at 20 ppm. Protein and peptide FDR was set to 0.01 (1%) and the decoy database was set to revert. Datasets were loaded into Perseus (1.5.2.6) and proteins identified by site, reverse and potential contaminants were removed. LFQ intensities were log2 transformed and missing values were imputed using a width of 0.3 and down shift of 1.8.

3.2.8 ELISA

Secreted VEGFa and proCOL1a1 levels were determined in triplicate using a Quantikine Mouse VEGF ELISA kit (R&D Systems) and Mouse Pro-Collagen I alpha 1 ELISA kit

(Abcam). Assays were performed according to the manufacturer's instructions, with 5 times dilution of conditioned media for VEGF assay. A standard curve was constructed for each assay (linear between 31.3 and 2000 pg/mL for ProCOL1a1 and between 7.8 and 500 pg/mL for VEGF).

3.2.9 Animals

Mice possessing a tamoxifen-dependent Cre recombinase under the control of a fibroblast-specific regulatory sequence from the proα2(I) collagen gene (Zheng, Zhang et al. 2002) were crossed with mice homozygous for a conditional CCN2 allele to generate Cre/CCN2 heterozygote mice, which were mated to generate mice hemizygous for Cre and homozygous for CCN2. For immunohistochemistry experiments these mice were mated with Col1a2-Cre(ER)T;Rosa26mTmG mice, generated as previously described (Liu and Leask 2013), resulting in Cre/CCN2/mTmG heterozygote mice which were mated to generate mice hemizygous for Cre and homozygous for CCN2 and mTmG. Animals used for experiments were genotyped by polymerase chain reaction (PCR) as described previously (Zheng, Zhang et al. 2002, Liu, Shi-wen et al. 2011). To delete CCN2 (CCN2-/-), excise tdTomato, and trigger expression of GFP in fibroblasts, 3-week-old mice were given intraperitoneal injections of tamoxifen suspension (0.1 ml of 10 mg/mL 4-hydroxitamoxifen, Sigma) over 5 days. Col1a2-Cre(ER)T;Rosa26mTmG were also injected with tamoxifen, and were used as controls (CCN2$^{fl/fl}$). For micro-CT experiments 3-week-old Cre/CCN2 mice were given intraperitoneal injections of tamoxifen suspension over 5 days to delete CCN2 (CCN2$^{-/-}$), and littermate contols injected with corn oil were used as controls (CCN2$^{fl/fl}$). All animal protocols were approved by the animal care committee at the University of Western Ontario.

3.2.10   *In vivo* tumour implantation

Subconfluent melanoma cells in the exponential growth phase were harvested by exposure to 0.25% trypsin/0.02% EDTA solution, resuspended in serum-free DMEM at a concentration of 3300 cells/μL, and 330,000 cells were injected subcutaneously into the right flank of each mouse. After appearance of a palpable tumour mice were monitored for 14 days before being euthanized. After euthanasia mice were either perfused with

micro-CT contrast agent as described below, or tumours were harvested, embedded in TissueTek O.C.T. compound (VWR), and frozen.

3.2.11 Immunohistochemistry

Frozen sections (20μm) were cut at -22°C using a refrigerated microtome Leica CM1900 UV cryostat (Leica, Concord, ON, Canada) and collected on Superfrost Plus slides (Fisher Scientific, Ottawa, ON, Canada). Excess O.C.T. compound was removed from sections by soaking in PBS for 30 minutes prior to blocking with 10% serum in 0.1% Triton X-100 in PBS for 1 hour and then in primary antibody in 10% serum in 0.1% Triton X-100 in PBS overnight in a humidified chamber at 4°C overnight. The primary antibodies used in this study were: anti-α-SMA (1:2000 dilution; Sigma), anti-vWF (1:200 dilution; Chemicon International), anti-SOX2 conjugated to Alexa Fluor 647 (1:100 dilution; abcam). After primary antibody incubation sections were rinsed and incubated in appropriate secondary antibodies (Jackson ImmunoResearch) at room temperature (~23°C) for 1 hour. Sections were rinsed, mounted and imaged on a Zeiss fluorescence microscope and Northern Eclipse software.

3.2.12 Vascular perfusion of micro-CT contrast agent

Mice were injected intraperitoneally with sodium heparin solution to prevent coagulation. After 15 minutes the mice were euthanized by isofluorane asphyxiation to preserve vascular structure. Each mouse had its chest opened to reveal the heart. A small incision was made in the right atrium to allow for drainage of blood, and a butterfly needle was inserted into the left ventricle. Heparinized saline was run through the butterfly needle at ~120 mmHg to flush the vasculature of blood. Once the vasculature was cleared of blood Microfil (Flow-Tech, Carver, MA) was run through the butterfly needle until vasculature was fully perfused. Microfil was allowed to polymerize for approximately 30 minutes before the butterfly needle was removed and the mouse was immersed in 4% PFA until fixed (approximately 24 hours). After preliminary CT scans to ensure full vascular perfusion of each mouse, tumours were removed and embedded in paraffin for high resolution X-ray micro-CT acquisition.

3.2.13   X-ray micro-CT acquisition

Samples were scanned on a GE Locus MS-8 x-ray conebeam micro-CT imaging system
(GE Medical Systems, London, ON) operating at a peak energy of 80 kVp and tube
current of 80 μA. 900 X-ray projections were acquired at 0.4 degree angular increments
during a full 360 degree rotation of the sample. Each projection was the average of 4
frames with an integration time of 3000 ms. The data was reconstructed into a 3D data
set with isotropic 11.473 μm voxel spacing using custom software employing a Feldkamp
filtered-backprojection algorithm. Water-filled compartments and air regions were
included in each scan as an internal reference in order to ensure that the final
reconstructions were properly calibrated in Hounsfield Units (HU). Visualization and
analysis of the 3D μCT data was performed in MicroView (GE Healthcare, Parallax
Innovations, London, ON).

3.2.14   Datasets and Analysis of Patient Samples

Level 3 TCGA RNAseqV2 gene expression data was obtained from the TCGA Data
Portal in January 2016. Enrichment for CCN2 associated gene sets was conducted using
Generally Applicable Gene-set Enrichment (GAGE, v2.12.3). Hallmark gene sets were
downloaded from the Molecular Signatures Database
(http://software.broadinstitute.org/gsea/msigdb) v5.0 on 10 August 2015 (Subramanian,
Tamayo et al. 2005). Enrichment was calculated against a formulated sample composed
of the mean expression values for each gene and sample-specific test statistics were
correlated to CCN2 expression values (log10[RSEM+1]) using Spearman's rank
correlation. The heatmap was constructed using genes from the Hallmark Angiogenesis
gene set that correlated with CCN2 expression values (log10[RSEM+1]) with a rho>0.25.
We conducted all analyses and visualizations in the RStudio programming environment
(v0.98.501). R/Bioconductor packages ggplot2, plyr, gplots, and GAGE were used where
appropriate.

3.3   Results

3.3.1 CCN2 in fibroblasts is required for the activation of contractile stroma

B16F(10) melanoma cells were injected subcutaneously into syngeneic C57 BL6 mice deleted for CCN2 or not in fibroblasts, and expressing GFP in fibroblasts. Melanoma cells were injected 2 weeks after gene deletion, and were allowed to grow for 14 days after the detection of a palpable tumour. Fresh tumour tissue was harvested and frozen in O.C.T. for sectioning. Sections were stained for anti-αSMA to determine the extent to which the stroma had adopted a contractile phenotype, and anti-SOX2 as myofibroblasts in fibrotic environments have been shown to largely express SOX2 (Tsang and Leask 2015) (Figure 1). While there was no difference in the proportion of stromal cells derived from fibroblasts (GFP positive cells), there was a significant reduction in the proportion of cells expressing SOX2 and almost no cells expressing αSMA in mice deleted for CCN2 in the stroma compared to wild-type. Additionally, the proportion of cells co-expressing GFP and SOX2 was also reduced.

These results indicate that CCN2 is not required for the recruitment of fibroblasts to the tumour stroma, but it is required for those fibroblasts to acquire SOX2 and αSMA expression, and also for non-fibroblast derived cells to acquire their expression.

3.3.2 Loss of CCN2 expression in the stroma resulted in impaired tumour vascularization *in vivo*

As lack of CCN2 causes perinatal death due to inadequate basement membrane formation and lack of pericyte recruitment to vasculature we investigated the effects of CCN2 on tumour vascularization. B16F(10) melanoma cells were injected subcutaneously into syngeneic C57 BL6 mice deleted for CCN2 in fibroblasts or not. After growing for 14 days after the appearance of a palpable tumour the mice were perfused with a micro-CT contrast agent, tumours were harvested and then scanned by x-ray micro-CT. After being calibrated against an air-water capsule, total volume of tumour and total volume of
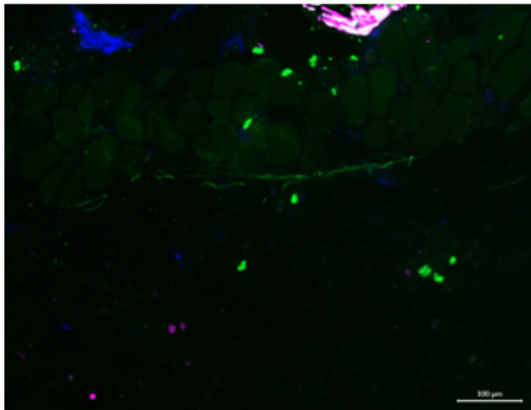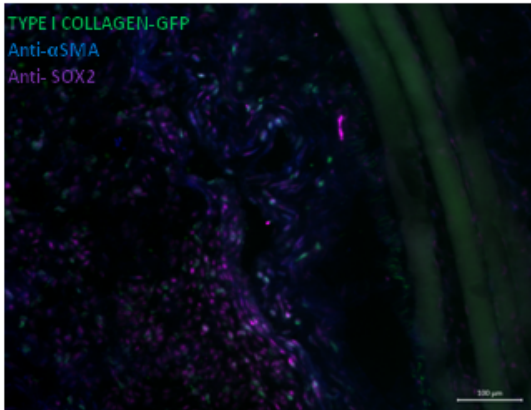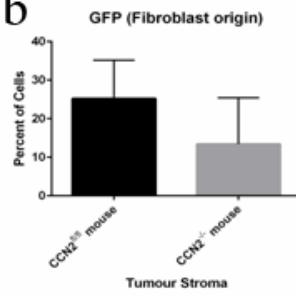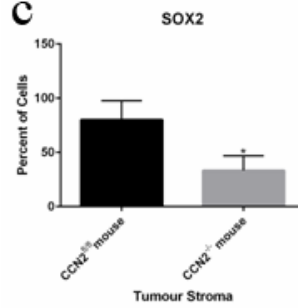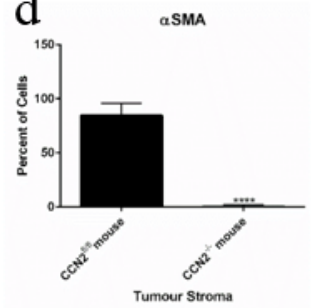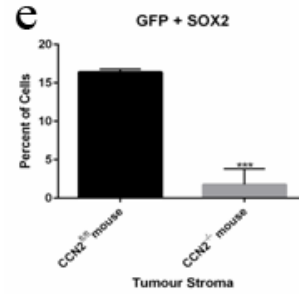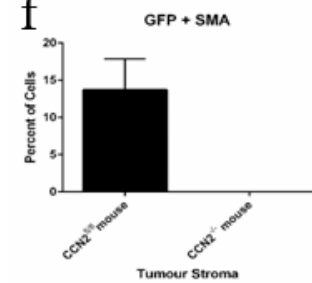
Figure 3-1 Loss of CCN2 prevents activation of αSMA and expression of plasticity marker SOX2

Sections of tumour stroma from wild-type or *Ccn2*-knockout mice (mice deleted for CCN2 in fibroblasts) which contain a GFP reporter for cells expressing collagen 1α2 (synthetic fibroblasts) at 3 weeks of age. **(a)** Sections were stained for αSMA (blue), SOX2 (violet), and GFP (green). *Ccn2*-knockout mice showed a significant reduction in **(b)** the number of cells of fibroblastic origin (GFP positive), **(c)** stromal SOX2 and **(d)** αSMA expression, as well as a significant reduction in the number of cells co-expressing GFP with **(e)** SOX2 and **(f)** αSMA (t-test, n = 3, * = p<0.05, *** = p<0.001, **** = p<0.0001)

tumour vasculature were calculated. Tumours in mice with CCN2 deleted in fibroblasts had significantly less vascular volume than those in wild-type mice (Figure 2). To see if this extended into human melanoma patients we looked at mRNA expression levels of 470 melanoma patient samples from The Cancer Genome Atlas (TCGA). CCN2 expression was strongly correlated with expression of genes in the angiogenesis gene set (Figure 3).

Taken together, this data indicates that stromal CCN2 expression is an important factor in the vascularization of tumours.

3.3.3 Loss of CCN2 in melanoma cells reduces secreted pro-angiogenic proteins and impairs vasculogenic mimicry *in vitro* and loss of CCN2 expression in the stroma impairs vasculogenic mimicry *in vivo*.

In order to determine what aspects of tumour vascularization were being affected by the loss of CCN2 we performed a matrigel tubule formation assay on B16F(10) melanoma cells that have been stably transfected with CCN2 shRNA or scrambled control shRNA. The cells transfected with CCN2 shRNA formed fewer tubules, which covered less area and met at fewer nodes, indicating a less robust network (Figure 4). This assay is typically used to determine the angiogenic potential of endothelial cells subjected to various treatments, and so is a reflection of the ability of the melanoma cells to mimic an endothelial cell phenotype by forming a tubule network. We also assessed the production and secretion of pro-angiogenic proteins by these cells. As a hypothesis-generating experiment we harvested conditioned media from the cells, concentrated the protein, and analyzed it by mass spectrometry. Analysis of secreted proteins with altered expression for functional groups revealed that pro-angiogenic proteins were reduced in the absence of CCN2 (Figure 6A). ELISAs were performed to confirm that secreted VEGFa (the major signaling ligand in angiogenesis) and proCOL1a1 (which increases angiogenic signaling through integrins and is required for capillary lumen formation) were reduced (Mongiat, Andreuzzi et al. 2016) (Figure 6B).

In order to determine the aspects of tumour vascularization being affected by loss of stromal CCN2 we implanted B16F(10) cells into mice deleted for CCN2 or not in the

Wild Type Stroma
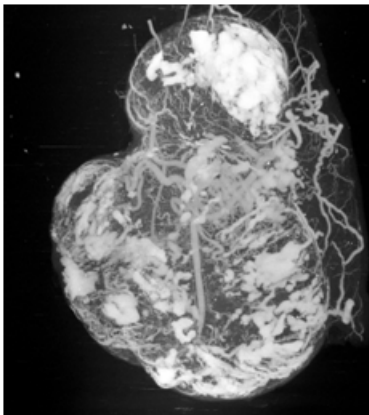
CCN2$^{-/-}$ Stroma

Volume of tumour occupied by vasculature
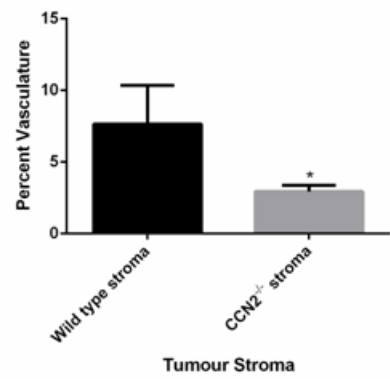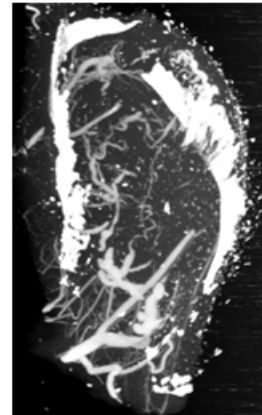
Figure 3-2 Deletion of Stromal CCN2 Reduces Tumour Vasculature

Tumours in wild-type or *Ccn2*-knockout mice (mice deleted for CCN2 in fibroblasts) were perfused with a CT-contrast agent (Microfil, Flow Tech Inc.) by injection through left ventricle and imaged. Percent volume of tumour occupied by vasculature was calculated. Mice lacking CCN2 in their fibroblasts had significantly reduced vascular volume (t-test, n = 3, p < 0.05)
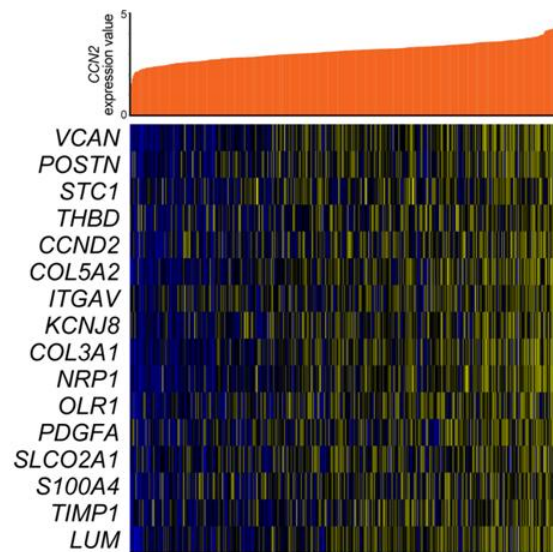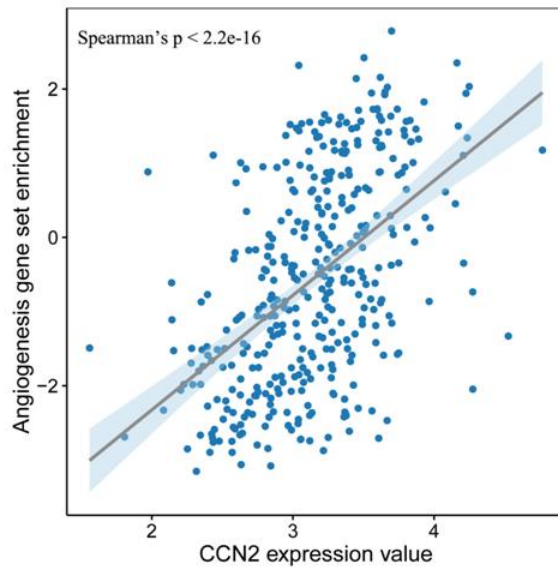
Figure 3-3 CCN2 expression correlates with angiogenesis in clinical samples

Gene expression data for melanoma patient samples (n = 468) from The Cancer Genome Atlas (TCGA) were analyzed for enrichment using the Generally Applicable Gene-set Enrichment (Gage, v2.12.3). Sample expression of CCN2 was strongly correlated with enrichment of genes in the Angiogenesis gene-set (Spearman's p<2.2e-16). Analysis was performed by Krista Vincent of the Postovit Lab at University of Alberta.

a

Control
shRNA

CCN2
shRNA

b — Number of Tubules

c — Luminal Area

d — Number of Nodes
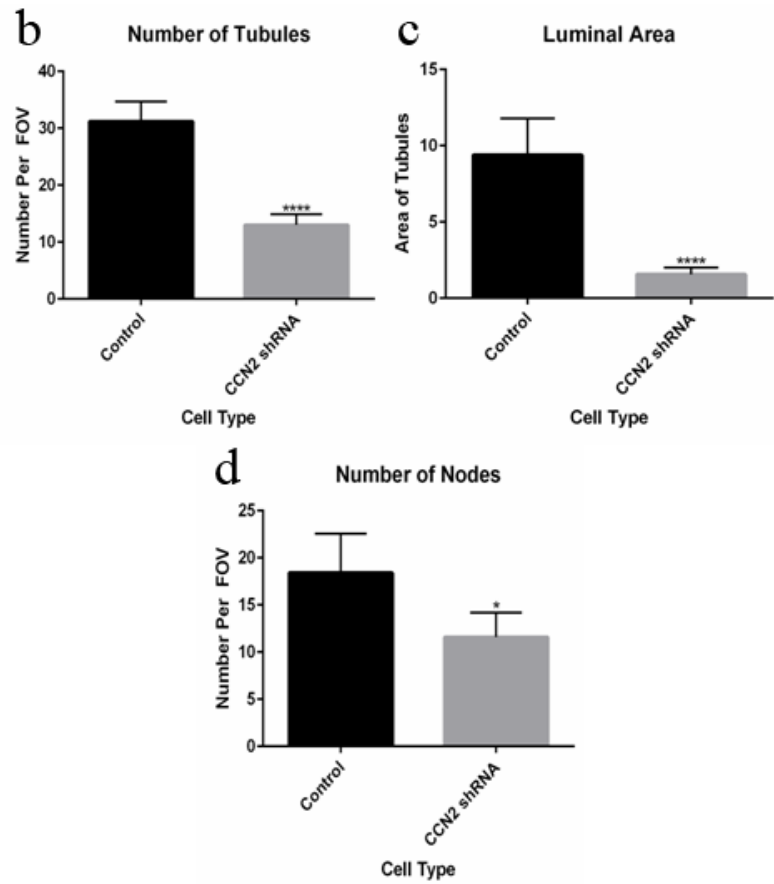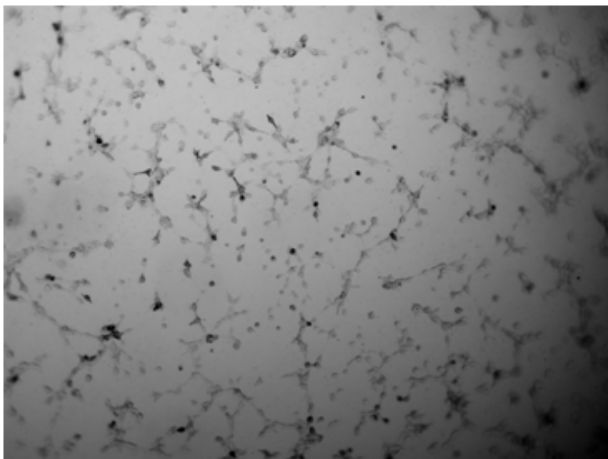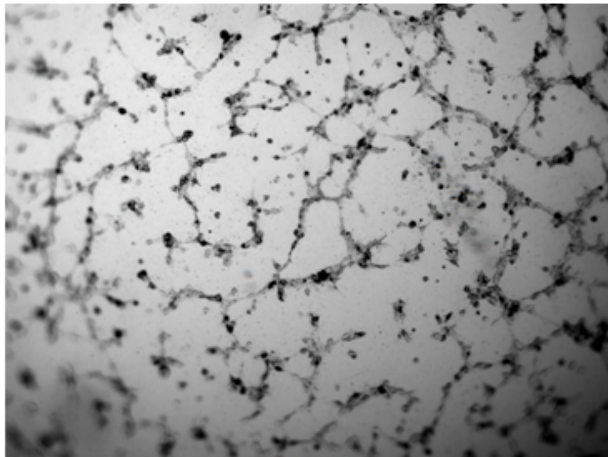
Figure 3-4 Loss of CCN2 decreases the capacity of B16F10 cells to form tubules *in vitro*

B16(F10) melanoma cells were transfected with either *CCN2* short hairpin RNA (shRNA), to produce a knockdown in *Ccn2* mRNA expression, or a scrambled shRNA, to act as a control. Cells were subjected to a tubule formation assay where 2000 cells/well were seeded in serum-free DMEM in a 96-well plate pre-coated in matrigel. After 8 hours incubation **(a)** images at the center of each well were taken. Cells transfected with *CCN2* shRNA showed a significantly decreased **(b)** number of tubules formed, **(c)** total area of tubules formed, and **(d)** number of nodes linking multiple tubules together (n = 7, * = p<0.05, **** = p<0.0001)
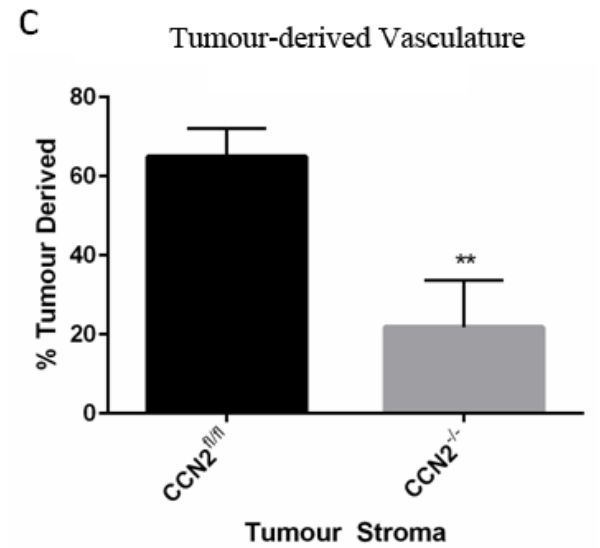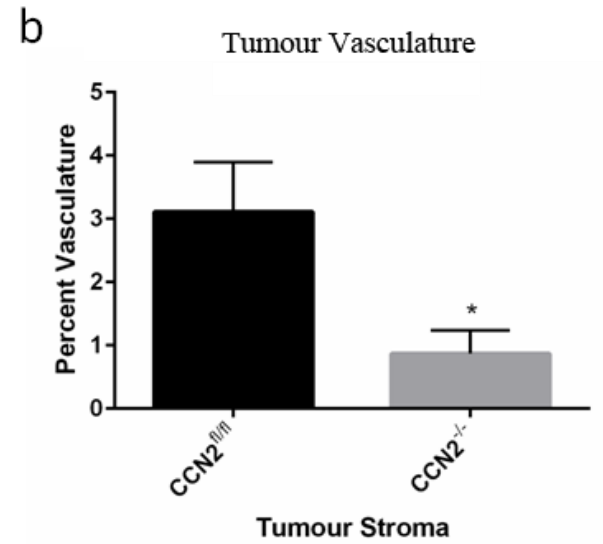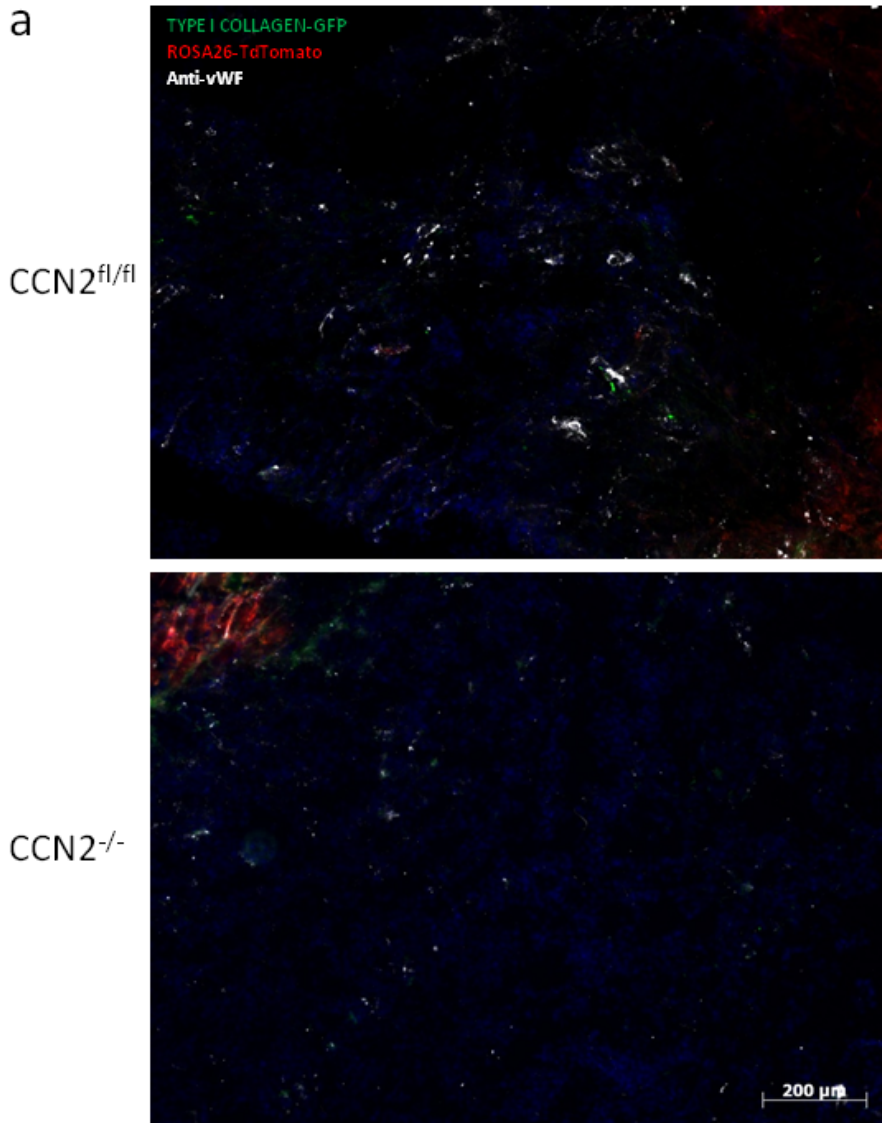
Figure 3-5 Loss of stromal CCN2 reduces tumour-derived vasculature *in vivo*

a) Sections of tumour stroma from wild-type or *Ccn2*-knockout mice (mice deleted for CCN2 in fibroblasts) which contain a GFP reporter for cells expressing collagen 1α2 (synthetic fibroblasts) at the time of deletion (3 weeks of age). Sections were stained with DAPI(blue), anti-vWF (white), tdTomato (red), and GFP (green). *Ccn2*-knockout mice have **(b)** reduced tumour vasculature, and **(c)** a reduced proportion of tumour vasculature derived from implanted tumour cells (n = 3, * = p<0.05, ** = p<0.01)

a

Protein	Expression [Log_2(CCN2shRNA) − Log_2(B16F10)]
B4galt1	-2.7318
Angpt2	-8.4071
Col1a1	-7.0607
Col5a1	-2.0109
CTGF	-8.463
Lama4	-2.1153
PGF	-1.7944
PDGFa	-4.9081
Serpine1	-7.0173
TGFb2	-2.9332
VEGFa	-6.5759
VEGFc	-1.7783

b
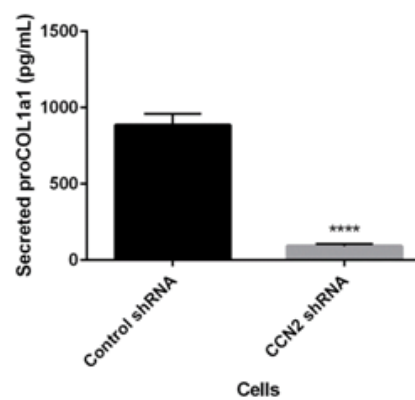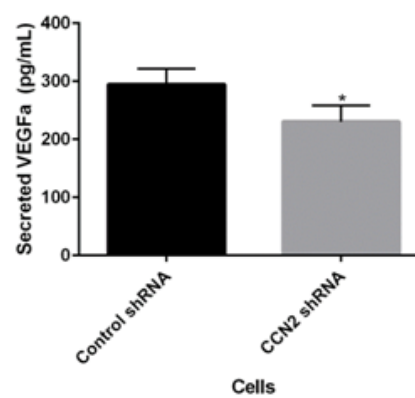
Figure 3-6 CCN2 knockdown reduces expression of secreted proteins associated with angiogenesis from B16(F10) cells

B16(F10) melanoma cells were transfected with either *CCN2* short hairpin RNA (shRNA), to produce a knockdown in *Ccn2* mRNA expression, or a scrambled shRNA, to act as a control. Cells were cultured in serum-free DMEM and conditioned media was collected. **a)** Secreted protein was analyzed by mass spectrometry to determine functional clusters affected by CCN2 deficiency (n = 1), and **(b)** ELISA to confirm changes in secreted VEGF (R&D Systems, MMV00) and COL1A1 (abcam, ab210579) (n = 3, * = p<0.05, **** = p<0.0001). Mass spectrometry performed by Dylan Dieters-Castator of Lajoie lab at University of Western Ontario.

fibroblasts, and which express GFP in fibroblasts and TdTomato in other cell types. Tumours were allowed to grow for 14 days after the appearance of a palpable tumour before being stained for anti-vWF to detect active vasculature (Figure 5A). The percentage of each section occupied by vasculature with blood flow at time of sacrifice was measured (Figure 5B), and then the percentage of that vascular area which was positive for either GFP or RFP, indicating that vessel was derived from host tissue, or was negative for both GFP and RFP, indicating that the vessel was derived from tumour cells, was calculated (Figure 5C). Tumours from mice with CCN2 deleted in fibroblasts had significantly lower vascular area, and significantly less of their vasculature was tumour derived.

3.4   Discussion

CCN2 in the tumour stroma has been shown to increase melanoma metastasis, but the mechanism behind how it does so is unclear (Hutchenreuther, Vincent et al. 2015). Our results in this report demonstrated that the loss of CCN2 from the fibroblasts of the tumour stroma resulted in a decrease of vascular volume of the tumour. They also demonstrate a reduced capability for the tumour stroma to acquire an activated, αSMA expressing phenotype in response to tumour implantation.

Tumours implanted into mice deleted for CCN2 or not in fibroblasts showed a significant reduction in stromal SOX2 expression (Fig. 3-1). SOX2 is a transcription factor that is required for stem-cell maintenance, and two major cell types that express SOX2 in the stroma are mesenchymal stromal cells and specific subpopulations of cancer associated fibroblasts (Domenech 2017). Cancer associated fibroblasts expressing higher levels of stem-markers like SOX2 belong to a subpopulation that exerts powerful promigratory effects on tumour cells through paracrine signaling (Herrera, Islam et al. 2013). This phenotype is also significantly associated with activation of αSMA expression in the fibroblasts (Herrera, Islam et al. 2013). Multipotent mesenchymal stromal cells can promote tumour vascularization by secreting factors that promote endothelial cell tubule formation, or by providing cells to form perivascular muscular layers of blood vessels,

and mesenchymal stromal cells expressing higher levels of SOX2 displayed an increased ability to revascularize wounded tissues (Rustad, Wong et al. 2012, Domenech 2017)

CCN2 has been implicated in angiogenesis, as CCN2 null mice die perinatally due in part to vascular defects such as poor basement membrane organization and lack of pericytes/smooth muscle cells (Mongiat, Andreuzzi et al. 2016). Additionally, CCN2 can induce VEGF expression through HIF-1α-dependent activation of PI3K, ERK, NF-κB and recombinant CCN2 promotes angiogenesis *in vivo* when applied to corneas (Leask and Abraham 2006, Mongiat, Andreuzzi et al. 2016). As such, we investigated the role of stromal CCN2 on the vascularization of melanoma.

While there has been a great deal of interest in developing anti-angiogenic therapies, most focus on VEGF and alternate pathways that can promote angiogenesis, or even alternate methods of vascularization that do not require angiogenesis have led to therapy failure (Maj, Papiernik et al. 2016). One of the mechanisms through which tumours can evade VEGF targeted therapies is through the expression of endothelial cell markers and the formation of vascular networks by the tumour cells themselves in a process called vasculogenic mimicry. We demonstrated that *in vitro* B16F(10) murine melanoma cells deleted for CCN2 showed a decreased capacity to form vasculogenic mimicry tubule networks, and reduced secretion of pro-angiogenic proteins. Among the secreted proteins reduced were VEGF, the major signaling ligand in sprouting angiogenesis, but also type I collagen α1 which induces survival signaling in endothelial cells and is required for proper capillary formation (Mongiat, Andreuzzi et al. 2016). By implanting tumours into mice that endogenously express GFP or TdTomato reporters in host cells but not tumour cells, and staining for vasculature we were demonstrated that the impaired vasculogenic mimicry *in vitro* was also seen *in vivo*.

In summation, this report demonstrates that loss of stromal CCN2 decreases vascular volume of tumours *in vivo*, that loss of CCN2 from melanoma cells decreases secretion of pro-angiogenic proteins *in vitro*, and that it decreases vasculogenic mimicry both *in vitro* and *in vivo*.

3.5 References

Bergers, G. and D. Hanahan (2008). "Modes of resistance to anti-angiogenic therapy." <u>Nat Rev Cancer</u> **8**(8): 592-603.

Cummins, D. L., J. M. Cummins, H. Pantle, M. A. Silverman, A. L. Leonard and A. Chanmugam (2006). "Cutaneous malignant melanoma." <u>Mayo Clin Proc</u> **81**(4): 500-507.

Domenech (2017). What are mesenchymal stromal cells? Origin and discovery of mesenchymal stromal cells. <u>Mesenchymal Stromal Cells as Tumor Stromal Modulators. 1st Edition</u>. B. a. Garcia. **37:** 1541.

Duan, X., R. Young, R. M. Straubinger, B. Page, J. Cao, H. Wang, H. Yu, J. M. Canty and J. Qu (2009). "A straightforward and highly efficient precipitation/on-pellet digestion procedure coupled with a long gradient nano-LC separation and Orbitrap mass spectrometry for label-free expression profiling of the swine heart mitochondrial proteome." <u>J Proteome Res</u> **8**(6): 2838-2850.

Felcht, M. and M. Thomas (2015). "Angiogenesis in malignant melanoma." <u>J Dtsch Dermatol Ges</u> **13**(2): 125-136.

Herrera, M., A. B. Islam, A. Herrera, P. Martin, V. Garcia, J. Silva, J. M. Garcia, C. Salas, I. Casal, A. G. de Herreros, F. Bonilla and C. Pena (2013). "Functional heterogeneity of cancer-associated fibroblasts from human colon tumors shows specific prognostic gene expression signature." <u>Clin Cancer Res</u> **19**(21): 5914-5926.

Hirata, E., M. R. Girotti, A. Viros, S. Hooper, B. Spencer-Dene, M. Matsuda, J. Larkin, R. Marais and E. Sahai (2015). "Intravital imaging reveals how BRAF inhibition generates drug-tolerant microenvironments with high integrin beta1/FAK signaling." <u>Cancer Cell</u> **27**(4): 574-588.

Hutchenreuther, J., K. M. Vincent, D. E. Carter, L. M. Postovit and A. Leask (2015). "CCN2 Expression by Tumor Stroma Is Required for Melanoma Metastasis." <u>J Invest Dermatol</u> **135**(11): 2805-2813.

Kulak, N. A., G. Pichler, I. Paron, N. Nagaraj and M. Mann (2014). "Minimal, encapsulated proteomic-sample processing applied to copy-number estimation in eukaryotic cells." <u>Nat Methods</u> **11**(3): 319-324.

Leask, A. and D. J. Abraham (2006). "All in the CCN family: essential matricellular signaling modulators emerge from the bunker." <u>J Cell Sci</u> **119**(Pt 23): 4803-4810.

Lim, S. Y., A. M. Menzies and H. Rizos (2017). "Mechanisms and strategies to overcome resistance to molecularly targeted therapy for melanoma." <u>Cancer</u> **123**(S11): 2118-2129.

Liu, S. and A. Leask (2013). "CCN2 modulates hair follicle cycling in mice." Mol Biol Cell **24**(24): 3939-3944.

Maj, E., D. Papiernik and J. Wietrzyk (2016). "Antiangiogenic cancer treatment: The great discovery and greater complexity (Review)." Int J Oncol **49**(5): 1773-1784.

Mongiat, M., E. Andreuzzi, G. Tarticchio and A. Paulitti (2016). "Extracellular Matrix, a Hard Player in Angiogenesis." Int J Mol Sci **17**(11).

Pastushenko, I., P. B. Vermeulen, G. G. Van den Eynden, A. Rutten, F. J. Carapeto, L. Y. Dirix and S. Van Laere (2014). "Mechanisms of tumor vascularization in cutaneous malignant melanoma: clinical implications." Br J Dermatol **171**(2): 220-233.

Reed, K. B., J. D. Brewer, C. M. Lohse, K. E. Bringe, C. N. Pruitt and L. E. Gibson (2012). "Increasing incidence of melanoma among young adults: an epidemiological study in Olmsted County, Minnesota." Mayo Clin Proc **87**(4): 328-334.

Rustad, K. C., V. W. Wong, M. Sorkin, J. P. Glotzbach, M. R. Major, J. Rajadas, M. T. Longaker and G. C. Gurtner (2012). "Enhancement of mesenchymal stem cell angiogenic capacity and stemness by a biomimetic hydrogel scaffold." Biomaterials **33**(1): 80-90.

Subramanian, A., P. Tamayo, V. K. Mootha, S. Mukherjee, B. L. Ebert, M. A. Gillette, A. Paulovich, S. L. Pomeroy, T. R. Golub, E. S. Lander and J. P. Mesirov (2005). "Gene set enrichment analysis: a knowledge-based approach for interpreting genome-wide expression profiles." Proc Natl Acad Sci U S A **102**(43): 15545-15550.

Tsang, M. and A. Leask (2015). "CCN2 is required for recruitment of Sox2-expressing cells during cutaneous tissue repair." J Cell Commun Signal **9**(4): 341-346.

van Zijl, F., G. Krupitza and W. Mikulits (2011). "Initial steps of metastasis: cell invasion and endothelial transmigration." Mutat Res **728**(1-2): 23-34.

Wessel, D. and U. I. Flugge (1984). "A method for the quantitative recovery of protein in dilute solution in the presence of detergents and lipids." Anal Biochem **138**(1): 141-143.

Zaki, K. A., B. Basu and P. Corrie (2012). "The role of angiogenesis inhibitors in the management of melanoma." Curr Top Med Chem **12**(1): 32-49.

Zheng, B., Z. Zhang, C. M. Black, B. de Crombrugghe and C. P. Denton (2002). "Ligand-dependent genetic recombination in fibroblasts : a potentially powerful technique for investigating gene function in fibrosis." Am J Pathol **160**(5): 1609-1617.

Bergers, G. and D. Hanahan (2008). "Modes of resistance to anti-angiogenic therapy." Nat Rev Cancer **8**(8): 592-603.

Cummins, D. L., J. M. Cummins, H. Pantle, M. A. Silverman, A. L. Leonard and A. Chanmugam (2006). "Cutaneous malignant melanoma." Mayo Clin Proc **81**(4): 500-507.

Domenech (2017). What are mesenchymal stromal cells? Origin and discovery of mesenchymal stromal cells. Mesenchymal Stromal Cells as Tumor Stromal Modulators. 1st Edition. B. a. Garcia. **37:** 1541.

Duan, X., R. Young, R. M. Straubinger, B. Page, J. Cao, H. Wang, H. Yu, J. M. Canty and J. Qu (2009). "A straightforward and highly efficient precipitation/on-pellet digestion procedure coupled with a long gradient nano-LC separation and Orbitrap mass spectrometry for label-free expression profiling of the swine heart mitochondrial proteome." J Proteome Res **8**(6): 2838-2850.

Felcht, M. and M. Thomas (2015). "Angiogenesis in malignant melanoma." J Dtsch Dermatol Ges **13**(2): 125-136.

Herrera, M., A. B. Islam, A. Herrera, P. Martin, V. Garcia, J. Silva, J. M. Garcia, C. Salas, I. Casal, A. G. de Herreros, F. Bonilla and C. Pena (2013). "Functional heterogeneity of cancer-associated fibroblasts from human colon tumors shows specific prognostic gene expression signature." Clin Cancer Res **19**(21): 5914-5926.

Hirata, E., M. R. Girotti, A. Viros, S. Hooper, B. Spencer-Dene, M. Matsuda, J. Larkin, R. Marais and E. Sahai (2015). "Intravital imaging reveals how BRAF inhibition generates drug-tolerant microenvironments with high integrin beta1/FAK signaling." Cancer Cell **27**(4): 574-588.

Hutchenreuther, J., K. M. Vincent, D. E. Carter, L. M. Postovit and A. Leask (2015). "CCN2 Expression by Tumor Stroma Is Required for Melanoma Metastasis." J Invest Dermatol **135**(11): 2805-2813.

Kulak, N. A., G. Pichler, I. Paron, N. Nagaraj and M. Mann (2014). "Minimal, encapsulated proteomic-sample processing applied to copy-number estimation in eukaryotic cells." Nat Methods **11**(3): 319-324.

Leask, A. and D. J. Abraham (2006). "All in the CCN family: essential matricellular signaling modulators emerge from the bunker." J Cell Sci **119**(Pt 23): 4803-4810.

Lim, S. Y., A. M. Menzies and H. Rizos (2017). "Mechanisms and strategies to overcome resistance to molecularly targeted therapy for melanoma." Cancer **123**(S11): 2118-2129.

Liu, S. and A. Leask (2013). "CCN2 modulates hair follicle cycling in mice." Mol Biol Cell **24**(24): 3939-3944.

Maj, E., D. Papiernik and J. Wietrzyk (2016). "Antiangiogenic cancer treatment: The great discovery and greater complexity (Review)." Int J Oncol **49**(5): 1773-1784.

Mongiat, M., E. Andreuzzi, G. Tarticchio and A. Paulitti (2016). "Extracellular Matrix, a Hard Player in Angiogenesis." Int J Mol Sci **17**(11).

Pastushenko, I., P. B. Vermeulen, G. G. Van den Eynden, A. Rutten, F. J. Carapeto, L. Y. Dirix and S. Van Laere (2014). "Mechanisms of tumour vascularization in cutaneous malignant melanoma: clinical implications." Br J Dermatol **171**(2): 220-233.

Reed, K. B., J. D. Brewer, C. M. Lohse, K. E. Bringe, C. N. Pruitt and L. E. Gibson (2012). "Increasing incidence of melanoma among young adults: an epidemiological study in Olmsted County, Minnesota." Mayo Clin Proc **87**(4): 328-334.

Rustad, K. C., V. W. Wong, M. Sorkin, J. P. Glotzbach, M. R. Major, J. Rajadas, M. T. Longaker and G. C. Gurtner (2012). "Enhancement of mesenchymal stem cell angiogenic capacity and stemness by a biomimetic hydrogel scaffold." Biomaterials **33**(1): 80-90.

Subramanian, A., P. Tamayo, V. K. Mootha, S. Mukherjee, B. L. Ebert, M. A. Gillette, A. Paulovich, S. L. Pomeroy, T. R. Golub, E. S. Lander and J. P. Mesirov (2005). "Gene set enrichment analysis: a knowledge-based approach for interpreting genome-wide expression profiles." Proc Natl Acad Sci U S A **102**(43): 15545-15550.

Tsang, M. and A. Leask (2015). "CCN2 is required for recruitment of Sox2-expressing cells during cutaneous tissue repair." J Cell Commun Signal **9**(4): 341-346.

van Zijl, F., G. Krupitza and W. Mikulits (2011). "Initial steps of metastasis: cell invasion and endothelial transmigration." Mutat Res **728**(1-2): 23-34.

Wessel, D. and U. I. Flugge (1984). "A method for the quantitative recovery of protein in dilute solution in the presence of detergents and lipids." Anal Biochem **138**(1): 141-143.

Zaki, K. A., B. Basu and P. Corrie (2012). "The role of angiogenesis inhibitors in the management of melanoma." Curr Top Med Chem **12**(1): 32-49.

Zheng, B., Z. Zhang, C. M. Black, B. de Crombrugghe and C. P. Denton (2002). "Ligand-dependent genetic recombination in fibroblasts : a potentially powerful technique for investigating gene function in fibrosis." Am J Pathol **160**(5): 1609-1617.

Chapter 4

4 CCN1 Expression in tumour stroma is required for collagen organization and melanoma metastasis

4.1 Introduction

Melanoma is an invasive cancer that is disproportionately found in young adults, and with an increasing frequency (Reed, Brewer et al. 2012). The high metastatic rate of melanoma makes it the most likely skin cancer to be fatal (Society 2013). Melanocytes are routinely assaulted by ultraviolet radiation and are highly resistant to apoptosis. Accordingly, melanoma is remarkably resistant to conventional anti-cancer treatments, leaving surgical excision as the only viable treatment (Soengas and Lowe 2003). Unfortunately, once metastasis has occurred surgical excision is no longer an effective treatment option with 5 year survival rates dropping from 90% for patients with no metastases to 36% in the presence of even local metastasis and 5% in the case of distant metastases (Homsi, Kashani-Sabet et al. 2005, Cummins, Cummins et al. 2006).

In order for cells to metastasize they have to leave the primary tumour and migrate through the activated stromal extracellular matrix. Activated cancer associated fibroblasts (CAFs) produce, organize and remodel the extracellular matrix and accordingly have significant effects on the rate and method of invasion. Stromal CAFs secrete a variety of cytokines, including transforming growth factor (TGF) β, that increase the adhesive and invasive abilities of cancer cells, and also remodel the extracellular matrix to increase stiffness and realign collagen fibres to facilitate cancer cell migration (Provenzano, Inman et al. 2008, Horimoto, Polanska et al. 2012, Kalluri 2016). Many of these pro-invasive processes are mediated by signaling and adhesion through integrins (Steeg 2006, Margadant and Sonnenberg 2010).

Abnormal expression of the CCN (named for the three prototypical members Cyr61, CTGF, and NOV) family of matricellular proteins is highly associated with metastatic melanoma as well as progression of breast, prostate, pancreatic cancers (Xie, Nakachi et al. 2001, Yang, Tuxhorn et al. 2005, Dornhofer, Spong et al. 2006, Sun, Wang et al.

2008, Sha and Leask 2011). Additionally, high levels of CCN1 and CCN2 can be stimulated in stromal tissues by tumourigenesis related inflammation (Coussens and Werb 2002, Leask and Abraham 2006, Wong and Rustgi 2013). We have previously demonstrated the importance of CCN2 expression in the tumour stroma for facilitating the metastasis of melanoma (Hutchenreuther, Vincent et al. 2015). *In vitro*, CCN1 has similar functions to CCN2 and i*n vivo*, CCN1 is also induced during tissue repair and fibrosis in a similar pattern to CCN2 (Chen, Mo et al. 2001, Leivonen, Hakkinen et al. 2005, Liu, Thompson et al. 2014). Additionally, CCN1 is induced in response to hypoxia in early melanomas and is constitutively overexpressed in advanced melanomas; CCN1 knockdown in human melanoma cells reduces cell adhesion to the integrin Very Late Antigen 4 (Kunz, Moeller et al. 2003, Schmitz, Gerber et al. 2013). While this suggests that CCN1 is active in melanoma progression it is unclear whether CCN1 is instrumental in metastasis, or what the mechanism behind its role may be.

In this report, we use C57 BL6 mice with a conditional deletion of CCN1 in fibroblasts and a syngeneic B16F(10) murine melanoma model (Wack, Kirst et al. 2002) to investigate the effect of stromal CCN1 deficiency on melanoma invasion and metastasis.

4.2   Methods

4.2.1 Cell culture and Western Blotting

B16(F10) murine melanoma cells were purchased (ATCC) and cultured in high glucose Dulbecco's Modified Eagle's Medium (DMEM), 10% fetal bovine serum (FBS) and 1% antibiotic/antimycotic solution (Invitrogen). Cells were cultured until confluence prior to harvesting for mRNA or protein extraction. CCN1 levels were evaluated by co-incubating cultures with 50μg/mL sodium heparin (Sigma). Sodium heparin was included to prevent rapid internalization and degradation of CCN1 via low density lipoprotein receptor-related protein 1 (LRP1) as endogenous CCN1 interacts similarly with LRP1 as CCN2 , which can be rapidly degraded by mouse cells (Segarini, Nesbitt et al. 2001, Juric, Chen et al. 2012). 1mL conditioned culture media was collected for every treatment, and total protein were concentrated using methanol/chloroform precipitation as previously described (Friedman, Hoving et al. 2009). The concentration of protein was

detected (Pierce) and equal amounts of protein (50 μg) were subjected to SDS/PAGE on a 10% TGX Stain-Free FastCast acrylamide gel (BioRad). Gels were then exposed to UV to activate stain-free labelling of protein, and blotted onto nitrocellulose (BioRad) and CCN1 was detected using a goat anti-CCN1 antibody (1:200 dilution, Santa Cruz) followed by a HRP-conjugated anti-rabbit antibody (1:2000; Jackson), a chemiluminescent detection kit (Pierce) and X-Ray film (Kodak). When indicated, cells were transfected with CYR61 (CCN1) shRNA, CTGF (CCN2) shRNA, or control shRNA Lentiviral Particles (Santa Cruz) using polybrene and selected for using puromycin as described by the manufacturer (Santa Cruz).

4.2.2 Real Time RT-PCR

B16(F10) murine melanoma cells were grown in high glucose DMEM containing 10% FBS until 75% confluence after which the media was replaced with low glucose DMEM containing 0.5% FBS and grown for 24 hours. RNA was harvested using Trizol (Invitrogen) and used for Real-Time RT-PCR. 25ng of RNA was reverse transcribed using qScript cDNA Supermix (Quanta Biosciences) and amplified using PerfeCTa SYBR Green FastMix and primers for genes of interest (Table 1) using the ABI Prism 7900 HT sequence detector (Applied Biosystems) according to manufacturer's instructions. Samples were run in triplicate, expression values were standardized to control values from β-actin primers using ΔΔCt method. Statistical analysis was done using Student's T-test on GraphPad.

4.2.3 Expression Profiling

Expression profiling was performed as described in prior publications (Guo, Carter et al. 2011, Guo, Carter et al. 2011, Hutchenreuther, Vincent et al. 2015) All sample labeling and processing was handled at the London Regional Genomics Centre (Robarts Research Institute, London, Ontario, Canada; http://www.lrgc.ca). Briefly, RNA quality was assessed on an Agilent 2100 Bioanalyzer (Agilent Technologies Inc.) and the RNA 6000 Nano kit (Caliper Life Sciences) before 5.5 μg of single-stranded cDNA was synthesized

Target	Forward	Reverse
B-actin	CACTGTCGAGTCGCGTCC	TCATCCATGGCGAACTGGTG
CCN1	TCTGCGCTAAACAACTCAACGA	GCAGATCCCTTTCAGAGCGG
P4Ha1	AAATGGGTATCCAACAAATGGC	GTGCGTTAGAGGACAACAGGA
LOX	ACTTCCAGTACGGTCTCCCG	GCAGCGCATCTCAGGTTGT
PLOD2	CAGGAACATGGGCATGGATTTC	GACGTGTCACAAGAGGAGCAA
COL1a1	CGATGGATTCCCGTTCGAGT	GAGGCCTCGGTGGACATTAG
α-SMA	CATCCGACACTGCTGACA	AGGTCTCAAACATAATCTGGGTCA

Table 1: Probes/Primers used in real time PCR

from 200 ng of total RNA, end-labeled, and hybridized, for 16 hours at 45 °C, to Human Gene 1.0 ST arrays. GeneChips were scanned with the GeneChip Scanner 3000 7G and probe level (.CEL file) data were generated using Affymetrix Command Console v3.2.4.

Probes were summarized to gene level data in Partek Genomics Suite v6.6 (Partek) using the RMA algorithm. Experiments were performed twice, and fold changes and P-values were generated using analysis of variance in Partek. Genes that significantly changed (at least 1.5 fold change, P-value <0.05) in response to CCN1 knockdown were compiled and exported into DAVID (http://david.abcc.ncifcrf.gov/) for further analysis.

4.2.4 *In vitro* invasion assay

10,000 CCN1 shRNA, and control shRNA B16(F10) cells were seeded in growth medium containing 0.5% FBS (and 5μg/mL puromycin hydrochloride for shRNA cells) onto a transwell filter insert with a pore size of 8 μm coated with 100μL of 10μg/mL purified bovine collagen (Advanced Biosystems) as previously described (Chen 2005). The transwell filter insert was suspended in a plate filled with growth medium containing 10% FBS (to create a chemotactic incentive to invade) and allowed to incubate at 37°C for 24 hours. After incubation all excess collagen and non-invasive cells were removed from the inside of the transwell filter insert. The remaining cells were fixed in methanol, and stained with 1μg/mL DAPI to allow for counting with microscopy.

4.2.5 Animals

Mice possessing a tamoxifen-dependent Cre recombinase under the control of a fibroblast-specific regulatory sequence from the proα2(I) collagen gene (Zheng, Zhang et al. 2002) were crossed with mice homozygous for a conditional CCN1 allele or a conditional CCN2 allele (Liu, Thompson et al. 2014) to generate Cre/CCN1 or Cre/CCN2 heterozygote mice, which were mated to generate mice hemizygous for Cre and homozygous for CCN1 or mice hemizygous for Cre and homozygous for CCN2. Animals used for experiments were genotyped by polymerase chain reaction (PCR) as described previously (Zheng, Zhang et al. 2002, Liu, Shi-wen et al. 2011). To delete CCN1 (CCN1$^{-/-}$) or CCN2 (CCN2$^{-/-}$) in fibroblasts, 3-week-old mice were given intraperitoneal injections of tamoxifen suspension (0.1 ml of 10 mg/mL 4-

hydroxitamoxifen, Sigma) over 5 days. Littermate mice of identical genotype were injected with corn oil and were used as controls (CCN1$^{fl/fl}$ or CCN2$^{fl/fl}$). All animal protocols were approved by the animal care committee at the University of Western Ontario.

4.2.6 *In vivo* tumour growth and metastasis

Subconfluent melanoma cells in the exponential growth phase were harvested by exposure to 0.25% trypsin/0.02% EDTA solution, resuspended in serum-free DMEM at a concentration of 3300 cells/μL, and 330,000 cells were injected subcutaneously into the right flank of each mouse. Upon appearance of a palpable tumour the volume of the tumour was measured daily using calipers and the following equation: Tumour Volume (mm^3) = 1/2(Length of Longest Tumour Dimension) x (Length of Narrowest Tumour Dimension)^2. Tumour growth was evaluated over the course of 14 days, and mice were euthanized on the 14th day. After euthanasia the lungs and tumour were collected from the mice and fixed in a 4% paraformaldehyde solution. After fixation, tissues were processed, embedded in paraffin, and prepared for histological sectioning. Lung sections were stained with hematoxylin and eosin (H&E; Fisher Scientific) to locate dense metastatic foci. Three non-serial sections per lung were examined.

4.2.7 Immunohistochemistry

Tumour tissue was stained for CCN1 using the Vectastain ABC Kit (Vector Laboratories). Briefly, sections (0.5 μm) were cut using a microtome (Leica), collected on Superfrost Plus slides (Fisher Scientific), de-waxed in xylene, and rehydrated by successive immersion in descending concentrations of alcohol. Antigen retrieval was performed by immersing slides in Na-citrate solution (pH 6.0) for 30 minutes at 98°C. After cooling, slides were rinsed, and non-specific binding was blocked by incubation with diluted normal serum. Sections were incubated with primary antibodies in diluted normal serum (1:100 rabbit anti-CCN1; Santa Cruz), followed by incubation with biotinylated secondary antibody solution and Vectastain ABC Reagent. After incubations, the sections were incubated in ImmPACT DAB peroxidise substrate (Vector Laboratories) and counterstained with hematoxylin. Tumour tissue was stained for

CCN2 by immunofluorescent immunohistochemistry as previously described (Liu and Leask 2013). Briefly, sections (0.5 µm) were cut using a microtome (Leica), collected on Superfrost Plus slides (Fisher Scientific), de-waxed in xylene, and rehydrated by successive immersion in descending concentrations of alcohol. Antigen retrieval was performed by immersing slides in Na-citrate solution (pH 6.0) for 30 minutes at 98°C. After cooling, slides were rinsed, and non-specific binding was blocked by incubation with 10% serum in 0.1% Triton X-100 in PBS for 1 hour and then in primary antibody (1:100 goat anti-CCN2; Santa Cruz) in 10% serum in 0.1% Triton X-100 in PBS overnight in a humidified chamber at 4°C overnight.

4.2.8 Proteomic analysis of skin

Skin from CCN1$^{fl/fl}$ and CCN1$^{-/-}$ mice was harvested, minced, and protein was dissolved in 8M urea. After eight-fold dilution with 50 mM NH_4HCO_3, pH 7.8, tryptic digestion was carried out for 18 h at 37°C, after the addition of 2% (w/w) sequencing-grade trypsin (Promega, Madison, WI, USA).

Peptide separation and mass spectrometric analyses were carried out with a nano-HPLC Proxeon (Thermo Scientific, San Jose, CA, USA) which allows in-line liquid chromatography with the capillary column, 75 µm×10 cm (Pico Tip™ EMITTER, New Objective, Woburn, MA) packed in-house using Magic C18 resin of 3 µm diameter and 200 Å pores size (Michrom BioResources, Auburn, CA) linked to mass spectrometer (LTQ-Velos, Thermo Scientific, San Jose, CA, USA) using an electrospray ionization in a survey scan in the range of m/z values 390–2000 tandem MS/MS. Equal amount of all samples were dried by rotary evaporator and re-suspended in 20 µl of 97.5 % H2O/2.4% acetonitrile/0.1% formic acid and then subjected to reversed-phase LC-ESI-MS/MS. The nano-flow reversed-phase HPLC was developed with linear 85 minutes gradient ranging from 5% to 55% of solvent B in 65 minutes (97.5% acetonitrile, 0.1% formic acid) at a flow rate of 200 nl/min with a maximum pressure of 280 bar. Electrospray voltage and the temperature of the ion transfer capillary were 1.8 kV and 250°C respectively. Each survey scan (MS) was followed by automated sequential selection of seven peptides for CID, with dynamic exclusion of the previously selected ions.

The obtained MS/MS spectra were searched against human protein databases (Swiss Prot and TrEMBL, Swiss Institute of Bioinformatics, Geneva, Switzerland, http://ca.expasy.org/sprot/) using SEQUEST algorithm in Proteome Discoverer 1.3 software (Thermo Scientific, San Jose, CA, USA). Search results were filtered for a False Discovery rate of 1% employing a decoy search strategy utilizing a reverse database. An addition inclusion criterion for positive identification of proteins was that the same protein passing the filter score from at least in three different MS analyses from the same group in a total of four MS analyses per group.

For quantitative proteome analysis, three MS raw files from each pooled group were analyzed using SIEVE software (Version 2.0 Thermo Scientific, San Jose, CA, USA). Signal processing was performed in a total of 12 MS raw files. The SIEVE experimental workflow was defined as "Control Compare Trend Analysis" where one class of samples are compared to one or more other class of samples. Here the control samples were compared to each of the samples that were treated with different percentages of NaF (1%, 2% and 5%). For the alignment step, a single MS raw file belonging to the HA group was selected as the reference file and all of the other files were adjusted to generate the best correlation to this reference file. After alignment, the feature detection and integration (or framing) process was performed using the MS level data with a feature called "Frames From MS2 Scans" only. When using this type of framing only MS mass-to-charge ratio (m/z) values that were associated with MS2 scan are used. Any m/z measurements that do not have MS2 were ignored. The parameters used consisted of a frame m/z width of 1500 ppm and a retention time width of 1.75 min. A total of 216,099 MS2 scans were present in all of the 12 RAW files that resulted in a total of 20,158 frames. Then peak integration was performed for each frame and these values were used for statistic analysis. Next, peptide sequences obtained from the database search using SEQUEST algorithm in Proteome Discoverer 1.3 were imported into SIEVE. A filter was applied to the peptide sequences during the import that eliminated all sequences with a Percolator q-value greater than 1% (false discovery rate). Peptides were grouped into proteins and a protein ratio and p-value were calculated. SIEVE uses a weighted average of the peptide intensities for the protein calculation. By using the weighted average, peptides with lower variance in their intensity measurements have a higher weight on the overall protein ratio.

This is done to decrease variance in protein level quantities based on variance of the peptides that compose proteins

4.2.9 Transmission Electron Microscopy of skin

Skin from CCN1$^{fl/fl}$ and CCN1$^{-/-}$ mice was harvested and cut into 0.5-1.0mm wedges, then fixed in 2.5% gluteraldehyde in cacodylate buffer overnight. Tissues were oriented and immobilized using mPREP system and workbench. All subsequent steps were conducted in mPREM system. Tissue was fixed/stained in 1% osmium tetroxide in cacodylate buffer (0.1M, pH 7.2) for 1 hour on ice, then rinsed 5 times in ddH$_2$O. Tissue was stained in 1% Tannic acid in cacodylate buffer for 2 hours on ice, then again in fresh 1% Tannic acid in cacodylate buffer for 2 more hours on ice. Samples were rinsed 5 times in ddH$_2$O, then incubated in 1% uranyl acetate at 4°C overnight in the dark. Samples were rinsed 5 times in ddH$_2$O before being dehydrated in successive baths of 20%, 50%, 70%, 90%, 95%, and 3 times in 100% acetone. After dehydration, samples were infiltrated overnight by mixtures of 1 part Epon-Araldite resin:2 parts acetone followed by 1 part resin:1 part acetone, followed by 2 parts resin:1 part acetone, followed by 100% resin. Samples were embedded in 100% resin, which was polymerized in 60°C oven for 5 days. Embedded samples were sectioned to a thickness of 70-80nm on the Ultracut E (Reichert-Jung) and collected on nickel grids. Grids were stained with 1% uranyl acetate for 15 minutes, rinsed 24 times before staining with Reynolds' lead citrate. Grids were rinsed 24 more times before being dried. Images were obtained on a Philips CM10 transmission electron microscope at 60 Kv.

4.3   Results

4.3.1 CCN1 is not regulated by CCN2 expression in B16F(10) murine melanoma cells or tumour stroma, and its loss decreases expression of different genes

Initial experiments were conducted in which B16F(10) melanoma cells were stably transfected with either CCN1 shRNA, CCN2 shRNA, or scrambled control shRNA. Extent of CCN1 knockdown relative to β-actin control was determined by real time PCR and Western Blot analyses (Figure 1A and 1B), and mRNA expression profiling was

performed using Human Gene 1.0 ST arrays. Genes reduced by CCN1 knockdown were compared to previously generated expression data of B16F(10) cells transfected with CCN2 shRNA (Hutchenreuther, Vincent et al. 2015) (Figure 2A). Additionally, CCN1 expression of CCN2 shRNA transfected cells was assayed by real time PCR (Figure 2B), and stromal CCN1 expression of cells implanted in mice with or without CCN2 expression in fibroblasts was detected by immunohistochemistry (Figure 2C). Expression profiling data revealed very little overlap (44/1117 genes downregulated total) in genes downregulated by both CCN1 and CCN2 loss in B16F(10) melanoma cells. Additionally, there was no significant difference in CCN1 mRNA expression from cells transfected with CCN2 shRNA, and stromal expression of CCN1 in C57 BL6 mice implanted with B16F(10) melanoma cells was still detected in mice lacking CCN2 in their fibroblasts.

4.3.2 Loss of CCN1 expression by B16F(10) murine melanoma cells results in impaired invasion

To assess the invasive ability of CCN1 deficient melanoma cells, B16F(10) melanoma cells that were transfected with either CCN1 shRNA or scrambled control shRNA were subjected to a transwell filter invasion assay. After incubation for 24 hours at 37°C, non-invasive cells and collagen were removed from the transwell membrane before it was mounted and cells were counted. Cells transfected with CCN1 shRNA showed significantly less invasion through type I collagen than cells transfected with scrambled control shRNA (Figure 1C).
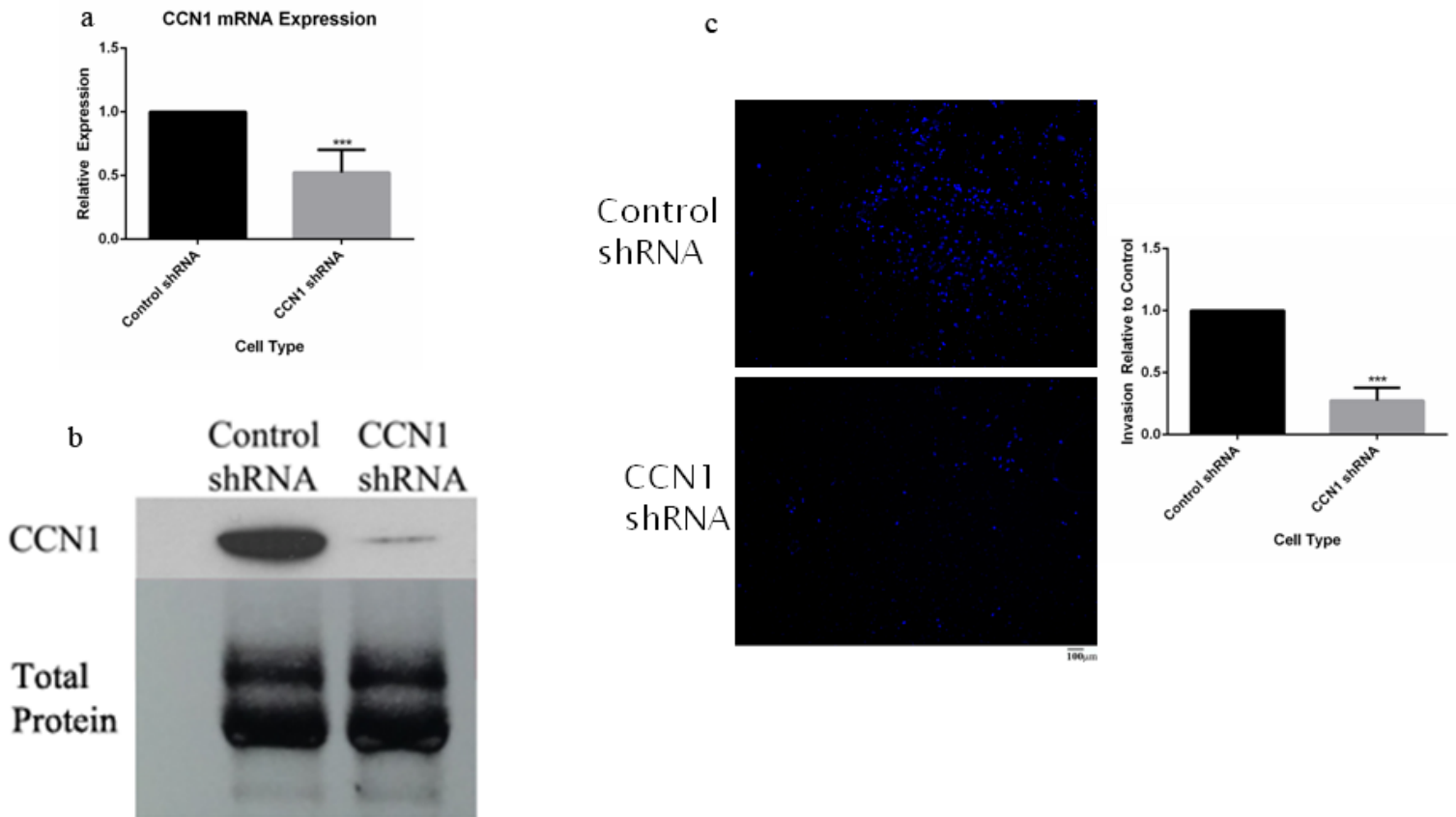
Figure 4-1 CCN1 knockdown impairs invasion through collagen

B16(F10) melanoma cells were transfected with *CCN1* shRNA, to produce a knockdown in *Ccn1* mRNA expression, or a scrambled shRNA, to act as a control. **(a)** Cells treated with *CCN1* shRNA lentiviral particles showed a significant decrease in *Ccn1* mRNA expression compared with cells treated with scrambled control shRNA (n = 3, p<0.001), and **(b)** reduced CCN1 protein present in growth media (Santa Cruz, sc-13100). **(c)** Both cell lines were subjected to a Boyden chamber assay to assess their ability to invade through a collagen matrix. After being given 24 hours to invade through collagen towards a chemotactic incentive, the non-invasive cells and collagen were removed. Invasive cells were stained with DAPI (4'6-diamidino-2-phenylindole). Cells deficient in CCN1 were significantly less invasive (n = 3, p<0.001).

a Genes showing 1.5 Fold Decrease Compared to Control

373   44   700

CCN2 shRNA (417)   CCN1 shRNA (744)

b CCN1 mRNA Expression

c CCN2$^{fl/fl}$ stroma   CCN2$^{-/-}$ stroma
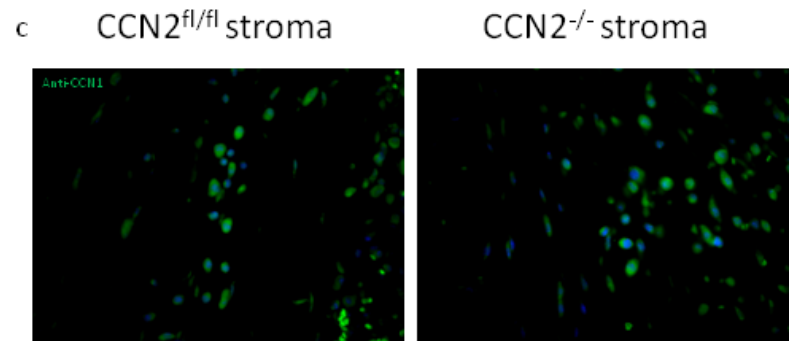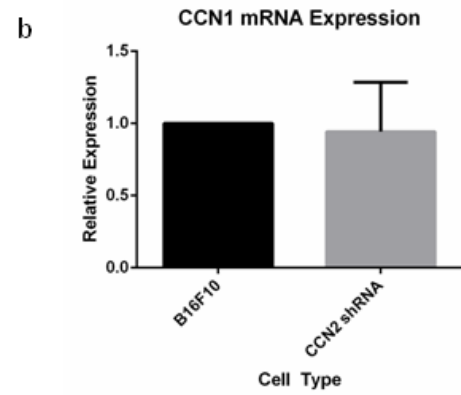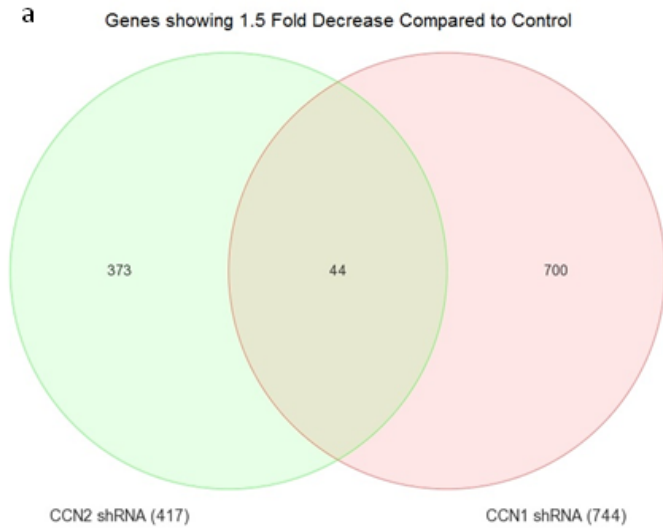
Figure 4-2 CCN1 likely acts through a different mechanism than, and is not regulated by CCN2 expression

B16(F10) melanoma cells were transfected with either *CCN2* short hairpin RNA (shRNA), to produce a knockdown in *Ccn2* mRNA expression, *CCN1* shRNA, to produce a knockdown in *Ccn1* mRNA expression, or a scrambled shRNA, to act as a control. **(a)** mRNA collected from cells was analyzed by microarray on the Human Gene 1.0 ST array (Affymetrix) to generate lists of genes with at least 1.5 fold decreased expression using Partek Genomics Suite v6.6 (Partek) when either CCN1 or CCN2 are knocked down. The majority of genes decreased by either CCN1 or CCN2 knockdown were exclusive. **(b)** Cells treated with *CCN2* shRNA showed no significant reduction in *Ccn1* mRNA expression, and **(c)** sections of tumour stroma from wild-type or *Ccn2*-knockout mice both stain positively for CCN1 expression in tumour stroma (Santa Cruz, sc-13100; n = 3, representative sections shown).

4.3.3 Loss of CCN1 expression by tumour stroma resulted in impaired metastasis *in vivo*

In order to determine if the invasive defect observed *in vitro* was seen *in vivo* as well we used a syngeneic model wherein we implanted B16F(10) melanoma cells (which are derived from C57 BL6 mice) subcutaneously into the right flank of C57 BL6 mice that had CCN1 deleted or not in their fibroblasts. Cells were suspended in serum-free DMEM and injected subcutaneously two weeks post-deletion of CCN1 and allowed to form a palpable tumour. Fourteen days later harvested lungs were sectioned, H&E stained, and assessed for extent of metastasis (Figure 3). Loss of CCN1 from the tumour stroma resulted in a significant reduction in metastasis. Loss of CCN1 from tumour stroma was confirmed by immunohistochemical analysis (Figure 5). These results indicate that CCN1 in tissue surrounding a tumour is essential for the metastasis of melanoma.

4.3.4 Loss of CCN1 expression by fibroblasts resulted in impaired collagen organization

In unpublished data generated by Katherine Quesnel of the Leask lab at the University of Western Ontario, mRNA was extracted from skin samples of wild-type and CCN1-deficient mice (mice deleted for CCN1 in the fibroblasts) and analyzed by real time PCR. Skin from CCN1-deficient mice showed a significantly reduced expression of mRNA encoding the collagen crosslinking enzymes prolyl 4-hydroxylase subunit alpha-1, lysyl oxidase, and lysyl hydroxylase 2 (translated from P4Ha1, LOX, and PLOD2 mRNA), but no reduction in the amount of type I collagen $\alpha 1$ being transcribed and no difference in transcription of α-smooth muscle actin, which is a major constituents of the contractile apparatus (Rockey, Weymouth et al. 2013). To determine if this change in mRNA expression carried over to a change in translation of functional enzymes, skin protein was dissolved in urea to solublize collagens, trypsin digested, and analyzed by LC-MS. Detected fragments were analyzed for hydroxylation of target sites for crosslinking enzymes, and a significant decrease in the number of potential target sites for PLOD2 modification that were oxidized was detected (Figure 4).

a

CCN1^{fl/fl}

CCN1^{-/-}

300μm

b
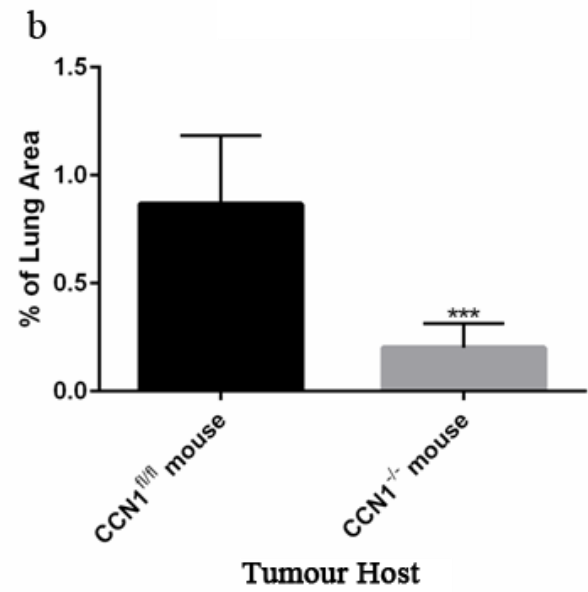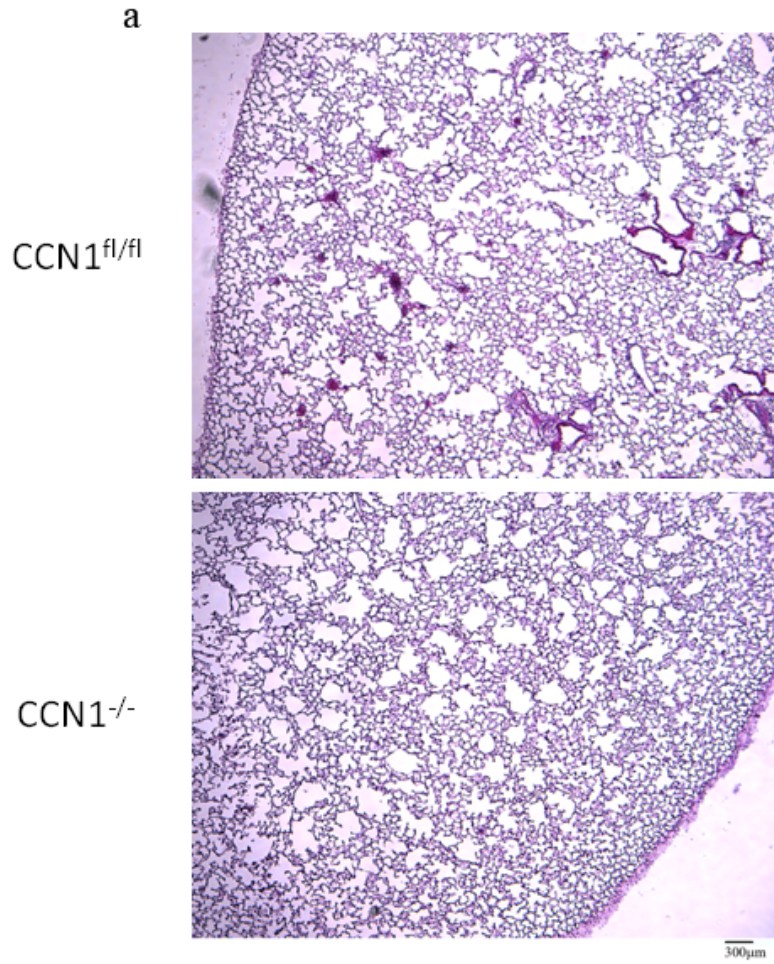
Figure 4-1 Loss of CCN1 in tumour stroma fibroblasts impairs metastasis *in vivo*

(a) Representative images of lung sections from wild-type or *Ccn1*-knockout mice (mice deleted for CCN1 in fibroblasts) following subcutaneous implantation of B16(F10) melanoma cells after 14 days of tumour growth. Hematoxylin and eosin (H&E) staining detects sites of pulmonary metastasis by staining dense metastatic foci purple. **(b)** Tumours implanted in *Ccn1*-knockout mice show a significant decrease in pulmonary metastasis compared to wild-type (n = 6, p<0.001).
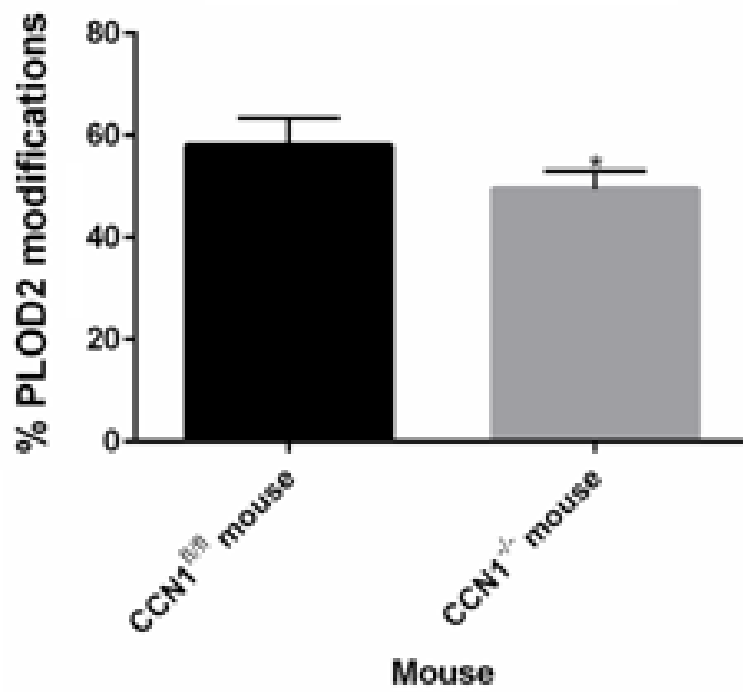
Figure 4-2 CCN1 Alters Collagen Processing and Stability

Collagen from skin samples collected from wild-type and *Ccn1*-deficient mice was solublized in Urea, digested with trypsin, and analyzed by HPLC-Mass Spectrometry. *Ccn1*-deficient samples showed a significantly reduced proportion of hydroxylation at sites targeted by crosslinking enzyme PLOD2 (n = 4, p<0.05). Mass Spectrometry performed by Yizhi Xiao of the Siqueira lab at University of Western Ontario.

| Mouse: | CCN1^{fl/fl} | CCN1^{-/-} |

Stain:

CCN1

Trichrome

CCN1   50 um
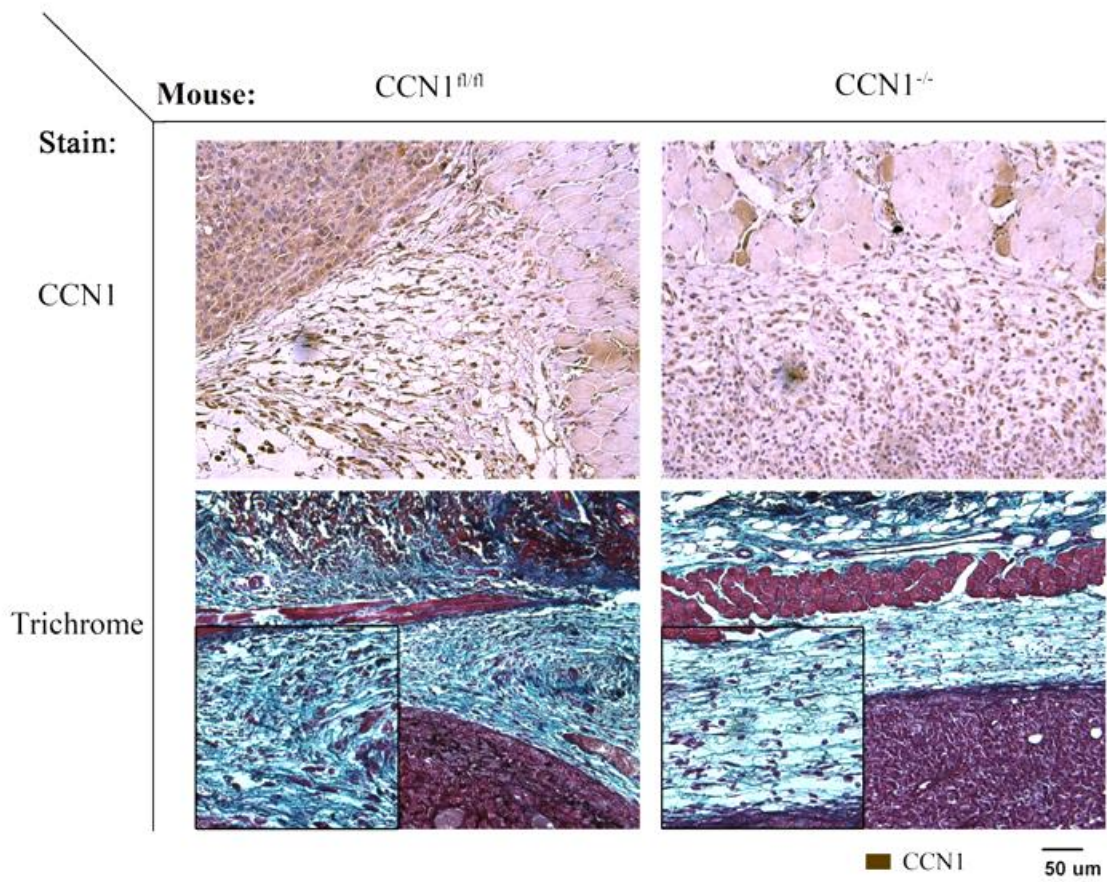
Figure 4-3 Stromal CCN1 Thickens and Organizes Collagen

Sections of tumour stroma from wild-type or *Ccn1*-knockout mice (mice deleted for CCN1 in fibroblasts) stained with anti-CCN1 (Santa Cruz, sc-13100) or Masson's trichrome. *Ccn1*-knockout stroma shows sparse blue staining, indicating a reduction in collagen, compared to wild-type stroma.

To determine the effects of CCN1 deletion from fibroblasts on the collagen architecture of the skin samples from wild-type and CCN1-deficient mice were analyzed by transmission electron microscopy after fixation and staining with uranyl acetate, osmium tetroxide, tannic acid, and Reynolds' lead citrate. High magnification cross-sectional images were used to measure the diameter of collagen fibrils (Figure 6), and lower magnification images were used to assess collagen fibre organization (Figure 7). Skin samples from CCN1-deficient mice had significantly reduced collagen fibril diameter compared to wild-type samples (Figure 6B), with the presence of abnormal interstitial spaces between fibrils making up a fiber (Figure 6A). CCN1-deficient mice also had highly disorganized collagen that failed to form thick, directional, organized fibres (Figure 7). To determine if these results were also seen in the stroma recruited by a primary melanoma tumour, sections of tumours harvested from wild-type and CCN1-deficient mice were stained for CCN1 expression to verify stromal CCN1 deletion, and by Masson's Trichrome which stains collagen fibres blue (Figure 5). Trichrome stains of CCN1-deficient mice showed a tumour stroma with more diffuse collagen than the thick, interwoven fibres formed by the stroma in the wild-type mouse.

4.4   Discussion

Our results demonstrate that CCN1 from the fibroblasts of the tumour stroma is required for the formation of an organized collagen matrix, and for melanoma metastasis. This is consistent with the concept that the cancer associated fibroblasts reshape the tumour microenvironment to encourage tumour cell invasion. This reinforces the idea that targeting the alterations to the stromal microenvironment induced by the tumour might be a viable strategy to develop widely effective anti-cancer therapies (Jewer, Findlay et al. 2012).

CCN1 is a member of the CCN family of matricellular proteins, and shows a high degree of spatiotemporal regulation due to its role as a regulatory molecule in the extracellular environment (Leask and Abraham 2006). In normal skin CCN1 shows low expression, but during wound healing is highly upregulated, secreted to the extracellular matrix where it

a

CCN1^fl/fl fibril diameter

CCN1^-/- fibril diameter

b
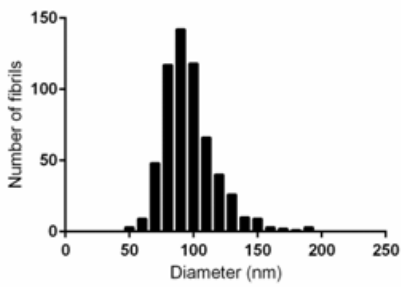
CCN1 loss reduces fibril diameter
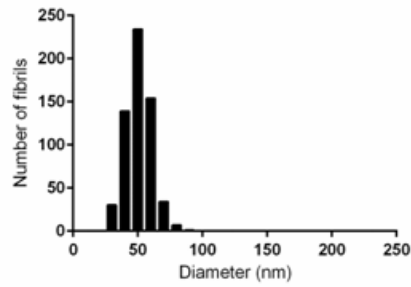
Figure 4-4 Loss of CCN1 decreases collagen fibril diameter

Sections of skin from wild-type or *Ccn1*-knockout mice (mice deleted for CCN1 in fibroblasts) were fixed and stained with gluteraldehyde, tannic acid, uranyl acetate, and Reynold's lead citrate. Samples were cut into ~70nm sections and imaged by transmission electron microscopy. **(a)** Representative cross-sectional images of collagen fibrils from wild-type and *Ccn1*-knockout mice, with diameter distribution graphs. Note the presence of interstitial spaces within each bundle of fibrils in *Ccn1*-knockout mice (indicated by arrows). **(b)** Average fibril diameter was significantly decreased in *Ccn1*-knockout mice compared to wild-type (n = 3, p<0.01)
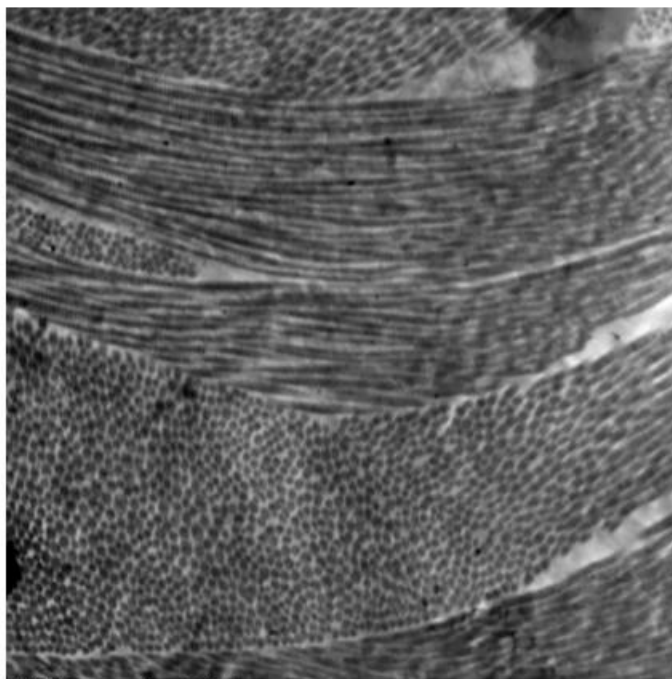
jAMES Hutchenreuther.066.tif
CCN1 f1/f1 3
Print Mag: 20600x @ 7.0 in
11:45 07/05/17
TEM Mode: Imaging
500 nm
HV=60.0kV
Direct Mag: 10500x
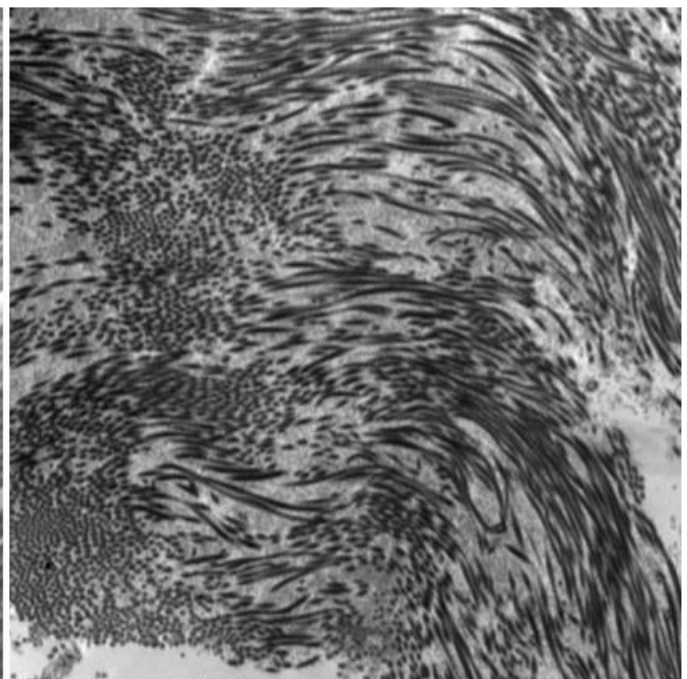
jAMES Hutchenreuther.025.tif
CCN1 -/- 2
Print Mag: 20600x @ 7.0 in
14:31 07/04/17
TEM Mode: Imaging
500 nm
HV=60.0kV
Direct Mag: 10500x

Figure 4-5 Loss of CCN1 decreases organization of collagen fibrils into fibers

Sections of skin from wild-type or *Ccn1*-knockout mice (mice deleted for CCN1 in fibroblasts) were fixed and stained with gluteraldehyde, tannic acid, uranyl acetate, and Reynolds lead citrate. Samples were cut into ~70nm sections and imaged by transmission electron microscopy. Collagen fibrils from *Ccn1*-knockout mice do not form organized, directional fibers like those seen in wild-type samples.

remains tightly associated with the tissue that produced it, and through integrin signaling and potentiation of other cytokine signaling it increases adhesion and migration in fibroblasts, as well as increasing angiogenic activity in endothelial cells (Chaqour and Goppelt-Struebe 2006, Lau 2011). In pathological conditions, CCN1 has been shown to play a role in inflammatory and fibrotic processes, as has been upregulated in fibrosis of several organs, and overexpression has been detected in a wide variety of cancers (Lai, Chen et al. 2013, Lai, Lin et al. 2014, Grazioli, Gil et al. 2015, Li, Ye et al. 2015). While it has been shown to be upregulated few studies have be done to elucidate the specific mechanisms by which CCN1 acts in cancers, but in melanoma CCN1 has been implicated in activation of the integrin VLA-4 in melanoma cells to increase their ability to extravasate at the site of metastasis, and in osteosarcoma CCN1 increases invasion and metastasis through integrin signaling (Schmitz, Gerber et al. 2013, Barreto, Ray et al. 2016). Our *in vitro* data showing that CCN1 deficient B16F(10) cells have impaired invasion through type I collagen are consistent with this, and suggesting that CCN1 might increase invasion through integrin signaling in melanoma as well. While CCN2 is known to upregulate genes associated with the deposition of new extracellular matrix in fibrotic stroma, including stimulating increased production of collagen, CCN1 has not typically been associated with such processes (Quan, Xu et al. 2014). This is understandable, given our data showing that loss of CCN1 does not affect the transcription of type I collagen, but the two proteins may act in concert by performing different functions to facilitate the accumulation of extracellular matrix proteins, with CCN2 increasing the production of collagen and CCN1 increasing the production of collagen cross-linking enzymes to stabilize and mature the collagen after production. The process of crosslinking is integral to the formation of a thick, patterned extracellular matrix that uses mechanical transduction to induce invasive phenotypes in cancer cells (Levental, Yu et al. 2009).

In summation, our *in vitro* invasion data are consistent with the hypothesis that CCN1 stimulates melanoma invasion through integrin signaling, and also shows that CCN1 is required for proper collagen matrix formation and melanoma metastasis. These data indicate that CCN1 is a potential target for disrupting the formation of a pro-metastatic tumour stroma, and is thus a novel approach to mitigate the progression of melanoma.

4.5   References

Barreto, S. C., A. Ray and P. Ag Edgar (2016). "Biological characteristics of CCN proteins in tumor development." J BUON **21**(6): 1359-1367.

Chaqour, B. and M. Goppelt-Struebe (2006). "Mechanical regulation of the Cyr61/CCN1 and CTGF/CCN2 proteins." FEBS J **273**(16): 3639-3649.

Chen, C. C., F. E. Mo and L. F. Lau (2001). "The angiogenic factor Cyr61 activates a genetic program for wound healing in human skin fibroblasts." J Biol Chem **276**(50): 47329-47337.

Chen, H. C. (2005). "Boyden chamber assay." Methods Mol Biol **294**: 15-22.

Coussens, L. M. and Z. Werb (2002). "Inflammation and cancer." Nature **420**(6917): 860-867.

Cummins, D. L., J. M. Cummins, H. Pantle, M. A. Silverman, A. L. Leonard and A. Chanmugam (2006). "Cutaneous malignant melanoma." Mayo Clin Proc **81**(4): 500-507.

Dornhofer, N., S. Spong, K. Bennewith, A. Salim, S. Klaus, N. Kambham, C. Wong, F. Kaper, P. Sutphin, R. Nacamuli, M. Hockel, Q. Le, M. Longaker, G. Yang, A. Koong and A. Giaccia (2006). "Connective tissue growth factor-specific monoclonal antibody therapy inhibits pancreatic tumor growth and metastasis." Cancer Res **66**(11): 5816-5827.

Friedman, D. B., S. Hoving and R. Westermeier (2009). "Isoelectric focusing and two-dimensional gel electrophoresis." Methods Enzymol **463**: 515-540.

Grazioli, S., S. Gil, D. An, O. Kajikawa, A. W. Farnand, J. F. Hanson, T. Birkland, P. Chen, J. Duffield, L. M. Schnapp, W. A. Altemeier and G. Matute-Bello (2015). "CYR61 (CCN1) overexpression induces lung injury in mice." Am J Physiol Lung Cell Mol Physiol **308**(8): L759-765.

Guo, F., D. E. Carter and A. Leask (2011). "Mechanical tension increases CCN2/CTGF expression and proliferation in gingival fibroblasts via a TGFbeta-dependent mechanism." PLoS One **6**(5): e19756.

Guo, F., D. E. Carter, A. Mukhopadhyay and A. Leask (2011). "Gingival fibroblasts display reduced adhesion and spreading on extracellular matrix: a possible basis for scarless tissue repair?" PLoS One **6**(11): e27097.

Homsi, J., M. Kashani-Sabet, J. L. Messina and A. Daud (2005). "Cutaneous melanoma: prognostic factors." Cancer Control **12**(4): 223-229.

Horimoto, Y., U. M. Polanska, Y. Takahashi and A. Orimo (2012). "Emerging roles of the tumor-associated stroma in promoting tumor metastasis." Cell Adh Migr **6**(3): 193-202.

Hutchenreuther, J., K. M. Vincent, D. E. Carter, L. M. Postovit and A. Leask (2015). "CCN2 Expression by Tumor Stroma Is Required for Melanoma Metastasis." <u>J Invest Dermatol</u> **135**(11): 2805-2813.

Jewer, M., S. D. Findlay and L. M. Postovit (2012). "Post-transcriptional regulation in cancer progression : Microenvironmental control of alternative splicing and translation." <u>J Cell Commun Signal</u> **6**(4): 233-248.

Juric, V., C. C. Chen and L. F. Lau (2012). "TNFalpha-induced apoptosis enabled by CCN1/CYR61: pathways of reactive oxygen species generation and cytochrome c release." <u>PLoS One</u> **7**(2): e31303.

Kalluri, R. (2016). "The biology and function of fibroblasts in cancer." <u>Nat Rev Cancer</u> **16**(9): 582-598.

Kunz, M., S. Moeller, D. Koczan, P. Lorenz, R. H. Wenger, M. O. Glocker, H. J. Thiesen, G. Gross and S. M. Ibrahim (2003). "Mechanisms of hypoxic gene regulation of angiogenesis factor Cyr61 in melanoma cells." <u>J Biol Chem</u> **278**(46): 45651-45660.

Lai, C. F., Y. M. Chen, W. C. Chiang, S. L. Lin, M. L. Kuo and T. J. Tsai (2013). "Cysteine-rich protein 61 plays a proinflammatory role in obstructive kidney fibrosis." <u>PLoS One</u> **8**(2): e56481.

Lai, C. F., S. L. Lin, W. C. Chiang, Y. M. Chen, V. C. Wu, G. H. Young, W. J. Ko, M. L. Kuo, T. J. Tsai and K. D. Wu (2014). "Blockade of cysteine-rich protein 61 attenuates renal inflammation and fibrosis after ischemic kidney injury." <u>Am J Physiol Renal Physiol</u> **307**(5): F581-592.

Lau, L. F. (2011). "CCN1/CYR61: the very model of a modern matricellular protein." <u>Cell Mol Life Sci</u> **68**(19): 3149-3163.

Leask, A. and D. J. Abraham (2006). "All in the CCN family: essential matricellular signaling modulators emerge from the bunker." <u>J Cell Sci</u> **119**(Pt 23): 4803-4810.

Leivonen, S. K., L. Hakkinen, D. Liu and V. M. Kahari (2005). "Smad3 and extracellular signal-regulated kinase 1/2 coordinately mediate transforming growth factor-beta-induced expression of connective tissue growth factor in human fibroblasts." <u>J Invest Dermatol</u> **124**(6): 1162-1169.

Levental, K. R., H. Yu, L. Kass, J. N. Lakins, M. Egeblad, J. T. Erler, S. F. Fong, K. Csiszar, A. Giaccia, W. Weninger, M. Yamauchi, D. L. Gasser and V. M. Weaver (2009). "Matrix crosslinking forces tumor progression by enhancing integrin signaling." <u>Cell</u> **139**(5): 891-906.

Li, J., L. Ye, S. Owen, H. P. Weeks, Z. Zhang and W. G. Jiang (2015). "Emerging role of CCN family proteins in tumorigenesis and cancer metastasis (Review)." <u>Int J Mol Med</u> **36**(6): 1451-1463.

Liu, S. and A. Leask (2013). "CCN2 modulates hair follicle cycling in mice." <u>Mol Biol Cell</u> **24**(24): 3939-3944.

Liu, S., X. Shi-wen, D. J. Abraham and A. Leask (2011). "CCN2 is required for bleomycin-induced skin fibrosis in mice." <u>Arthritis Rheum</u> **63**(1): 239-246.

Liu, S., K. Thompson and A. Leask (2014). "CCN2 expression by fibroblasts is not required for cutaneous tissue repair." <u>Wound Repair Regen</u> **22**(1): 119-124.

Margadant, C. and A. Sonnenberg (2010). "Integrin-TGF-beta crosstalk in fibrosis, cancer and wound healing." <u>EMBO Rep</u> **11**(2): 97-105.

Provenzano, P. P., D. R. Inman, K. W. Eliceiri, J. G. Knittel, L. Yan, C. T. Rueden, J. G. White and P. J. Keely (2008). "Collagen density promotes mammary tumor initiation and progression." <u>BMC Med</u> **6**: 11.

Quan, T., Y. Xu, Z. Qin, P. Robichaud, S. Betcher, K. Calderone, T. He, T. M. Johnson, J. J. Voorhees and G. J. Fisher (2014). "Elevated YAP and its downstream targets CCN1 and CCN2 in basal cell carcinoma: impact on keratinocyte proliferation and stromal cell activation." <u>Am J Pathol</u> **184**(4): 937-943.

Reed, K. B., J. D. Brewer, C. M. Lohse, K. E. Bringe, C. N. Pruitt and L. E. Gibson (2012). "Increasing incidence of melanoma among young adults: an epidemiological study in Olmsted County, Minnesota." <u>Mayo Clin Proc</u> **87**(4): 328-334.

Rockey, D. C., N. Weymouth and Z. Shi (2013). "Smooth muscle alpha actin (Acta2) and myofibroblast function during hepatic wound healing." <u>PLoS One</u> **8**(10): e77166.

Schmitz, P., U. Gerber, N. Schutze, E. Jungel, R. Blaheta, A. Naggi, G. Torri and G. Bendas (2013). "Cyr61 is a target for heparin in reducing MV3 melanoma cell adhesion and migration via the integrin VLA-4." <u>Thromb Haemost</u> **110**(5): 1046-1054.

Segarini, P. R., J. E. Nesbitt, D. Li, L. G. Hays, J. R. Yates, 3rd and D. F. Carmichael (2001). "The low density lipoprotein receptor-related protein/alpha2-macroglobulin receptor is a receptor for connective tissue growth factor." <u>J Biol Chem</u> **276**(44): 40659-40667.

Sha, W. and A. Leask (2011). "CCN2 expression and localization in melanoma cells." <u>J Cell Commun Signal</u> **5**(3): 219-226.

Society, A. C. (2013). "Melanoma Skin Cancer."   Retrieved January 6, 2013, from http://www.cancer.org/cancer/skincancer-melanoma/detailedguide/index.

Soengas, M. S. and S. W. Lowe (2003). "Apoptosis and melanoma chemoresistance." <u>Oncogene</u> **22**(20): 3138-3151.

Steeg, P. S. (2006). "Tumor metastasis: mechanistic insights and clinical challenges." <u>Nat Med</u> **12**(8): 895-904.

Sun, Z. J., Y. Wang, Z. Cai, P. P. Chen, X. J. Tong and D. Xie (2008). "Involvement of Cyr61 in growth, migration, and metastasis of prostate cancer cells." <u>Br J Cancer</u> **99**(10): 1656-1667.

Wack, C., A. Kirst, J. C. Becker, W. K. Lutz, E. B. Brocker and W. H. Fischer (2002). "Chemoimmunotherapy for melanoma with dacarbazine and 2,4-dinitrochlorobenzene elicits a specific T cell-dependent immune response." <u>Cancer Immunol Immunother</u> **51**(8): 431-439.

Wong, G. S. and A. K. Rustgi (2013). "Matricellular proteins: priming the tumor microenvironment for cancer development and metastasis." <u>Br J Cancer</u> **108**(4): 755-761.

Xie, D., K. Nakachi, H. Wang, R. Elashoff and H. P. Koeffler (2001). "Elevated levels of connective tissue growth factor, WISP-1, and CYR61 in primary breast cancers associated with more advanced features." <u>Cancer Res</u> **61**(24): 8917-8923.

Yang, F., J. A. Tuxhorn, S. J. Ressler, S. J. McAlhany, T. D. Dang and D. R. Rowley (2005). "Stromal expression of connective tissue growth factor promotes angiogenesis and prostate cancer tumorigenesis." <u>Cancer Res</u> **65**(19): 8887-8895.

Zheng, B., Z. Zhang, C. M. Black, B. de Crombrugghe and C. P. Denton (2002). "Ligand-dependent genetic recombination in fibroblasts : a potentially powerful technique for investigating gene function in fibrosis." <u>Am J Pathol</u> **160**(5): 1609-1617.

Chapter 5

5   Discussion

Melanoma is a highly invasive cancer with an increasing incidence that is responsible for a disproportionately large number of skin cancer fatalities for its incidence of diagnosis (Reed, Brewer et al. 2012). The two major reasons for its high rate of fatalities are that it is highly metastatic, and its high resistance to conventional anti-cancer therapies like chemo- and radiotherapy due to its melanocytic origins (Soengas and Lowe 2003). Even newly developed therapies targeting the mutations driving tumours, such as inhibition of mutant BRAF, show little efficacy as almost all tumours eventually acquire therapy resistance (Lim, Menzies et al. 2017). One prominent theory as to the source of this resistance is that tumour cell interaction with stromal extracellular matrix components activates survival signaling through the extracellular matrix association with integrin β1, which activates phosphoinositide 3-kinase (PI3K) signaling which compensates for the loss of constitutive BRAF activation (Hirata, Girotti et al. 2015).

Additionally, melanoma shows low susceptibility to anti-angiogenic therapies, with no studies showing a significant increase in overall survival in metastatic melanoma patients (Felcht and Thomas 2015). The reasons for therapeutic failure are multifactorial, but have been shown to include the infiltration of tumour stroma such as by endothelial progenitor cells, immature myeloid cells, and cancer associated fibroblasts all of which can promote the activation of alternate pro-angiogenic signaling pathways (Pastushenko, Vermeulen et al. 2014, Lupo, Caporarello et al. 2016). In addition to renewed angiogenesis, tumours can resist anti-angiogenic therapy by vasculogenic mimicry, where tumour cells themselves form a vascular network that compensates for a lack of sprouting angiogenesis as well as providing an easy route into the circulatory system for metastasis (Hendrix, Seftor et al. 2003, Felcht and Thomas 2015).

While these vasculogenic networks are formed from tumour cells, the extent of their composition and formation has been shown to depend on interactions with the tumour stroma. Mesenchymal stem cells can be reprogrammed into an endothelial cell-like

phenotype by melanoma, and the degree of vasculogenic mimicry in melanoma *in vitro* and *in vivo* can be reduced by inhibition of matrix metalloproteinase (MMP) 2 (Bergers and Hanahan 2008, Vartanian, Karshieva et al. 2016, Liang, Sun et al. 2017, Wang, You et al. 2017). Treatment of dermal fibroblasts with conditioned media from melanoma cells promotes myofibroblast differentiation, which among other things increases MMP2 secretion, and the treatment of melanoma cells with conditioned media of cells with a secretory phenotype similar to the activated fibroblasts of the stroma results in increased MMP2 expression in melanoma cells (Albinet, Bats et al. 2014, Menicacci, Laurenzana et al. 2017). These results indicate that the stroma is instrumental in vasculogenic mimicry, which is consistent with the emerging concept that alterations in the tumour microenvironment play a major role in the progression, survival, and metastasis of tumours (Jewer, Findlay et al. 2012, Quail, Taylor et al. 2012).

The CCN proteins are a family of matricellular proteins that are highly spatiotemporally regulated, with CCN1 and CCN2 showing low basal expression in adult fibroblasts that is significantly increased during wound healing and fibrosis (Leask and Abraham 2006). Additionally, abnormal expression of CCN1 and CCN2 have been associated with progression of malignant melanoma, breast, prostate, and pancreatic cancers (Xie, Nakachi et al. 2001, Yang, Tuxhorn et al. 2005, Dornhofer, Spong et al. 2006, Sha and Leask 2011). A large source of increased CCN protein expression is from activated cancer associated fibroblasts, which adopt a phenotype similar to the myofibroblasts seen in fibrosis (Albinet, Bats et al. 2014). Given that CCN2 is required for the development of fibrosis, CCN1 has been shown to have similar functions to CCN2 *in vitro* and similar expression patterns in tissue repair and fibrosis *in vivo* we used both shRNA *in vitro* and genetic knockouts *in vivo* to investigate the roles of CCN1 and CCN2 in melanoma (Chen, Mo et al. 2001, Leivonen, Hakkinen et al. 2005, Liu, Parapuram et al. 2013, Liu, Thompson et al. 2014).

In this thesis I found that knockdown of both CCN1 and CCN2 in B16F(10) melanoma cells each reduced the ability of the cells to invade through type I collagen. This is consistent with literature showing that CCN1 increases invasion in osteosarcoma, breast cancer, and pancreatic cancer, while CCN2 and invasion both increase in response to

increased YAP/TAZ signaling (Haque, Mehta et al. 2011, Jim Leu, Sung et al. 2013, Nallet-Staub, Marsaud et al. 2014, Nguyen, Song et al. 2016). Additionally, since the time of initial publication of my results it has been shown that CCN2 derived from mesenchymal stem cells increases *in vitro* invasion of squamous cell carcinoma (Wu, Li et al. 2017). Interestingly, while CCN1 has been shown to increase invasion in other cancers, it has previously been shown to decrease invasion in melanoma (Dobroff, Wang et al. 2009). Dobroff *et al.* showed that overexpression of CCN1 in highly invasive melanoma cells decreased their ability to invade through Matrigel, and knockdown of CCN1 increased their invasive ability. This is potentially explained by differences in methodologies used between their study and mine. The composition of Matrigel is very similar to that of the basement membrane separating the epidermis and the dermis, with its primary collagen being type IV while my experiments measured the ability of cells to invade through type I collagen, which is the dominant form of collagen found in the dermis (Hughes, Postovit et al. 2010, Krieg and Aumailley 2011). Thus, it is possible that CCN1 impedes the ability of melanoma cells to invade through the basement membrane, but once invasion has happened it enhances the ability of cells to invade rapidly through the dermis.

Given the similar *in vitro* functions of CCN1 and CCN2 and their similar patterns of *in vivo* expression in wound repair and fibrosis it was speculated that the genes might have similar functions in melanoma progression as well, however when the gene expression alterations of B16F(10) melanoma cells transfected with CCN2 shRNA were compared to those of cells transfected with CCN1 shRNA I found that there was very little overlap in genes with reduced expression. This suggests that while loss of CCN1 and CCN2 both reduced invasive capacity of cells *in vitro*, they are likely acting through a different mechanism. Previous studies indicate that CCN1-induced increases in melanoma invasion are likely a result of integrin signaling, as shown by the blockade of α_V integrin activation by CCN1 resulting in decrease in invasion in breast cancer and blockade of CCN1 associating with the integrin VLA-4 resulting in a decrease in invasion in melanoma (Jim Leu, Sung et al. 2013, Schmitz, Gerber et al. 2013), but the mechanisms through which CCN2 increases metastasis are less well established. Our results showing

CCN2 induces invasion through increased expression of periostin (POSTN) are consistent with previous observations that POSTN expression correlates with metastasis in several cancers, promotes invasiveness in pancreatic cancer cells, and that recombinant CCN2 can induce POSTN expression in periodontal ligament cells (Asano, Kubota et al. 2005, Baril, Gangeswaran et al. 2007, Tilman, Mattiussi et al. 2007, Kotobuki, Yang et al. 2014).

When B16F(10) melanoma cells with CCN2 knockdown or not were implanted into syngeneic C57 BL6 mice with CCN2 deleted in fibroblasts or not I found that loss of CCN2 in the fibroblasts significantly impaired the metastasis of the tumour. This is consistent with previous studies showing that not only are high levels of CCN2 a prognositic factor for aggressive pancreatic cancer, but also that antibodies blocking CCN2 block anchorage independent growth *in vitro* and significantly reduce metastasis of pancreatic cancer *in vivo* (Dornhofer, Spong et al. 2006, Bennewith, Huang et al. 2009). Additionally, high levels of stromal CCN2 expression are poor prognostic markers in glioma, pancreatic, and prostate cancers (Wells, Howlett et al. 2015). Interestingly, the co-culture of squamous cell carcinoma cells with mesenchymal stem cells induced increase expression of CCN2 in the mesenchymal stem cells that in turn enhanced the invasion of the cancer cells *in vitro* (Wu, Li et al. 2017). In multiple cancers, including melanoma, CCN2 is upregulated by hypoxia and by YAP/TAZ/Hippo, and suppression of YAP-TEAD complex activity in ovarian cancer using verteporfin decreased CCN2 expression without significantly affecting expression of upstream Hippo components yielding a decreased volume of gross ascites in preclinical models (Minchenko, Kharkova et al. 2014, Nallet-Staub, Marsaud et al. 2014, Feng, Gou et al. 2016). These data support my findings that stromal CCN2 is essential for the metastasis of melanoma and suggest that depriving the tumour of stromal CCN2 is a viable therapy to reduce the metastasis of melanoma.

Loss of CCN2 from the fibroblasts of the mouse did not significantly alter the recruitment of resident synthetic fibroblasts to the tumour stroma, but it did reduce the proportion of stromal cells expressing stemness marker SOX2, and also almost completely eliminated αSMA expression in the stroma which is indicative of the activation of myofibroblasts

(Hinz 2016). This is significant because activation of fibroblasts in the tumour stroma has been shown to cause increased matrix metalloproteinase secretion, increased expression of TGFβ, tenascin C, POSTN, and cytokines that recruit more cells to the activated stroma (Horimoto, Polanska et al. 2012, Kalluri 2016). Loss of CCN2 preventing activation of the tumour stroma also serves to further link together the stromal microenvironment and fibrosis, as it establishes that in both pathologies fibroblasts are differentiated into myofibroblasts in a CCN2 dependent fashion that differs from that seen in normal wound repair (Liu, Shi-wen et al. 2011, Liu, Parapuram et al. 2013, Liu, Thompson et al. 2014). The impaired induction of both αSMA and SOX2 as well as the reduced pulmonary metastasis in the absence of stromal CCN2 are consistent with the findings of Herrera *et al* that cancer associated fibroblasts expressing high levels of αSMA and stemness markers like SOX2 correlate with the induction of a strong pro-migratory effect in cancer cells by the stroma (Herrera, Islam et al. 2013).

Another finding of this study is that tumours lacking CCN2 in the fibroblasts of their stroma have significantly reduced vasculature. This is consistent with prior studies showing that CCN2 is upregulated by hypoxia, promotes endothelial cell proliferation and tubule formation, and induces VEGF expression through hypoxia inducible factor (HIF)-1α-dependent pathways (Leask and Abraham 2006, Jun and Lau 2011, Mongiat, Andreuzzi et al. 2016). Additionally, recombinant CCN2 applied to corneas promotes angiogenesis, and CCN2 null mice die shortly after birth and show vascular defects (Leask and Abraham 2006). CCN2 expression is spatiotemporally correlated with the expansion of blood vessels seen in repair of ischemic, hyperoxic, and hyperglycemic injuries (Krupska, Bruford et al. 2015). In agreement with the results of this study showing CCN2 is strongly correlated with pro-angiogenic gene expression in clinical patients CCN2 blocking antibodies have been shown to prevent angiogenesis and the formation of microvasculature in pancreatic and breast cancer models (Aikawa, Gunn et al. 2006, Shimo, Kubota et al. 2006).

B16F(10) cells with CCN2 knockdown showed a reduction in secreted pro-angiogenic proteins. Reduced VEGFa and type I collagen α1 secretion were confirmed by ELISA of

conditioned media. VEGFa is highly expressed in most cancers, and is one of the primary molecules involved in driving angiogenesis (Pastushenko, Vermeulen et al. 2014). In addition, cells with higher expression of VEGF and its receptors have been shown to have a greater capacity for vasculogenic mimicry, and blockade of VEGF *in vitro* has been shown to inhibit tubule formation associated with vasculogenic mimicry in melanoma, ovarian carcinoma, and osteosarcoma (Vartanian, Burova et al. 2007, Mei, Gao et al. 2008, Wang, Sun et al. 2008). Additionally, type I collagen has been shown to be required for the proper formation of capillaries, and has been seen focally in some intratumoural patterns formed through vasculogenic mimicry and has been shown to have 97-fold increased expression in invasive vasculognic mimicry capable melanoma cells when compared to cells that are incapable of vasculogenic mimicry (Lin, Maniotis et al. 2005).

Consistent with these facts, this study showed that loss of CCN2 both *in vitro* and *in vivo* reduced vasculogenic mimicry. B16F(10) cells transfected with CCN2 shRNA to produce a knockdown in CCN2 expression formed fewer tubules in a matrigel-based tubule formation assay than those transfected with a scrambled control shRNA did, indicating they have a reduced capacity to form vasculogenic networks. Since vasculogenic mimicry is associated with poor prognosis in melanoma and is largely impervious to current anti-angiogenic therapies despite the loss of vasculogenic mimicry when VEGF is blocked *in vitro*, the ability to impede its development *in vivo* is of potential clinical signifigance (Wang, You et al. 2017).

A novel finding of this study is that reduced vasculogenic mimicry was observed *in vivo* when CCN2 was deleted in fibroblasts. C57 BL6 mice expressing either GFP or TdTomato in all endogenous tissues and with CCN2 deleted or not in fibroblasts had B16F(10) melanoma cells implanted subcutaneously. Once a tumour had grown, it was harvested and stained for vWF, a marker expressed in both mouse and tumour derived vasculature (Dunleavey and Dudley 2012). Not only did tumours with CCN2 deleted in fibroblasts show reduced vascular area, but they also showed a significantly reduced proportion of vasculature arising from vasculogenic mimicry. While there has been little research has been done on the role of activated tumour stroma on inducing a vasculogenic

mimicry phenotype on tumour cells, with most studies focusing on either the activated stroma's impact on total vascularization or the tumour's ability to induce vasculogenic mimicry in non-endothelial stromal cells, these results are consistent with and build upon the few *in vitro* studies on cancer cell lines that have been performed. Menicacci *et al.* have shown that melanoma cells grown in the conditioned media of fibroblasts with a similar secretory phenotype to cancer associated fibroblasts show an increase in their production of matrix metalloproteinase (MMP) 2 (Menicacci, Laurenzana et al. 2017), and two recent studies independently show that inhibition of MMP2 *in vitro* reduces vasculogenic mimicry (Liang, Sun et al. 2017, Wang, You et al. 2017). Additionally, dermal fibroblasts grown in conditioned medium from melanoma cells differentiate into myofibroblasts and display increased MMP2 production, representing a potential additional source of MMP2 to induce vasculogenic mimicry (Albinet, Bats et al. 2014). The results of this study indicate that, similar to fibrosis, myofibroblast differentiation is dependent on CCN2, and thus the lack of myofibroblasts in the tumour stroma may be responsible for the decreased vasculogenic mimicry observed in tumours with CCN2 deleted in their fibroblasts (Liu, Parapuram et al. 2013, Liu, Thompson et al. 2014).

When B16F(10) melanoma cells were implanted into syngeneic mice with CCN1 deleted in fibroblasts or not I found that loss of CCN1 in the fibroblasts significantly impaired the pulmonary metastasis of the tumour. This is consistent with literature showing that CCN1 expression is increased in aggressive or advanced prostate cancer, glioma, breast cancer, colorectal cancer, ovarian cancer, and osteosarcoma (Leask and Abraham 2006, Li, Ye et al. 2015, Barreto, Ray et al. 2016). It is worth noting that while these correlations are well established, and tumour-cell derived CCN1 has been shown to increase cancer progression through association with α_v integrin that to my knowledge no study has been done directly testing the effects of stromal CCN1 on tumour progression has been performed (Monnier, Farmer et al. 2008). However, the results of this study are consistent with the observation that low molecular weight heparin administered to patients reduces their incidence of metastasis by preventing VLA-4/V-CAM1 binding, that CCN1 mediates this binding, and that heparin binds to CCN1 and prevents this mediation (Fritzsche, Simonis et al. 2008, Schmitz, Gerber et al. 2013).

To determine the mechanism by which the deletion or blockade of CCN1 might prevent the metastasis of melanoma, skin from mice with CCN1 deleted in their fibroblasts or not was analyzed. In unpublished work from Katherine Quesnel in our lab, CCN1 deletion in fibroblasts was shown to reduce the transcription of genes encoding crosslinking enzymes P4Ha1, LOX, and PLOD2. In order to determine if there was any functional difference in collagen crosslinking resultant from this decrease, protein from the skin was dissolved in Urea and analyzed by mass spectrometry. When peptide sequences were analyzed I found that there was no difference in hydroxylation of sites associated with P4Ha1 crosslinking, which is consistent with the fact that collagen lacking P4Ha1 crosslinking results in collagens that are not stable at physiological temperatures so any collagens not crosslinked due to reduced activity would rapidly degrade (Bella 2016), but there was a significant reduction in the hydroxylation of sites associated with PLOD2 crosslinking. The observed reduction in PLOD2 and its activity is consistent with the results of previous studies showing that PLOD2 is transcribed in response to SMAD3-dependent TGFβ induction, and that CCN1 enhances profibrotic TGFβ/SMAD3 signaling in myofibroblasts, and that fibroblasts associated with melanoma show a significant increase in PLOD2 expression (Slany, Meshcheryakova et al. 2014, Kurundkar, Kurundkar et al. 2016, Du, Pang et al. 2017).

To determine if the lack of PLOD2 activity translated into any defects in collagen architecture, tumours were stained with Masson's Trichrome. The collagen surrounding the tumour was more sparse in mice with CCN1 deleted in their fibroblasts than in wild type. Additionally, skin samples from both types of mice were imaged by transmission electron microscopy, and mice with CCN1 deleted in their fibroblasts displayed a significantly reduced collagen fibril diameter, and a lack of organized fibre structure like that seen in wild type. These results are consistent with previous studies showing that cancer associated fibroblasts and myofibroblasts organize the collagen of the extracellular matrix into highly aligned fibers, that the stability of these fibers are primarily mediated by PLOD2-catalyzed crosslinking that occurs both intracellularly and extracellularly, and that depletion of PLOD2 from the stroma of melanoma reduces the proinvasive effects of cancer associated fibroblasts on the tumour (Chen, Guo et al. 2016, Du, Pang et al. 2017). In fibrotic tissues, excessive PLOD2-catalyzed crosslinking reduces degradation by

collagenases leading to the accumulation of a stiff matrix (Gjaltema, de Rond et al. 2015). The stiffness of this matrix then serves to stimulate myofibroblast differentiation, leading to more collagen production in both fibrotic conditions and in cancer associated fibroblasts (Gjaltema, de Rond et al. 2015, Zhang, Grither et al. 2016). In addition to further activating the fibroblasts of the stromal microenvironment this stiff matrix can exert mechanical stress on cancer cells and in doing so reprogram them into more pro-invasive phenotypes in prostate cancer, breast cancer, and non-small cell lung cancer (Zaman, Trapani et al. 2006, Goetz, Minguet et al. 2011, Fenner, Stacer et al. 2014, Navab, Strumpf et al. 2016).

While these results are consistent with and expand on other work in the literature, there are some limitations to the experiments used that might impact the translatability of the results. These results were derived largely from experiments performed *in vitro* and in animal models, and as such they might not be directly representative of the processes occurring in patients due to both the differences between human and mouse physiology and the differences in genetic diversity between an inbred mouse line and the patients seen in clinic. Additionally, while the promoter used to achieve knockout of CCN1 and CCN2 in fibroblasts is specific to fibroblasts in adult mice (Bou-Gharios, Garrett et al. 1996), it is only effective in synthetic fibroblasts, and would not successfully delete CCN1 or CCN2 in non-synthetic, senescent fibroblast populations that might contribute to the formation of an activated tumour stroma. While this is a limitation in the deletion given the results showing reduced pulmonary metastasis and tumour vascularization, the absence of deleted proteins from the stroma of tumours, and the efficacy with which knockout of CCN2 in synthetic fibroblasts using this promoter prevents the development of fibrosis it is unlikely that senescent fibroblasts contribute to the activated tumour stroma significantly. It is also of note that the deletion occurs in every synthetic fibroblast in the body, not just those in the dermis that might be recruited to the stroma. Because of this, it is possible that the deletion of CCN1 and CCN2 from the fibroblasts in the lung is having some effect on the ability of cells to properly extravasate and survive during metastasis. For example, it has been reported that increased periostin expression from pulmonary fibroblasts is required for the survival of cancer stem cells which extravasate into the lung to form pulmonary metastases (Malanchi, Santamaria-Martinez

et al. 2011). Given that deletion of CCN2 prevented expression of periostin in the tumour stroma it is conceivable that it is having the same effect in pulmonary fibroblasts and this lack of pulmonary periostin is influencing the amount of detected metastasis. While I elected to use syngeneic implantation of tumour cells due to the effects of the primary tumour on the microenvironment making it a closer mimic of the conditions of metastasis in patients, the impact of primary tumour stroma CCN proteins and pulmonary metastatic site CCN proteins could be deconvoluted in future studies by tail vein injection of melanoma cells. A limitation in the micro-CT scans that determined tumour vascularity is that the Microfil compound that was used to perfuse the tumours was injected at a pressure that replicates physiological conditions. This means that any vessels temporarily occluded, as occurs during cycling hypoxia, would not have been detected (Muz, de la Puente et al. 2015). While this might be overcome by increasing the injection pressure, that would likely result in the rupture of capillaries. Since the vascular area of tumour sections showed the same reduction in mice with CCN2 deleted from their fibroblasts as the vascular volume in micro-CT scans it is unlikely this significantly altered the data collected.

Despite these limitations, it is clear that CCN1 and CCN2 in the tumour stroma play important roles in the metastasis of melanoma. Future work to build off of these discoveries should include tail vein injection of cells to determine the extent to which CCN2 in the pulmonary metastatic microenvironment is contributing to metastasis through periostin expression. Additionally, implantation of tumours into mice which have been subjected to an experimental model of dermal fibrosis, such as bleomycin injection or deletion of PTEN from the fibroblasts, would serve to increase evidence that the fibrotic nature of the microenvironment is enhancing the metastasis of the tumour. Finally since CCN1 and CCN2 are both important for metastasis, but seem to have different functions it would be useful to find a therapy that targets both proteins at once. Since elevated YAP has been shown to induce expression of CCN1 and CCN2, and a widely clinically used drug (verteporfin) that prevents the activity of YAP has been shown to be effective at controlling the progression of other cancers in mouse models it would be an ideal first target for studies either administering verteporfin to mice

implanted with melanoma, or implanting the cells into mice which have had YAP deleted in their fibroblasts(Quan, Xu et al. 2014, Feng, Gou et al. 2016).

In summation, I found that both CCN1 and CCN2 in the tumour stroma contribute to the metastasis of melanoma, but they do so in distinct ways. CCN1 is required for the formation of organized collagen fibres which promote invasion and metastasis through the transduction of mechanical stress onto cancer cells, through the activation of pro-invasive phenotypes by integrin signaling, and by forming directional channels through which the tumour cells can move. CCN2 is required for the activation of the tumour stroma into a fibrotic environment containing myofibroblasts, and for the vascularization of the tumour which provides easy access to the circulatory system for metastasis. Given the stroma's demonstrated role in promoting the progression and metastasis of melanoma, and its hypothesized role in contributing to therapy resistance by tumours, my findings indicate that the CCN family of proteins represent an exciting potential therapeutic target for the disruption of pro-tumourigenic stroma.

5.1   References

Aikawa, T., J. Gunn, S. M. Spong, S. J. Klaus and M. Korc (2006). "Connective tissue growth factor-specific antibody attenuates tumor growth, metastasis, and angiogenesis in an orthotopic mouse model of pancreatic cancer." <u>Mol Cancer Ther</u> **5**(5): 1108-1116.

Albinet, V., M. L. Bats, A. Huwiler, P. Rochaix, C. Chevreau, B. Segui, T. Levade and N. Andrieu-Abadie (2014). "Dual role of sphingosine kinase-1 in promoting the differentiation of dermal fibroblasts and the dissemination of melanoma cells." <u>Oncogene</u> **33**(26): 3364-3373.

Asano, M., S. Kubota, T. Nakanishi, T. Nishida, T. Yamaai, G. Yosimichi, K. Ohyama, T. Sugimoto, Y. Murayama and M. Takigawa (2005). "Effect of connective tissue growth factor (CCN2/CTGF) on proliferation and differentiation of mouse periodontal ligament-derived cells." <u>Cell Commun Signal</u> **3**: 11.

Baril, P., R. Gangeswaran, P. C. Mahon, K. Caulee, H. M. Kocher, T. Harada, M. Zhu, H. Kalthoff, T. Crnogorac-Jurcevic and N. R. Lemoine (2007). "Periostin promotes invasiveness and resistance of pancreatic cancer cells to hypoxia-induced cell death: role of the beta4 integrin and the PI3k pathway." <u>Oncogene</u> **26**(14): 2082-2094.

Barreto, S. C., A. Ray and P. Ag Edgar (2016). "Biological characteristics of CCN proteins in tumor development." <u>J BUON</u> **21**(6): 1359-1367.

Bella, J. (2016). "Collagen structure: new tricks from a very old dog." <u>Biochem J</u> **473**(8): 1001-1025.

Bennewith, K. L., X. Huang, C. M. Ham, E. E. Graves, J. T. Erler, N. Kambham, J. Feazell, G. P. Yang, A. Koong and A. J. Giaccia (2009). "The role of tumor cell-derived connective tissue growth factor (CTGF/CCN2) in pancreatic tumor growth." <u>Cancer Res</u> **69**(3): 775-784.

Bergers, G. and D. Hanahan (2008). "Modes of resistance to anti-angiogenic therapy." <u>Nat Rev Cancer</u> **8**(8): 592-603.

Bou-Gharios, G., L. A. Garrett, J. Rossert, K. Niederreither, H. Eberspaecher, C. Smith, C. Black and B. Crombrugghe (1996). "A potent far-upstream enhancer in the mouse pro alpha 2(I) collagen gene regulates expression of reporter genes in transgenic mice." <u>J Cell Biol</u> **134**(5): 1333-1344.

Chaqour, B. and M. Goppelt-Struebe (2006). "Mechanical regulation of the Cyr61/CCN1 and CTGF/CCN2 proteins." <u>FEBS J</u> **273**(16): 3639-3649.

Chen, C. C., F. E. Mo and L. F. Lau (2001). "The angiogenic factor Cyr61 activates a genetic program for wound healing in human skin fibroblasts." <u>J Biol Chem</u> **276**(50): 47329-47337.

Chen, H. C. (2005). "Boyden chamber assay." <u>Methods Mol Biol</u> **294**: 15-22.

Chen, Y., H. Guo, M. Terajima, P. Banerjee, X. Liu, J. Yu, A. A. Momin, H. Katayama, S. M. Hanash, A. R. Burns, G. B. Fields, M. Yamauchi and J. M. Kurie (2016). "Lysyl Hydroxylase 2 Is Secreted by Tumor Cells and Can Modify Collagen in the Extracellular Space." J Biol Chem **291**(50): 25799-25808.

Coussens, L. M. and Z. Werb (2002). "Inflammation and cancer." Nature **420**(6917): 860-867.

Cummins, D. L., J. M. Cummins, H. Pantle, M. A. Silverman, A. L. Leonard and A. Chanmugam (2006). "Cutaneous malignant melanoma." Mayo Clin Proc **81**(4): 500-507.

Dobroff, A. S., H. Wang, V. O. Melnikova, G. J. Villares, M. Zigler, L. Huang and M. Bar-Eli (2009). "Silencing cAMP-response element-binding protein (CREB) identifies CYR61 as a tumor suppressor gene in melanoma." J Biol Chem **284**(38): 26194-26206.

Dornhofer, N., S. Spong, K. Bennewith, A. Salim, S. Klaus, N. Kambham, C. Wong, F. Kaper, P. Sutphin, R. Nacamuli, M. Hockel, Q. Le, M. Longaker, G. Yang, A. Koong and A. Giaccia (2006). "Connective tissue growth factor-specific monoclonal antibody therapy inhibits pancreatic tumor growth and metastasis." Cancer Res **66**(11): 5816-5827.

Du, H., M. Pang, X. Hou, S. Yuan and L. Sun (2017). "PLOD2 in cancer research." Biomed Pharmacother **90**: 670-676.

Dunleavey, J. M. and A. C. Dudley (2012). "Vascular Mimicry: Concepts and Implications for Anti-Angiogenic Therapy." Curr Angiogenes **1**(2): 133-138.

Felcht, M. and M. Thomas (2015). "Angiogenesis in malignant melanoma." J Dtsch Dermatol Ges **13**(2): 125-136.

Feng, J., J. Gou, J. Jia, T. Yi, T. Cui and Z. Li (2016). "Verteporfin, a suppressor of YAP-TEAD complex, presents promising antitumor properties on ovarian cancer." Onco Targets Ther **9**: 5371-5381.

Fenner, J., A. C. Stacer, F. Winterroth, T. D. Johnson, K. E. Luker and G. D. Luker (2014). "Macroscopic stiffness of breast tumors predicts metastasis." Sci Rep **4**: 5512.

Friedman, D. B., S. Hoving and R. Westermeier (2009). "Isoelectric focusing and two-dimensional gel electrophoresis." Methods Enzymol **463**: 515-540.

Fritzsche, J., D. Simonis and G. Bendas (2008). "Melanoma cell adhesion can be blocked by heparin in vitro: suggestion of VLA-4 as a novel target for antimetastatic approaches." Thromb Haemost **100**(6): 1166-1175.

Gjaltema, R. A., S. de Rond, M. G. Rots and R. A. Bank (2015). "Procollagen Lysyl Hydroxylase 2 Expression Is Regulated by an Alternative Downstream Transforming Growth Factor beta-1 Activation Mechanism." J Biol Chem **290**(47): 28465-28476.

Goetz, J. G., S. Minguet, I. Navarro-Lerida, J. J. Lazcano, R. Samaniego, E. Calvo, M. Tello, T. Osteso-Ibanez, T. Pellinen, A. Echarri, A. Cerezo, A. J. Klein-Szanto, R. Garcia, P. J. Keely, P. Sanchez-Mateos, E. Cukierman and M. A. Del Pozo (2011). "Biomechanical remodeling of the microenvironment by stromal caveolin-1 favors tumor invasion and metastasis." Cell **146**(1): 148-163.

Grazioli, S., S. Gil, D. An, O. Kajikawa, A. W. Farnand, J. F. Hanson, T. Birkland, P. Chen, J. Duffield, L. M. Schnapp, W. A. Altemeier and G. Matute-Bello (2015). "CYR61 (CCN1) overexpression induces lung injury in mice." Am J Physiol Lung Cell Mol Physiol **308**(8): L759-765.

Guo, F., D. E. Carter and A. Leask (2011). "Mechanical tension increases CCN2/CTGF expression and proliferation in gingival fibroblasts via a TGFbeta-dependent mechanism." PLoS One **6**(5): e19756.

Guo, F., D. E. Carter, A. Mukhopadhyay and A. Leask (2011). "Gingival fibroblasts display reduced adhesion and spreading on extracellular matrix: a possible basis for scarless tissue repair?" PLoS One **6**(11): e27097.

Haque, I., S. Mehta, M. Majumder, K. Dhar, A. De, D. McGregor, P. J. Van Veldhuizen, S. K. Banerjee and S. Banerjee (2011). "Cyr61/CCN1 signaling is critical for epithelial-mesenchymal transition and stemness and promotes pancreatic carcinogenesis." Mol Cancer **10**: 8.

Hendrix, M. J., E. A. Seftor, A. R. Hess and R. E. Seftor (2003). "Vasculogenic mimicry and tumour-cell plasticity: lessons from melanoma." Nat Rev Cancer **3**(6): 411-421.

Herrera, M., A. B. Islam, A. Herrera, P. Martin, V. Garcia, J. Silva, J. M. Garcia, C. Salas, I. Casal, A. G. de Herreros, F. Bonilla and C. Pena (2013). "Functional heterogeneity of cancer-associated fibroblasts from human colon tumors shows specific prognostic gene expression signature." Clin Cancer Res **19**(21): 5914-5926.

Hinz, B. (2016). "Myofibroblasts." Exp Eye Res **142**: 56-70.

Hirata, E., M. R. Girotti, A. Viros, S. Hooper, B. Spencer-Dene, M. Matsuda, J. Larkin, R. Marais and E. Sahai (2015). "Intravital imaging reveals how BRAF inhibition generates drug-tolerant microenvironments with high integrin beta1/FAK signaling." Cancer Cell **27**(4): 574-588.

Homsi, J., M. Kashani-Sabet, J. L. Messina and A. Daud (2005). "Cutaneous melanoma: prognostic factors." Cancer Control **12**(4): 223-229.

Horimoto, Y., U. M. Polanska, Y. Takahashi and A. Orimo (2012). "Emerging roles of the tumor-associated stroma in promoting tumor metastasis." Cell Adh Migr **6**(3): 193-202.

Hughes, C. S., L. M. Postovit and G. A. Lajoie (2010). "Matrigel: a complex protein mixture required for optimal growth of cell culture." Proteomics **10**(9): 1886-1890.

Hutchenreuther, J., K. M. Vincent, D. E. Carter, L. M. Postovit and A. Leask (2015). "CCN2 Expression by Tumor Stroma Is Required for Melanoma Metastasis." J Invest Dermatol **135**(11): 2805-2813.

Jewer, M., S. D. Findlay and L. M. Postovit (2012). "Post-transcriptional regulation in cancer progression : Microenvironmental control of alternative splicing and translation." J Cell Commun Signal **6**(4): 233-248.

Jim Leu, S. J., J. S. Sung, M. L. Huang, M. Y. Chen and T. W. Tsai (2013). "A novel anti-CCN1 monoclonal antibody suppresses Rac-dependent cytoskeletal reorganization and migratory activities in breast cancer cells." Biochem Biophys Res Commun **434**(4): 885-891.

Jun, J. I. and L. F. Lau (2011). "Taking aim at the extracellular matrix: CCN proteins as emerging therapeutic targets." Nat Rev Drug Discov **10**(12): 945-963.

Juric, V., C. C. Chen and L. F. Lau (2012). "TNFalpha-induced apoptosis enabled by CCN1/CYR61: pathways of reactive oxygen species generation and cytochrome c release." PLoS One **7**(2): e31303.

Kalluri, R. (2016). "The biology and function of fibroblasts in cancer." Nat Rev Cancer **16**(9): 582-598.

Kotobuki, Y., L. Yang, S. Serada, A. Tanemura, F. Yang, S. Nomura, A. Kudo, K. Izuhara, H. Murota, M. Fujimoto, I. Katayama and T. Naka (2014). "Periostin accelerates human malignant melanoma progression by modifying the melanoma microenvironment." Pigment Cell Melanoma Res **27**(4): 630-639.

Krieg, T. and M. Aumailley (2011). "The extracellular matrix of the dermis: flexible structures with dynamic functions." Exp Dermatol **20**(8): 689-695.

Krupska, I., E. A. Bruford and B. Chaqour (2015). "Eyeing the Cyr61/CTGF/NOV (CCN) group of genes in development and diseases: highlights of their structural likenesses and functional dissimilarities." Hum Genomics **9**: 24.

Kunz, M., S. Moeller, D. Koczan, P. Lorenz, R. H. Wenger, M. O. Glocker, H. J. Thiesen, G. Gross and S. M. Ibrahim (2003). "Mechanisms of hypoxic gene regulation of angiogenesis factor Cyr61 in melanoma cells." J Biol Chem **278**(46): 45651-45660.

Kurundkar, A. R., D. Kurundkar, S. Rangarajan, M. L. Locy, Y. Zhou, R. M. Liu, J. Zmijewski and V. J. Thannickal (2016). "The matricellular protein CCN1 enhances TGF-beta1/SMAD3-dependent profibrotic signaling in fibroblasts and contributes to fibrogenic responses to lung injury." FASEB J **30**(6): 2135-2150.

Lai, C. F., Y. M. Chen, W. C. Chiang, S. L. Lin, M. L. Kuo and T. J. Tsai (2013). "Cysteine-rich protein 61 plays a proinflammatory role in obstructive kidney fibrosis." PLoS One **8**(2): e56481.

Lai, C. F., S. L. Lin, W. C. Chiang, Y. M. Chen, V. C. Wu, G. H. Young, W. J. Ko, M. L. Kuo, T. J. Tsai and K. D. Wu (2014). "Blockade of cysteine-rich protein 61 attenuates renal inflammation and fibrosis after ischemic kidney injury." Am J Physiol Renal Physiol **307**(5): F581-592.

Lau, L. F. (2011). "CCN1/CYR61: the very model of a modern matricellular protein." Cell Mol Life Sci **68**(19): 3149-3163.

Leask, A. and D. J. Abraham (2006). "All in the CCN family: essential matricellular signaling modulators emerge from the bunker." J Cell Sci **119**(Pt 23): 4803-4810.

Leivonen, S. K., L. Hakkinen, D. Liu and V. M. Kahari (2005). "Smad3 and extracellular signal-regulated kinase 1/2 coordinately mediate transforming growth factor-beta-induced expression of connective tissue growth factor in human fibroblasts." J Invest Dermatol **124**(6): 1162-1169.

Levental, K. R., H. Yu, L. Kass, J. N. Lakins, M. Egeblad, J. T. Erler, S. F. Fong, K. Csiszar, A. Giaccia, W. Weninger, M. Yamauchi, D. L. Gasser and V. M. Weaver (2009). "Matrix crosslinking forces tumor progression by enhancing integrin signaling." Cell **139**(5): 891-906.

Li, J., L. Ye, S. Owen, H. P. Weeks, Z. Zhang and W. G. Jiang (2015). "Emerging role of CCN family proteins in tumorigenesis and cancer metastasis (Review)." Int J Mol Med **36**(6): 1451-1463.

Liang, X., R. Sun, X. Zhao, Y. Zhang, Q. Gu, X. Dong, D. Zhang, J. Sun and B. Sun (2017). "Rictor regulates the vasculogenic mimicry of melanoma via the AKT-MMP-2/9 pathway." J Cell Mol Med.

Lim, S. Y., A. M. Menzies and H. Rizos (2017). "Mechanisms and strategies to overcome resistance to molecularly targeted therapy for melanoma." Cancer **123**(S11): 2118-2129.

Lin, A. Y., A. J. Maniotis, K. Valyi-Nagy, D. Majumdar, S. Setty, S. Kadkol, L. Leach, J. Pe'er and R. Folberg (2005). "Distinguishing fibrovascular septa from vasculogenic mimicry patterns." Arch Pathol Lab Med **129**(7): 884-892.

Liu, S. and A. Leask (2013). "CCN2 modulates hair follicle cycling in mice." Mol Biol Cell **24**(24): 3939-3944.

Liu, S., S. K. Parapuram and A. Leask (2013). "Fibrosis caused by loss of PTEN expression in mouse fibroblasts is crucially dependent on CCN2." Arthritis Rheum **65**(11): 2940-2944.

Liu, S., X. Shi-wen, D. J. Abraham and A. Leask (2011). "CCN2 is required for bleomycin-induced skin fibrosis in mice." Arthritis Rheum **63**(1): 239-246.

Liu, S., K. Thompson and A. Leask (2014). "CCN2 expression by fibroblasts is not required for cutaneous tissue repair." Wound Repair Regen **22**(1): 119-124.

Lupo, G., N. Caporarello, M. Olivieri, M. Cristaldi, C. Motta, V. Bramanti, R. Avola, M. Salmeri, F. Nicoletti and C. D. Anfuso (2016). "Anti-angiogenic Therapy in Cancer: Downsides and New Pivots for Precision Medicine." Front Pharmacol **7**: 519.

Malanchi, I., A. Santamaria-Martinez, E. Susanto, H. Peng, H. A. Lehr, J. F. Delaloye and J. Huelsken (2011). "Interactions between cancer stem cells and their niche govern metastatic colonization." Nature **481**(7379): 85-89.

Margadant, C. and A. Sonnenberg (2010). "Integrin-TGF-beta crosstalk in fibrosis, cancer and wound healing." EMBO Rep **11**(2): 97-105.

Mei, J., Y. Gao, L. Zhang, X. Cai, Z. Qian, H. Huang and W. Huang (2008). "VEGF-siRNA silencing induces apoptosis, inhibits proliferation and suppresses vasculogenic mimicry in osteosarcoma in vitro." Exp Oncol **30**(1): 29-34.

Menicacci, B., A. Laurenzana, A. Chilla, F. Margheri, S. Peppicelli, E. Tanganelli, G. Fibbi, L. Giovannelli, M. Del Rosso and A. Mocali (2017). "Chronic Resveratrol Treatment Inhibits MRC5 Fibroblast SASP-Related Protumoral Effects on Melanoma Cells." J Gerontol A Biol Sci Med Sci.

Minchenko, O. H., A. P. Kharkova, K. I. Kubaichuk, D. O. Minchenko, N. A. Hlushchak and O. V. Kovalevska (2014). "Effect of hypoxia on the expression of CCN2, PLAU, PLAUR, SLURP1, PLAT and ITGB1 genes in ERN1 knockdown U87 glioma cells." Ukr Biochem J **86**(4): 79-89.

Mongiat, M., E. Andreuzzi, G. Tarticchio and A. Paulitti (2016). "Extracellular Matrix, a Hard Player in Angiogenesis." Int J Mol Sci **17**(11).

Monnier, Y., P. Farmer, G. Bieler, N. Imaizumi, T. Sengstag, G. C. Alghisi, J. C. Stehle, L. Ciarloni, S. Andrejevic-Blant, R. Moeckli, R. O. Mirimanoff, S. L. Goodman, M. Delorenzi and C. Ruegg (2008). "CYR61 and alphaVbeta5 integrin cooperate to promote invasion and metastasis of tumors growing in preirradiated stroma." Cancer Res **68**(18): 7323-7331.

Muz, B., P. de la Puente, F. Azab and A. K. Azab (2015). "The role of hypoxia in cancer progression, angiogenesis, metastasis, and resistance to therapy." Hypoxia (Auckl) **3**: 83-92.

Nallet-Staub, F., V. Marsaud, L. Li, C. Gilbert, S. Dodier, V. Bataille, M. Sudol, M. Herlyn and A. Mauviel (2014). "Pro-invasive activity of the Hippo pathway effectors YAP and TAZ in cutaneous melanoma." J Invest Dermatol **134**(1): 123-132.

Navab, R., D. Strumpf, C. To, E. Pasko, K. S. Kim, C. J. Park, J. Hai, J. Liu, J. Jonkman, M. Barczyk, B. Bandarchi, Y. H. Wang, K. Venkat, E. Ibrahimov, N. A. Pham, C. Ng, N. Radulovich, C. Q. Zhu, M. Pintilie, D. Wang, A. Lu, I. Jurisica, G. C. Walker, D. Gullberg and M. S. Tsao (2016). "Integrin alpha11beta1 regulates cancer stromal stiffness and promotes tumorigenicity and metastasis in non-small cell lung cancer." Oncogene **35**(15): 1899-1908.

Nguyen, L. T., Y. W. Song and S. K. Cho (2016). "Baicalein Inhibits Epithelial to Mesenchymal Transition via Downregulation of Cyr61 and LOXL-2 in MDA-MB231 Breast Cancer Cells." Mol Cells **39**(12): 909-914.

Pastushenko, I., P. B. Vermeulen, G. G. Van den Eynden, A. Rutten, F. J. Carapeto, L. Y. Dirix and S. Van Laere (2014). "Mechanisms of tumour vascularization in cutaneous malignant melanoma: clinical implications." Br J Dermatol **171**(2): 220-233.

Provenzano, P. P., D. R. Inman, K. W. Eliceiri, J. G. Knittel, L. Yan, C. T. Rueden, J. G. White and P. J. Keely (2008). "Collagen density promotes mammary tumor initiation and progression." BMC Med **6**: 11.

Quail, D. F., M. J. Taylor and L. M. Postovit (2012). "Microenvironmental regulation of cancer stem cell phenotypes." Curr Stem Cell Res Ther **7**(3): 197-216.

Quan, T., Y. Xu, Z. Qin, P. Robichaud, S. Betcher, K. Calderone, T. He, T. M. Johnson, J. J. Voorhees and G. J. Fisher (2014). "Elevated YAP and its downstream targets CCN1 and CCN2 in basal cell carcinoma: impact on keratinocyte proliferation and stromal cell activation." Am J Pathol **184**(4): 937-943.

Reed, K. B., J. D. Brewer, C. M. Lohse, K. E. Bringe, C. N. Pruitt and L. E. Gibson (2012). "Increasing incidence of melanoma among young adults: an epidemiological study in Olmsted County, Minnesota." Mayo Clin Proc **87**(4): 328-334.

Rockey, D. C., N. Weymouth and Z. Shi (2013). "Smooth muscle alpha actin (Acta2) and myofibroblast function during hepatic wound healing." PLoS One **8**(10): e77166.

Schmitz, P., U. Gerber, N. Schutze, E. Jungel, R. Blaheta, A. Naggi, G. Torri and G. Bendas (2013). "Cyr61 is a target for heparin in reducing MV3 melanoma cell adhesion and migration via the integrin VLA-4." Thromb Haemost **110**(5): 1046-1054.

Segarini, P. R., J. E. Nesbitt, D. Li, L. G. Hays, J. R. Yates, 3rd and D. F. Carmichael (2001). "The low density lipoprotein receptor-related protein/alpha2-macroglobulin receptor is a receptor for connective tissue growth factor." J Biol Chem **276**(44): 40659-40667.

Sha, W. and A. Leask (2011). "CCN2 expression and localization in melanoma cells." J Cell Commun Signal **5**(3): 219-226.

Shimo, T., S. Kubota, N. Yoshioka, S. Ibaragi, S. Isowa, T. Eguchi, A. Sasaki and M. Takigawa (2006). "Pathogenic role of connective tissue growth factor (CTGF/CCN2) in osteolytic metastasis of breast cancer." J Bone Miner Res **21**(7): 1045-1059.

Slany, A., A. Meshcheryakova, A. Beer, H. J. Ankersmit, V. Paulitschke and C. Gerner (2014). "Plasticity of fibroblasts demonstrated by tissue-specific and function-related proteome profiling." Clin Proteomics **11**(1): 41.

Society, A. C. (2013). "Melanoma Skin Cancer."   Retrieved January 6, 2013, from http://www.cancer.org/cancer/skincancer-melanoma/detailedguide/index.

Soengas, M. S. and S. W. Lowe (2003). "Apoptosis and melanoma chemoresistance." Oncogene **22**(20): 3138-3151.

Steeg, P. S. (2006). "Tumor metastasis: mechanistic insights and clinical challenges." Nat Med **12**(8): 895-904.

Sun, Z. J., Y. Wang, Z. Cai, P. P. Chen, X. J. Tong and D. Xie (2008). "Involvement of Cyr61 in growth, migration, and metastasis of prostate cancer cells." Br J Cancer **99**(10): 1656-1667.

Tilman, G., M. Mattiussi, F. Brasseur, N. van Baren and A. Decottignies (2007). "Human periostin gene expression in normal tissues, tumors and melanoma: evidences for periostin production by both stromal and melanoma cells." Mol Cancer **6**: 80.

Vartanian, A., S. Karshieva, V. Dombrovsky and A. Belyavsky (2016). "Melanoma educates mesenchymal stromal cells towards vasculogenic mimicry." Oncol Lett **11**(6): 4264-4268.

Vartanian, A. A., O. S. Burova, E. V. Stepanova and A. Y. Baryshnikov (2007). "The involvement of apoptosis in melanoma vasculogenic mimicry." Melanoma Res **17**(1): 1-8.

Wack, C., A. Kirst, J. C. Becker, W. K. Lutz, E. B. Brocker and W. H. Fischer (2002). "Chemoimmunotherapy for melanoma with dacarbazine and 2,4-dinitrochlorobenzene elicits a specific T cell-dependent immune response." Cancer Immunol Immunother **51**(8): 431-439.

Wang, J. Y., T. Sun, X. L. Zhao, S. W. Zhang, D. F. Zhang, Q. Gu, X. H. Wang, N. Zhao, S. Qie and B. C. Sun (2008). "Functional significance of VEGF-a in human ovarian carcinoma: role in vasculogenic mimicry." Cancer Biol Ther **7**(5): 758-766.

Wang, Z., D. You, M. Lu, Y. He and S. Yan (2017). "Inhibitory effect of norcantharidin on melanoma tumor growth and vasculogenic mimicry by suppressing MMP-2 expression." Oncol Lett **13**(3): 1660-1664.

Wells, J. E., M. Howlett, C. H. Cole and U. R. Kees (2015). "Deregulated expression of connective tissue growth factor (CTGF/CCN2) is linked to poor outcome in human cancer." Int J Cancer **137**(3): 504-511.

Wong, G. S. and A. K. Rustgi (2013). "Matricellular proteins: priming the tumour microenvironment for cancer development and metastasis." Br J Cancer **108**(4): 755-761.

Wu, Y. L., H. Y. Li, X. P. Zhao, J. Y. Jiao, D. X. Tang, L. J. Yan, Q. Wan and C. B. Pan (2017). "Mesenchymal stem cell-derived CCN2 promotes the proliferation, migration and invasion of human tongue squamous cell carcinoma cells." Cancer Sci **108**(5): 897-909.

Xie, D., K. Nakachi, H. Wang, R. Elashoff and H. P. Koeffler (2001). "Elevated levels of connective tissue growth factor, WISP-1, and CYR61 in primary breast cancers associated with more advanced features." Cancer Res **61**(24): 8917-8923.

Yang, F., J. A. Tuxhorn, S. J. Ressler, S. J. McAlhany, T. D. Dang and D. R. Rowley (2005). "Stromal expression of connective tissue growth factor promotes angiogenesis and prostate cancer tumorigenesis." Cancer Res **65**(19): 8887-8895.

Zaman, M. H., L. M. Trapani, A. L. Sieminski, D. Mackellar, H. Gong, R. D. Kamm, A. Wells, D. A. Lauffenburger and P. Matsudaira (2006). "Migration of tumor cells in 3D matrices is governed by matrix stiffness along with cell-matrix adhesion and proteolysis." Proc Natl Acad Sci U S A **103**(29): 10889-10894.

Zhang, K., W. R. Grither, S. Van Hove, H. Biswas, S. M. Ponik, K. W. Eliceiri, P. J. Keely and G. D. Longmore (2016). "Mechanical signals regulate and activate SNAIL1 protein to control the fibrogenic response of cancer-associated fibroblasts." J Cell Sci **129**(10): 1989-2002.

Zheng, B., Z. Zhang, C. M. Black, B. de Crombrugghe and C. P. Denton (2002). "Ligand-dependent genetic recombination in fibroblasts : a potentially powerful technique for investigating gene function in fibrosis." Am J Pathol **160**(5): 1609-1617.

5.2

Appendices

Appendix A: Publication permission

Chapter 2 was published in the Journal of Investigative Dermatology and was reproduced with permission as listed on their website (https://www.elsevier.com/about/our-business/policies/copyright/permissions), as seen below.
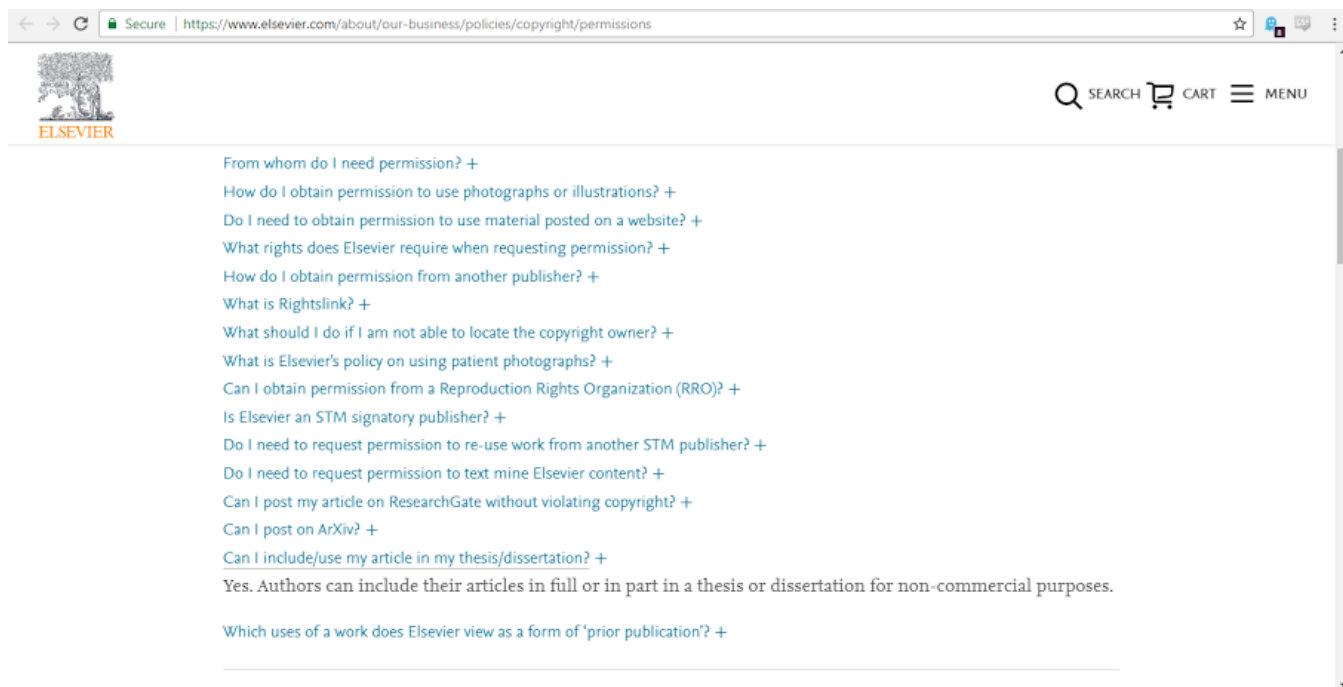
Figure 1-1 was published in Cancer Cell under the terms of the Creative Commons Attribution-Non-Commercial-No Derivatives License as Hirata, E., M. R. Girotti, A. Viros, S. Hooper, B. Spencer-Dene, M. Matsuda, J. Larkin, R. Marais and E. Sahai (2015). "Intravital imaging reveals how BRAF inhibition generates drug-tolerant microenvironments with high integrin beta1/FAK signaling." Cancer Cell **27**(4): 574-588 DOI: 10.1016/j.ccell.2015.03.008

Figure 1-2 was Reprinted from Cancer Cell, 31/3, Kristin G. Anderson, Ingunn M. Stromnes, Philip D. Greenberg, Obstacles Posed by the Tumor Microenvironment to T cell Activity: A Case for Synergistic Therapies, 311-325, 2017, with permission from Elsevier (See license below)

ELSEVIER LICENSE
TERMS AND CONDITIONS

Dec 04, 2017

This Agreement between University of Western Ontario -- James Hutchenreuther ("You") and Elsevier ("Elsevier") consists of your license details and the terms and conditions provided by Elsevier and Copyright Clearance Center.

License Number	4241940216893
License date	Dec 04, 2017
Licensed Content Publisher	Elsevier
Licensed Content Publication	Cancer Cell
Licensed Content Title	Obstacles Posed by the Tumor Microenvironment to T cell Activity: A Case for Synergistic Therapies
Licensed Content Author	Kristin G. Anderson,Ingunn M. Stromnes,Philip D. Greenberg
Licensed Content Date	Mar 13, 2017
Licensed Content Volume	31
Licensed Content Issue	3
Licensed Content Pages	15
Start Page	311
End Page	325
Type of Use	reuse in a thesis/dissertation
Portion	figures/tables/illustrations
Number of figures/tables/illustrations	1
Format	both print and electronic
Are you the author of this Elsevier article?	No
Will you be translating?	No

Original figure numbers	Figure 1
Title of your thesis/dissertation	CCN Proteins in Metastatic Melanoma
Expected completion date	Dec 2017
Estimated size (number of pages)	160
Requestor Location	University of Western Ontario 1151 Richmond St London, ON N6A 3K7 Canada Attn: James Hutchenreuther
Total	0.00 CAD

Appendix B: Ethics Approvals

Ethics approval for use of animals was granted under animal use protocols 2010-253, 2011-046, which became 2016-004 upon renewal (Below).

Western

AUP Number: 2010-253
PI Name: Leask, Andrew
AUP Title: The Role Of Adhesive Signaling In Fibrogenesis
Approval Date: 12/02/2014

Official Notice of Animal Use Subcommittee (AUS) Approval: Your new Animal Use Protocol (AUP) entitled "The Role Of Adhesive Signaling In Fibrogenesis" has been APPROVED by the Animal Use Subcommittee of the University Council on Animal Care. This approval, although valid for four years, and is subject to annual Protocol Renewal.2010-253::5

1. This AUP number must be indicated when ordering animals for this project.
2. Animals for other projects may not be ordered under this AUP number.
3. Purchases of animals other than through this system must be cleared through the ACVS office. Health certificates will be required.

The holder of this Animal Use Protocol is responsible to ensure that all associated safety components (biosafety, radiation safety, general laboratory safety) comply with institutional safety standards and have received all necessary approvals. Please consult directly with your institutional safety officers.

Submitted by: Copeman, Laura
on behalf of the Animal Use Subcommittee
University Council on Animal Care

Western

2016-004::1:
AUP Number: 2016-004
AUP Title: The role of CCN proteins in melanoma
Yearly Renewal Date: 03/01/2017
The YEARLY RENEWAL to Animal Use Protocol (AUP) 2016-004 has been approved, and will be approved for one year following the above review date.

1. This AUP number must be indicated when ordering animals for this project.
2. Animals for other projects may not be ordered under this AUP number.
3. Purchases of animals other than through this system must be cleared through the ACVS office.
   Health certificates will be required.

REQUIREMENTS/COMMENTS
Please ensure that individual(s) performing procedures on live animals, as described in this protocol, are familiar with the contents of this document.
The holder of this Animal Use Protocol is responsible to ensure that all associated safety components (biosafety, radiation safety, general laboratory safety) comply with institutional safety standards and have received all necessary approvals. Please consult directly with your institutional safety officers.
Submitted by: Schoelier, Marianne
on behalf of the Animal Use Subcommittee

James Hutchenreuther

Department of Physiology and Pharmacology
University of Western Ontario
1151 Richmond Street
London, Ontario, N6A 3K7

Education

Ph.D. Candidate (Physiology), University of Western Ontario, London, Ontario, Canada   2012 - 2017
Thesis Title: The role of CCN proteins in Metastatic Melanoma
Advisor: Drs. Andrew Leask & Lynne-Marie Postovit

Science Laboratory Techology Diploma, Fanshawe College, London, Ontario, Canada   2008 - 2011

B.Sc, Honours Biological Sciences, University of Guelph, Guelph, Ontario, Canada   2003 - 2007

Other Positions and Employment

Lab Technician, Department of Dentistry, University of Western Ontario, London, Ontario, Canada   2010 - 2011

Lab Techician, A&L Labs, London, Ontario, Canada   2009

Honors and Awards

Ontario Graduate Scholarship   2016 - 2017

Lucille and Norton Wolfe London Health Research Day Trainee Publication Award   2016

Dentistry Research Day 1st Place Poster Award, senior category   2015

Publications

Peer-reviewed publications

1. Hutchenreuther J, Leask A. A tale of two origins: do myofibroblasts originate from different sources in wound healing and fibrosis? Cell and Tissue Research 365 (3): pp 507-509 (2016).

2. Hutchenreuther J, Vincent KM, Carter DE, Postovit LM, Leask A. CCN2 Expression by Tumor Stroma is Required for Melanoma Metastasis. Journal of Investigative Dermatology 135(11): pp 2805-2813 (2015)

3. Kuk H, Hutchenreuther J, Murphy-Marshman H, Carter D, Leask A. 5Z-7-Oxozeaenol Inhibits the Effects of TGFβ1 on Human Gingival Fibroblasts. PLoS One 10(4) eCollection (2015)

4. Parampuram SK, Thompson K, Tsang M, Hutchenreuther J, Bekking C, Liu S, Leask A. Loss of PTEN expression by mouse fibroblasts results in lung fibrosis through a CCN2-dependent mechanism. Matrix Biology 43: pp 35-41 (2015)

5. Guo F, Hutchenreuther J, Carter DE, Leask A. TAK1 is required for dermal wound healing and homeostasis. Journal of Investigative Dermatology 133(6): pp 1646-1654 (2013)

Books & Chapters

1. Hutchenreuther J, Leask A, Thompson K. Studying the CCN Proteins in Fibrosis. in Methods in Molecular Biology pp 423-429. Springer (2016).

Non-peer-reviewed publications

1. Leask A, Hutchenreuther J. Activation of latent TGFβ by αvβ1 integrin: of potential importance in myofibroblast activation in fibrosis. Journal of Cell Communication and Signaling 8(2): pp 171-172 (2014)

2. Hutchenreuther J. CCN1 is a novel target to reduce the metastasis of melanoma. Journal of Cell Communication and Signaling 8(1): pp 65-66 (2014)

Invited Presentations

Local

Cancer-Associated Fibroblasts are Essential for Melanoma Metastasis, Stevenson Distinguished Lecture Series, University of Western Ontario, London, Ontario, Canada	Nov 1, 2016

Other Presentations, Posters & Abstracts

International

Hutchenreuther J, Vincent KM, Norley C, Postovit LM, Leask A. Fibrotic mediator CCN2 is required in tumour stroma for melanoma metastasis and angiogenesis. 2017 Gordon Research Conference on Tissue Regeneration and Repair. Abstract and Poster Presentation.	June 4 - 9, 2017
Hutchenreuther J, Vincent KM, Carter DE, Postovit LM, Leask A. The role of CCN2 in melanoma metastasis. ASMB 2016 Biennial Meeting. Oral Presentation, Abstract, and Poster	November 13-16, 2016
Hutchenreuther J, Vincent KM, Carter DE, Postovit LM, Leask A. CCN2 Expression by the Tumor Stroma is Required for Melanoma Metastasis. 2015 American Society for Cell Biology (ASCB) Annual Meeting. Abstract and Poster Presentation	December 12-16, 2015
Hutchenreuther J, Vincent KM, Carter DE, Postovit LM Leask A. CCN2 Expression by the Tumor Stroma is Required for Melanoma Metastasis. British Society of Matrix Biology Spring 2015 Meeting – Location, Location, Location: The Matrix and the Microenvronment. Oral Presentation, Abstract, and Poster.	March 30 - 31, 2015
Hutchenreuther J and Leask A. TAK1 signaling is required for fibrotic gene expression in human fibroblasts. 12th Annual International Workshop on Scleroderma Research (2011). Abstract and Poster Presentation.	July 23 - 27, 2011

National

Hutchenreuther J, Vincent KM, Carter DE, Postovit LM, Leask A. CCN2 Expression by the Tumor Stroma is Required for Melanoma Metastasis. 2016 Canadian Student Health Research Forum (CSHRF). Abstract and Poster Presentation.	June 7 - 9, 2016
Hutchenreuther J, Vincent KM, Quesnel K, Postovit LM, Leask A. CCN1 Expression by Tumor Stroma is Required for Melanoma Metastasis. 2016 Canadian Bone and Joint Conference. Abstract and Poster Presentation.	April 8 - 9, 2016

Local

Hutchenreuther J, Vincent KM, Carter DE, Postovit LM, Leask A. CCN2 Expression by the Tumor Stroma is Required for Melanoma Metastasis. 2016 London Health Research Day. Abstract and Poster Presentation.	March 29, 2016
Hutchenreuther J, Vincent KM, Carter DE, Postovit LM, Leask A. CCN2 Expression by Tumor Stroma is Required for Melanoma Metastasis. 2015 Dentistry Research Day. Poster Presentation	October 14, 2015

Educational Activities

Teaching Activities

Introduction to Human Physiology (Phys 1021), TA, ~90 students in my sections 400 in the course	2015 - 2017
Human Physiology (Phys 2130), TA, ~80 students in my sections ~700 in the course	2014 - 2015
Cell Signaling in Tissue Injury and Repair, TA, ~40 students in the course	2014

Clinical Teaching and Supervision

Dental SIM clinic after-hours supervisor, responsible for health and safety policy enforcement for dental students in after hours simulation clinic, University of Western Ontario, London, Ontario, Canada	2015 - 2017

Committee Assignments and Administrative Service

External Professional Service

Graduate Management Consulting Association Western Chapter Executive Committee (Director of Member and Professional Relations), GMCA Canada	2015 - 2017

Advising and Mentoring

Students

Courtney Wallingford, Department of Biology, Undergraduate Thesis Student	2016 - 2017
Sabina Strashun, Department of Biology, Undergraduate Thesis Student	2016